



**HAL**  
open science

# Integration of proteins with organic electrochemical transistors for sensing applications

Xenofon Strakosas

► **To cite this version:**

Xenofon Strakosas. Integration of proteins with organic electrochemical transistors for sensing applications. Other. Ecole Nationale Supérieure des Mines de Saint-Etienne, 2015. English. NNT : 2015EMSE0774 . tel-01151130

**HAL Id: tel-01151130**

**<https://theses.hal.science/tel-01151130>**

Submitted on 12 May 2015

**HAL** is a multi-disciplinary open access archive for the deposit and dissemination of scientific research documents, whether they are published or not. The documents may come from teaching and research institutions in France or abroad, or from public or private research centers.

L'archive ouverte pluridisciplinaire **HAL**, est destinée au dépôt et à la diffusion de documents scientifiques de niveau recherche, publiés ou non, émanant des établissements d'enseignement et de recherche français ou étrangers, des laboratoires publics ou privés.



NNT : 2015 EMSE 0774.

## THÈSE

présentée par

**Xenofon Strakosas**

pour obtenir le grade de  
Docteur de l'École Nationale Supérieure des Mines de Saint-Étienne

Spécialité : Bioélectronique

## INTEGRATION OF PROTEINS WITH ORGANIC ELECTROCHEMICAL TRANSISTORS FOR SENSING APPLICATIONS

soutenue à Gardanne, le 12 Janvier 2015

### Membres du jury

Président :	Dermot DIAMOND	Professeur, DCU, Dublin
Rapporteurs :	Thomas ANTHOPOULOS Pascal MAILLEY	Professeur, Imperial college, London PhD - HDR, CEA, Grenoble
Examineur(s) :	Susan DANIEL	Professeur, Cornell University, Ithaca
Directeur(s) de thèse :	George MALLIARAS	Professeur, ENSMSE, Gardanne
Co-encadrant :	Roisin OWENS	Maitre-Assistant, ENSMSE, Gardanne

Spécialités doctorales	Responsables	Spécialités doctorales	Responsables
SCIENCES ET GENIE DES MATERIAUX	K. Wolski Directeur de recherche	MATHEMATIQUES APPLIQUEES	O. Roustant, Maître-assistant
MECANIQUE ET INGENIERIE	S. Drapier, professeur	INFORMATIQUE	O. Boissier, Professeur
GENIE DES PROCEDES	F. Gruy, Maître de recherche	IMAGE, VISION, SIGNAL	JC. Pinoli, Professeur
SCIENCES DE LA TERRE	B. Guy, Directeur de recherche	GENIE INDUSTRIEL	A. Dolgui, Professeur
SCIENCES ET GENIE DE L'ENVIRONNEMENT	D. Grailot, Directeur de recherche	MICROELECTRONIQUE	S. Dauzere Peres, Professeur

**EMSE : Enseignants-chercheurs et chercheurs autorisés à diriger des thèses de doctorat (titulaires d'un doctorat d'état ou d'une HDR)**

ABSI	Nabil	CR		CMP
AVRIL	Stéphane	PR2	Mécanique et ingénierie	CIS
BALBO	Flavien	PR2		FAYOL
BASSEREAU	Jean-François	PR		SMS
BATTON-HUBERT	Mireille	PR2	Sciences et génie de l'environnement	FAYOL
BERGER DOUCE	Sandrine	PR2		FAYOL
BERNACHE-ASSOLLANT	Didier	PRO	Génie des Procédés	CIS
BIGOT	Jean Pierre	MR(DR2)	Génie des Procédés	SPIN
BILAL	Essaid	DR	Sciences de la Terre	SPIN
BOISSIER	Olivier	PR1	Informatique	FAYOL
BORBELY	Andras	MR(DR2)	Sciences et génie des matériaux	SMS
BOUCHER	Xavier	PR2	Génie Industriel	FAYOL
BRODHAG	Christian	DR	Sciences et génie de l'environnement	FAYOL
BRUCHON	Julien	MA(MDC)	Mécanique et ingénierie	SMS
BURLAT	Patrick	PR2	Génie Industriel	FAYOL
COURNIL	Michel	PRO	Génie des Procédés	DIR
DARRIEULAT	Michel	IGM	Sciences et génie des matériaux	SMS
DAUZERE-PERES	Stéphane	PR1	Génie Industriel	CMP
DEBAYLE	Johan	CR	Image Vision Signal	CIS
DELAFOSSSE	David	PR1	Sciences et génie des matériaux	SMS
DESRAYAUD	Christophe	PR2	Mécanique et ingénierie	SMS
DOLGUI	Alexandre	PRO	Génie Industriel	FAYOL
DRAPIER	Sylvain	PR1	Mécanique et ingénierie	SMS
FEILLET	Dominique	PR2	Génie Industriel	CMP
FEVOTTE	Gilles	PR1	Génie des Procédés	SPIN
FRACZKIEWICZ	Anna	DR	Sciences et génie des matériaux	SMS
GARCIA	Daniel	MR(DR2)	Génie des Procédés	SPIN
GERINGER	Jean	MA(MDC)	Sciences et génie des matériaux	CIS
GOEURIOT	Dominique	DR	Sciences et génie des matériaux	SMS
GRAILLOT	Didier	DR	Sciences et génie de l'environnement	SPIN
GROSSEAU	Philippe	DR	Génie des Procédés	SPIN
GRUY	Frédéric	PR1	Génie des Procédés	SPIN
GUY	Bernard	DR	Sciences de la Terre	SPIN
HAN	Woo-Suck	CR	Mécanique et ingénierie	SMS
HERRI	Jean Michel	PR1	Génie des Procédés	SPIN
KERMOUCHE	Guillaume	PR2	Mécanique et Ingénierie	SMS
KLOCKER	Helmut	DR	Sciences et génie des matériaux	SMS
LAFOREST	Valérie	MR(DR2)	Sciences et génie de l'environnement	FAYOL
LERICHE	Rodolphe	CR	Mécanique et ingénierie	FAYOL
LI	Jean-Michel		Microélectronique	CMP
MALLIARAS	Georges	PR1	Microélectronique	CMP
MOLIMARD	Jérôme	PR2	Mécanique et ingénierie	CIS
MONTHEILLET	Frank	DR	Sciences et génie des matériaux	SMS
MOUTTE	Jacques	CR	Génie des Procédés	SPIN
NEUBERT	Gilles			FAYOL
NIKOLOVSKI	Jean-Pierre			CMP
NORTIER	Patrice	PR1		SPIN
PIJOLAT	Christophe	PRO	Génie des Procédés	SPIN
PIJOLAT	Michèle	PR1	Génie des Procédés	SPIN
PINOLI	Jean Charles	PRO	Image Vision Signal	CIS
POURCHEZ	Jérémy	CR	Génie des Procédés	CIS
ROBISSON	Bruno			CMP
ROUSSY	Agnès	MA(MDC)		CMP
ROUSTANT	Olivier	MA(MDC)		FAYOL
ROUX	Christian	PR		CIS
STOLARZ	Jacques	CR	Sciences et génie des matériaux	SMS
TRIA	Assia	Ingénieur de recherche	Microélectronique	CMP
VALDIVIESO	François	MA(MDC)	Sciences et génie des matériaux	SMS
VIRICELLE	Jean Paul	MR(DR2)	Génie des Procédés	SPIN
WOLSKI	Krzystof	DR	Sciences et génie des matériaux	SMS
XIE	Xiaolan	PR1	Génie industriel	CIS
YUGMA	Gallian	CR	Génie industriel	CMP

**ENISE : Enseignants-chercheurs et chercheurs autorisés à diriger des thèses de doctorat (titulaires d'un doctorat d'état ou d'une HDR)**

BERGHEAU	Jean-Michel	PU	Mécanique et Ingénierie	ENISE
BERTRAND	Philippe	MCF	Génie des procédés	ENISE
DUBUJET	Philippe	PU	Mécanique et Ingénierie	ENISE
FEULVARCH	Eric	MCF	Mécanique et Ingénierie	ENISE
FORTUNIER	Roland	PR	Sciences et Génie des matériaux	ENISE
GUSSAROV	Andrey	Enseignant contractuel	Génie des procédés	ENISE
HAMDI	Hédi	MCF	Mécanique et Ingénierie	ENISE
LYONNET	Patrick	PU	Mécanique et Ingénierie	ENISE
RECH	Joël	PU	Mécanique et Ingénierie	ENISE
SMUROV	Igor	PU	Mécanique et Ingénierie	ENISE
TOSCANO	Rosario	PU	Mécanique et Ingénierie	ENISE
ZAHOUANI	Hassan	PU	Mécanique et Ingénierie	ENISE

NNT : 2015 EMSE 0774

Xenofon Strakosas

## INTEGRATION OF PROTEINS WITH ORGANIC ELECTROCHEMICAL TRANSISTORS FOR SENSING APPLICATIONS

Spécialité: Bioélectronique

Mots clefs: OECT, enzymatic sensors, biofunctionalization

### **Résumé:**

Le domaine de la bioélectronique, qui couple l'électronique et la biologie, présente un fort potentiel pour le développement de nouveaux outils biomédicaux. Les dispositifs à base d'électronique organique sont particulièrement prometteurs; l'utilisation de ces matériaux organiques confère une interface idéale entre les mondes biologique et électronique en raison de leur biocompatibilité et de leur possible grande flexibilité. Le transistor électrochimique organique (OECT) représente un dispositif prometteur dans ce domaine. Une des caractéristiques importante de l'OECT réside dans son amplification locale permettant une amélioration du rapport signal sur bruit et donc une augmentation de la sensibilité et de la limite de détection d'événements biologiques. Des OECT ont par exemple été intégrés dans des systèmes permettant de détecter localement l'activité ionique/biomoléculaire, de mesurer l'activité d'une cellule unique, mais aussi d'effectuer la caractérisation de tissus et le suivi du fonctionnement d'organes entiers. L'OECT est un dispositif extrêmement polyvalent qui apparaît comme un outil thérapeutique et de diagnostic de première importance.

L'utilisation de matériaux organiques tels que les polymères conducteurs, rend l'OECT adaptable pour une large gamme d'applications. Un exemple représentatif est le capteur de glucose. La majorité des capteurs de glucose disponibles dans le commerce s'appuient sur la détection électrochimique dans laquelle une enzyme catalyse le glucose. L'utilisation d'un médiateur permet alors le transfert d'électrons à l'électrode, créant ainsi un courant qui dépend de la concentration de glucose. L'amplitude de ces courants biologiques est cependant faible. L'OECT, en raison de ses propriétés d'amplification, peut augmenter ces courants de plusieurs ordres de grandeurs. Utilisé comme capteur de glucose, il montre une forte sensibilité et des limites de détection des concentrations de l'ordre du nanomolar. Cependant, en dehors d'une meilleure précision de mesure, la stabilité est nécessaire pour les applications à long terme. Par exemple, ces capteurs se doivent d'enregistrer en continu les variations de glycémie chez des personnes pendant plusieurs jours et sans défaillance. Dans un autre registre, l'OECT a été utilisé pour des enregistrements cérébraux de zones épileptiques avec un meilleur rapport signal sur bruit que des électrodes classiques ou que des transistors à base de matériaux inorganiques. Le glucose est la source d'énergie principale du cerveau. Ainsi, l'enregistrement de la modulation des niveaux de glucose avant et/ou pendant la crise d'épilepsie peut donner beaucoup d'informations dans la compréhension de cette maladie.

La stabilité à long terme peut être atteinte par la biofonctionnalisation, méthode consistant à fixer une biomolécule sur le dispositif de mesure. La nature de la liaison peut varier: liaisons faibles et réversibles de Van der Waals ou liaisons fortes et irréversibles de type covalentes. Les besoins en biofonctionnalisation dépendent de chaque application. Pour des applications à long termes, une liaison covalente de la biomolécule est préférable. Cependant, pour des biomolécules telles que des enzymes, dans lequel la fonction dépend de leur conformation, une perte d'activité peut se produire. La biofonctionnalisation des polymères conducteurs, qui sont utilisés comme matières actives dans les OECTs, est une étape obligatoire qui mettra en évidence les propriétés de l'OECT telles que la biocompatibilité, la stabilité, et la fonctionnalité. Dans ce travail, des méthodes de biofonctionnalisation du poly(3,4-éthylènedioxythiophène) dopé avec des anions de tosylate (PEDOT: TOS) ou dopé avec du poly(styrène sulfonate) (PEDOT: PSS) ont été développées et ont conduit à des améliorations telles que la biocompatibilité accrue avec les cellules et à une stabilité accrue pour les applications de détection. En outre, nous avons étudié l'utilisation de liquides ioniques en combinaison avec des polymères réticulables comme alternatives aux électrolytes conventionnelles. Ces gels ioniques électrolytes ont amélioré la stabilité des enregistrements

électrophysiologiques. Enfin, des mesures *in vitro* de l'activité métabolique de la cellule ont été effectuées. Le suivi de l'absorption du glucose et de la conversion en lactate fournit des informations sur la santé des cellules et comment ses activités métaboliques sont affectées par la présence de composés toxiques et d'agents pathogènes.

NNT : 2015 EMSE 0774

Xenofon Strakosas

## INTEGRATION OF PROTEINS WITH ORGANIC ELECTROCHEMICAL TRANSISTORS FOR SENSING APPLICATIONS

Speciality: Bioelectronics

Keywords: OECT, enzymatic sensors, biofunctionalization

### **Abstract:**

The rising field of bioelectronics, which couples the realms of electronics and biology, holds huge potential for the development of novel biomedical devices for therapeutics and diagnostics. Organic electronic devices are particularly promising; the use of robust organic electronic materials provides an ideal bio-interface due to their reported biocompatibility, and mechanical matching between the sensor element and the biological environment, are amongst the advantages unique to this class of materials. One promising device emerging from this field is the organic electrochemical transistor (OECT). Arguably the most important feature of an OECT is that it provides local amplification and as such can be used as a high fidelity transducer of biological events. Additionally, the OECT combines properties and characteristics that can be tuned for a wide spectrum of biological applications. These applications have allowed the development of OECTs to sense local ionic/biomolecular and single cell activity,

as well characterization of tissue and even monitoring of function of whole organs. The OECT is an extremely versatile device that emerges as an important player for therapeutics and diagnostics.

The use of organic materials, such as conducting polymers, makes the OECT tunable for a wide range of applications. For example, OECTs have been used for sensing applications. A representative example is the glucose sensor. The majority of current commercially available glucose sensors rely on electrochemical detection, in which the enzyme glucose oxidase is catalyzing the glucose and through a mediator an electron is transferred to the electrode, thereby creating a current which depends in the concentration of glucose. However, the magnitude of these biological currents is low. The OECT, owing to its amplification properties, can amplify these currents many orders of magnitude. The OECT has been used as glucose sensor and has shown high sensitivities and low limit of detection for concentrations at the nanomolar range. However, apart from high sensitivities, stability and reproducibility are common necessities for long term applications. For example, it is of equal importance for these sensors to continuously record variations of glucose for diabetic patients, since multiple measurements per day without failure are necessary. Additionally, stability is necessary for implantable sensors. The OECT has been used in connection with the brain and has made recordings with better signal to noise ratio in epileptic rats. For brain cells such as neurons, glucose is the main energy source. Thus recording modulations of glucose levels before or during an epileptic crisis will enhance our understanding of this disease.

Long-term stabilities for these sensors can be achieved through biofunctionalization, which is a method to attach a biomolecule to a device. The nature of the biofunctionalization can vary from weak van der Waals reversible bonds to strong covalent irreversible bonds. The type of biofunctionalization depends on the needs of each application. For long term applications a covalent binding of the biomolecule is preferred.

Biofunctionalization of conducting polymers, which are used as active materials in OECTs, is a mandatory step that can enhance OECT properties such as biocompatibility, stability, and functionality. In this work, different biofunctionalization methods of poly(3,4-ethylenedioxythiophene) doped with tosylate anions (PEDOT:TOS) or doped with poly(styrene sulfonate) (PEDOT:PSS) have been explored. The biofunctionalization methods have led to improvements for different applications such as better interfaces with living cells, and better stability for enzymatic sensors. Additionally, we have employed the use of ionic liquids in combination with cross-linkable polymers as alternative solid state electrolytes. These electrolytes are improving the stability of recordings in electrophysiology. Finally, *in vitro* measurements of metabolic

activities in cells have been explored. The monitoring of glucose uptake and its conversion to lactate is a sensitive indicator of the viability of these cells. Furthermore, in the presence of toxic compounds and pathogens, the nature or kinetics of these metabolic activities is getting affected. Therefore, OECTs used for glucose and lactate sensing can at the same time be used for Immunosensing.

# Acknowledgements

These three years in south France, and more specifically at the Center of Microelectronics in Provence, have been marked in my brain as the most enjoyable, creative, challenging, with lots of new experiences, years of my life. Countless memories: In all these parties meeting new people with different mentalities, nights out with friends, small trips to the beautiful Provence, and the best working environment. The crucial parameter that contributed in all these are the people around me, and I would like to mention few of them. First of all, I would like to thank my supervisor Roisin Owens for the patience she showed during these years her amazing supervision, and the way she was always happy and cool. Also, I want to thank my second supervisor George Malliaras for his advice and supervision, also for giving me the chance to come and work with him.

Additionally, I want to thank the people from the Lab that made my working life so pleasant from the beginning. These people, who belong to the first generation of BEL, are no less than my **friends** and I will need several pages to write for everyone. I will always be grateful to you guys for the memories and experiences you gave me.

The new generation of BEL is keeping the same level of great people and they will write their own stories soon.

After that I want to thank the people from CMP that help me a lot in the beginning. We still hang out and play soccer with many of them.

I want to thank people that I have collaborated either by going to their labs or people that have come to our lab.

Then I thank few Greeks that I have met in Aix en Provence that made my stay a joyful experience.

Also I want to thank my friends and relatives from Greece for their great support.

Special thanks to my girlfriend for her patience, support and all the good moments. She made the difficult moments seem easy.

At the end and most important, I want to thank my parents Giannis and Roza Strakosas for all their support because without them none of this would have ever happened.

# Contents :

Résumé: .....	3
Abstract: .....	6
Acknowledgements.....	9
Contents :.....	10
1. Introduction .....	13
1.1. The organic electrochemical transistor for biological applications.....	13
1.1.1. Bioelectronics.....	13
1.1.2. The organic electrochemical transistor .....	14
1.1.3. Conducting Polymers .....	15
1.2. Applications in biology.....	19
1.2.1. OECTs coupled with biological moieties for sensing. ....	19
1.2.2. OECTs as ion sensors.....	19
1.2.3. OECTs as enzymatic sensors .....	22
1.2.4. OECTs as Immunosensors / nucleotide sensors.....	26
1.3. OECT coupled with whole cells for electrophysiology .....	28
1.3.1. Integration of OECTs with non-electrogenic cells .....	28
1.3.2. OECT for stimulation and recording of electrogenic cells .....	34
1.4. Conclusions.....	36
1.5. References .....	37
2. Biofunctionalization of PEDOT:TOS and exploration of enzyme wiring for realization of 3 <sup>rd</sup> generation enzymatic sensors .....	45
2.1. PEDOT :TOS :PEG with increased conductivity and surface functionality. ....	45
2.2. Vapor Phase Polymerization (VPP).....	47
2.2.1. Characterization of films and devices .....	48
2.2.2. Biofunctionalization of the films.....	51
2.3. Discussion.....	53
2.4. Experimental section .....	53
2.5. Stuffing of biomolecules and enzyme in PEDOT:TOS for enhanced cell adhesion and for 3 <sup>rd</sup> generation enzymatic sensors .....	55

2.5.1.	Characterization of PEDOT:TOS:Gelatin. ....	57
2.5.2.	Adhesion of BBB cells .....	59
2.5.3.	Stuffing of enzymes in PEDOT:TOS.....	62
2.6.	Discussion.....	66
2.7.	Experimental section .....	67
2.8.	Supplementary Information .....	69
2.9.	References .....	70
3.	A novel biofunctionalization route for solution processed PEDOT:PSS based devices.....	75
3.1.1.	Biofunctionalization strategy using PVA and silane.....	77
3.1.2.	Efficiency of the biofunctionalization .....	78
3.1.3.	Electrical properties of PEDOT:PSS:PVA as active material on OECTs. ....	80
3.2.	Applications.....	82
3.2.1.	Glucose sensing using biofunctionalized transistors .....	82
3.2.2.	Patterning of cells on active materials .....	83
3.3.	Discussion.....	85
3.4.	Experimental section .....	85
3.5.	Supplementary information .....	89
3.6.	References .....	89
4.	Ionic liquid gels integrated with conformal electrodes for long-term cutaneous recordings and with organic electrochemical transistors for sensing applications. ....	94
4.1.	Fabrication and characterization of electrodes with ionic liquid gel.....	96
4.2.	Ionic liquid gels integrated with OECTs for multianalyte sensors. ....	100
4.3.	Discussion.....	102
4.4.	Experimental section .....	103
4.5.	References .....	105
5.	In vitro enzymatic sensing using biofunctionalized OECTs.....	108
5.1.	Fabrication and functionalization process of the OECT .....	109
5.2.	Discussion.....	115
5.3.	Experimental section .....	115
5.4.	Supplementary Information .....	118

5.5. References .....	120
6. Conclusion.....	122
6.1. Outlook .....	123
7. Publications .....	124
Chapter 1.....	124
Chapter 2.....	124
Chapter 3.....	124
Chapter 4.....	124
Chapter 5.....	125
8. Glossary .....	126

# Chapter 1

---

## 1. Introduction

### 1.1. The organic electrochemical transistor for biological applications

#### 1.1.1. Bioelectronics

The coupling of organic electronics with biology is an emerging and continuously growing field.<sup>1</sup> The motivation for organic bioelectronics is to address and anticipate the current and future diagnostic and therapeutic needs of the biomedical community.<sup>2,3</sup> Those needs include detecting low concentrations of biological analytes, low amplitude brain activity, and pathogens, as well as improving compatibility with the biological environment.<sup>4</sup> Electrical methods for biological sensing are considered advantageous, in particular due to the fact that they are label-free, and do not require expensive and time consuming techniques involving fluorophores or chromophores (optical methods). Current diagnostic approaches using electrical sensors involve electrochemical biosensors, passive metal electrodes, and/or large scale integrated systems, in which the operating principle is based on redox reactions, changes in the local potential, or impedance. However, for electrochemical sensors and passive recording sites for electrophysiology the biological signals are often challenging to record and require further amplification to become detectable, necessitating a push towards more active, sensitive and biocompatible devices.<sup>5,6</sup> A promising technology that has the potential to overcome such limitations and respond to these specific requirements is the organic electrochemical transistor (OECT).

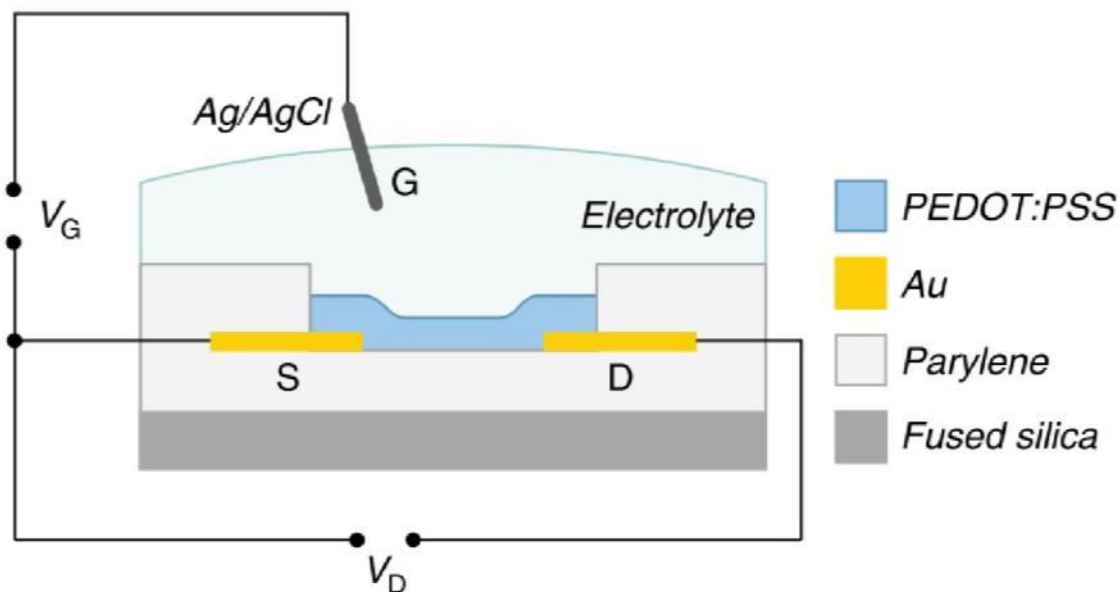


**Figure 1.1:** The organic electrochemical transistor: a. schematic cross-section of an OECT b. (reproduced from [7], with permission from [Nature Publishing Group])

### 1.1.2. The organic electrochemical transistor

The OECT, first reported by White *et al.*,<sup>8</sup> is a three terminal device in a transistor configuration (source, gate, and drain) (figure 1.1). The source and drain are connected by an organic conducting material in which an electronic current is generated ( $I_d$ ) in response to a potential difference. A variable potential at the gate controls the magnitude of the drain current ( $I_d$ ) by doping and de-doping the channel.

The OECT belongs to a broader class of transistors called electrolyte gated transistors (EGTs), in which the electrolyte is an integral part of the device.<sup>9</sup> This property makes the EGT compatible with aqueous environments. Apart from OECTs, a major subclass of the EGT is the electrolyte gated organic field effect transistor (EGOFET),<sup>10</sup> which has also been used as a diagnostic tool.<sup>11-13</sup> The difference between OECTs and EGOFETs lies in the interface between the channel and the electrolyte.<sup>14</sup> Specifically, in EGOFETs, the ions of the electrolyte create an electrical double layer (EDL) with the charges (electrons/holes) of the channel. By contrast, in OECTs, ions from the electrolyte can penetrate the whole bulk of the polymeric channel. This key difference enables the OECT to exhibit high amplification properties in sub-volt operation regimes, preventing electrolysis, and extending operating times necessary for *in-*

*vitro* and *in-vivo* applications.<sup>7</sup> The latter affords high sensitivity sensing for a wide spectrum of applications without additional amplification.

The OECT offers a unique set of advantages for biomedical tools. One notable advantage includes adaptability to a wide variety of fabrication methods, from simple to complex; OECTs have been fabricated using low-cost printing techniques,<sup>15-19</sup> high current modulation and fast response.<sup>20</sup> OECTs exhibit high stability in aqueous solutions and in one example showed reproducible, reliable performance when maintained in cell culture media under physiological conditions for five weeks.<sup>21</sup> Simple, planar, all PEDOT:PSS transistors on the macroscale have been shown to be capable of detecting glucose levels that exist in human saliva.<sup>22, 23</sup> For more challenging applications, OECTs are equally compatible with ongoing miniaturization techniques to the micro-scale, necessitated for the fabrication of high density electrode arrays for better interfacing with single neurons,<sup>24,25</sup> integration with microfluidics for detection of multiple analytes,<sup>26,27</sup> and lab on chip technologies.<sup>27</sup> The use of robust and versatile organic materials has also facilitated the fabrication of conformal OECTs (figure 1.4a) for non-invasive, long term, continuous recordings.<sup>28</sup> Additionally, OECTs have been integrated with natural and synthetic fibers for fully integrated sensors and wearable circuits compatible with human skin.<sup>29-31</sup> All OECTs reported to date have been fabricated with conducting polymers (CPs), as the active material in the channel due to their highly desirable properties, as discussed below.

### 1.1.3. Conducting Polymers

CPs, first discovered in 1976 by Alan MacDiarmid, Hideki Shirakawa and Alan Heeger, exhibit a wide spectrum of desired characteristics.<sup>32,33</sup> Of particular interest to biomedical applications, is that they exhibit mixed conductivity; ionic and electronic. Some of the first applications of CPs in the biomedical arena were their use as coatings on metal electrodes, where they were shown to improve recordings of brain activity by lowering the impedance of the electrode.<sup>14, 34</sup> CPs are chemically tunable, and can be designed according to the needs of each application. For instance, CPs have been designed to entrap enzymes and mediators.<sup>35,36</sup> Direct wiring of the active site of enzymes to electrodes has been explored using polyelectrolytes with redox active groups and conducting polymers.<sup>37-39</sup> Electrochemical biosensors have enlisted these types of CPs to improve stability and sensitivity. Finally, CPs have been shown repeatedly to be biocompatible, hosting a wide variety of cell types.<sup>40,41</sup> Part of their compatibility with live cells is most likely due to the fact that these polymeric materials

contain no broken bonds and are oxide-free, resulting in a closer interaction with cells hosted on their surface, possibly facilitating adhesion and promoting ionic interactions.<sup>41-45</sup> This concept has been extensively discussed by Rivnay and co-workers and is key to the understanding that CPs work well in electrolytes and, unlike other devices with semi-conducting polymers, are not isolated from the sensing events taking place in the aqueous milieu.<sup>45</sup>

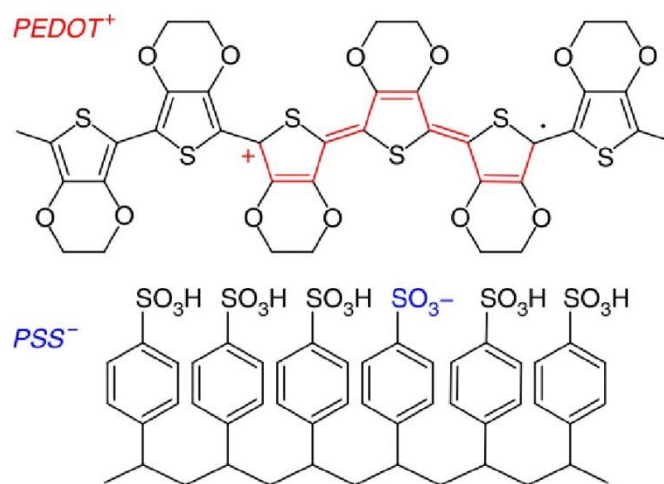


**Figure 1.2:** PEDOT:PSS structure. (reproduced from [7], with permission from [Nature Publishing Group])

Other advantages of CPs that will be highlighted below include their optical transparency and their mechanical flexibility akin to tissue, providing benefits for tissue engineering.

A well-studied and widely used CP is poly(3,4-ethylenedioxythiophene) doped with poly(styrene sulfonate) (PEDOT:PSS), a p-type conducting polymer in which the negative charge of PSS is compensated by a hole in the PEDOT backbone (figure 1.2). This conducting polymer exhibits high electronic conductivities, with typical conductivity values of commercially available PEDOT:PSS reaching approximately 1000 S/cm. Cross-linking of PEDOT:PSS with a silane (GOPS; 3-glycidoxypropyltrimethoxysilane) is a frequently used strategy for improving adhesion of PEDOT:PSS with substrates, and preventing delamination in aqueous milieu.<sup>7,12</sup> The conductivity of PEDOT:PSS drops with the addition of the crosslinker. However, conductivity measured after the addition of the crosslinker is in the order of 300 s/cm which is adequate for biological applications. Such cross-linked PEDOT:PSS films have been shown to swell in aqueous solutions, although to a lesser extent than uncrosslinked films, speaking to their ‘hydrogel’ type nature and implying their compatibility with electrolyte

solutions. Furthermore, PEDOT:PSS shows high ionic conductivities: ionic mobilities for small ions migrating in PEDOT:PSS can reach values that exist in dilute electrolytes.<sup>46</sup> Indeed, a novel class of devices based on PEDOT:PSS have been reported, which have ions as their main charge carrier (Iontronics), with subsequent development of ion transistors and ion pumps demonstrated for delivery of ions, neurotransmitters and other small molecules.<sup>47-49</sup> The combined high ionic and electronic mobilities are key reasons for PEDOT:PSS emerging as the champion material for devices such as OECTs.

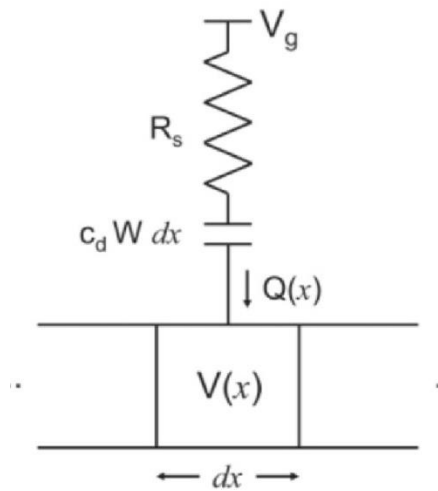


**Figure 1.3:** Ionic circuit of an OECT (c reproduced from [50], with permission from [Wiley-VCH ])

Apart from choosing the optimal materials for an OECT, it is important to understand its operating principle. Bernards and Malliaras,<sup>50</sup> have reproduced the transient behavior, the speed with which the transistor responds to external changes such as biological signals, and the steady state behavior of an OECT by modeling it as an ionic and electronic circuit (figure 1.3). The electronic circuit refers to the current flux of holes inside the channel and the changes of its magnitude upon de-doping. The ionic circuit (figure 1.3), has been modeled as a capacitor and resistor in series. For simplicity, the capacitance of the gate has been neglected. The resistor in the model refers to the ionic strength of the electrolyte and the capacitor to the amount of ions that can be stored in the bulk of the channel. The model explains the operating principle of the OECT which is affected by the interplay between the ionic and electronic currents. Thus, an understanding of the parameters that influence these properties must be taken into consideration and tuned according to the specific applications at hand. These parameters include: the material / size of the gate, the resistance of the electrolyte, and the size and geometry of the channel. Once defined, optimal parameters must be weighed with considerations such as fabrication - for

instance, micrometer scale transistors exhibit fast responses which are stable for higher frequencies, making them suitable and more specific for fast biological events (such as neuronal signaling). However, scaling down the dimensions requires somewhat complex lithographic techniques (figure 1.4a).

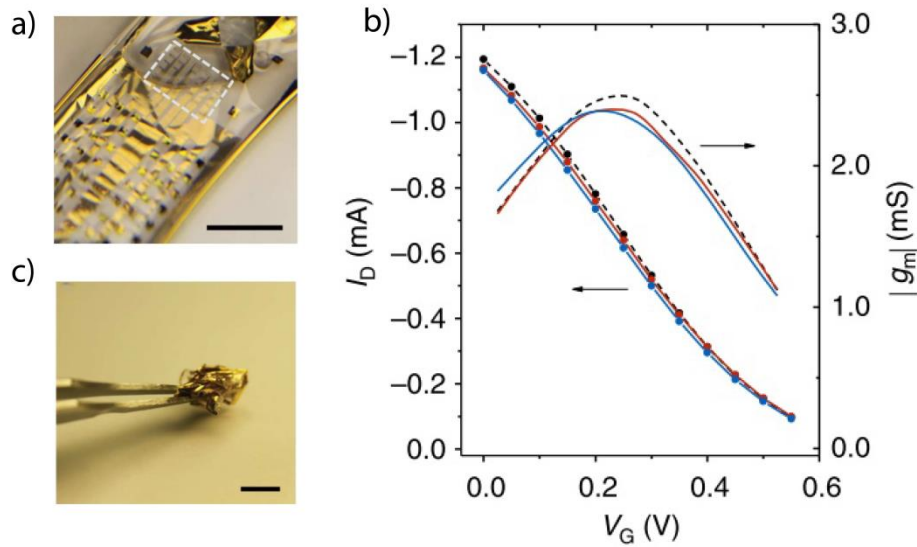


**Figure 1.4:** Robust micrometer scale, high amplification OEETs: a. an array of OEETs on a thin flexible substrate: scale bar = 1 cm b. the array is extensively crumpled c. (left axis) transfer characteristics of device before (red) and after (blue) crumpling (right axis) transconductance and time response for devices before (red) and after (blue) crumpling. (a, b, c reproduced from [7], with permission from [Nature Publishing Group])

Arguably, the most important device property of the OEET is related to its amplification properties. High amplification is a common necessity for unraveling biological information; to increase signal to noise ratio and to lower detection limits thus increasing sensitivity. For example, in electrophysiology, it is important to record brain activity that has a wide spectrum of frequencies and amplitudes. The potential difference of this activity is on the order of a few microvolts, and by taking advantage of its inherent transistor properties, OEETs can be used to locally amplify the signal.<sup>51</sup> The efficiency of the amplification can be measured by the transconductance, which is defined as  $g_m = \frac{\Delta I_d}{\Delta V_g}$ . Therefore, the higher the value of the transconductance, the better the gain. Khodagholy *et al.*,<sup>7</sup> have shown that the OEET reaches transconductance values in the miliSiemens range, outperforming traditional and other organic transistors (figure 1.4b), an impressive feat for a device fabricated with solution processed materials at room temperature. Furthermore, as shown in figure 1.4b and 1.4c, the transconductance and the time characteristics are not affected even after

extensive use and harsh manipulation. Finally, by carefully selecting and varying geometrical characteristics such as channel length, width and thickness, Rivnay *et al.*,<sup>52</sup> have engineered OECTs with peak transconductance values at zero gate voltage. This is of importance in many applications where very low voltages are required, for example when cell or lipid bilayer integrity has to be maintained over an extended period of biasing.<sup>53</sup> Moreover, omitting additional biasing facilitates simple integration with circuits and recording systems, something desirable for lab on chip applications. From the above, we see how individual properties and characteristics of an OECT may be tuned for a broad range of biological applications.

## 1.2. Applications in biology

### 1.2.1. OECTs coupled with biological moieties for sensing.

In this section work related to the coupling of OECTs with a variety of different biological molecules and macromolecules will be discussed, including ions, proteins (enzymes and antibodies), lipids and nucleic acids. These devices have been reported for applications in basic research but particularly as new alternatives for low-cost diagnostics.

### 1.2.2. OECTs as ion sensors

The electrolyte is an integral part of an OECT; variations in its ionic concentration affect the device properties. Therefore, sensing of ions, which is of great importance in healthcare diagnostics, has been possible with the OECT. Lin *et al.*,<sup>54</sup> have shown that altering the ionic concentration of an electrolyte affects its channel current ( $I_d$ ). Figure 1.5a shows a transfer curve, which is a function of the drain current with respect to the sweep of the gate voltage, for a range of concentrations of a potassium chloride (KCl) electrolyte. The transfer characteristics display the decrease in  $I_d$  with increase of the  $V_g$ , with a shift of these curves to lower values of  $V_g$  when the ionic concentration increases. This behavior can be explained by the ionic circuit in figure 1.5a; the higher the ionic concentration in the electrolyte the higher the ionic charge at the interface with PEDOT:PSS. So, the increase of the charge shifts the effective gate voltage ( $V_{g,eff}$ )

(constituting the potential drop to the channel) to higher values and in turns de-dopes the channel. Apart from changes in electrolyte concentration, changes in electrolyte composition can shift the  $V_{g,eff}$  in the OEET, a principle used by Tarabella *et al.*,<sup>55,56</sup> for sensing liposomes and micelle formation of cetyltrimethylammonium bromide (CTAB).

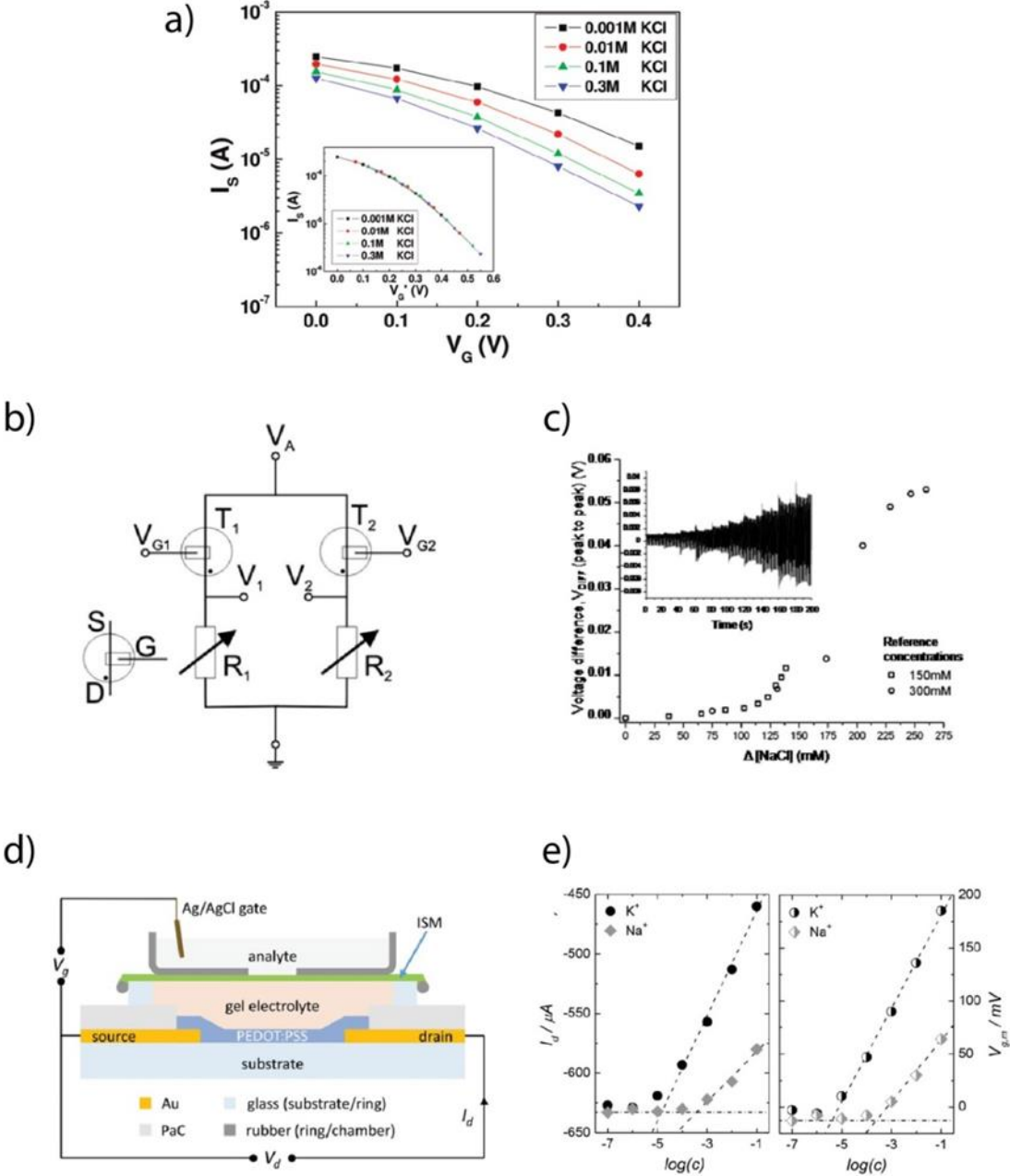


**Figure 1.5:** OEETs used as ion sensors *a.* Transfer characteristics of an OEET for different concentrations of KCl solutions ( $V_d = -0.1$  V). (reproduced from [54], with permission from [ACS Publications]). *b.* Wheatstone bridge circuit diagram. *c.* The peak-to-peak voltage difference as a function of concentration difference of NaCl solution, inset curve shows the raw data. (*b, c* reproduced from [57], with permission from [American Institute of Physics]). *d.* schematic of Ion-selective OEET. *e.* Calibration curves ( $I_d$ ,  $V_{g,m}$  vs concentration) of pure KCl and NaCl

*solutions performed using ion selective OECT (IS-OECT). (d, e reproduced from [58], with permission from [Wiley Online Library]).*

Svensson *et al.*,<sup>57</sup> have integrated OECTs in circuits for ion sensing in order to improve its sensitivity. In this case, two transistors were connected with two resistors in a Wheatstone bridge circuit configuration (figure 1.5b). After application of a small constant drain voltage the transistors operate in a resistive mode and the potential difference ( $V_{diff}$ ) between the two transistors is continuously recorded. By the additional application of a sinusoidal gate voltage of 10 Hz, a change of the resistance in the electrolyte and thus the  $V_{diff}$  can be measured. When the ionic concentration of the electrolyte in both transistors is the same, no potential difference is observed. However, by changing the concentration of the electrolyte in the second transistor, a potential difference is observed. In figure 1.5c (inset; raw data), we see how the phase of the potential between the two transistors shifts versus the concentration difference in the two electrolytes.

The importance of sensing specific ions has prompted the development of ion-selective OECT sensors (IS-OECT). Sessolo *et al.*,<sup>58</sup> as well as Mousavi *et al.*,<sup>59</sup> have combined OECTs with polymeric membranes that permit the passage of specific ions. In figure 1.5d the lay-out of an ion-selective OECT is shown. Briefly, a polyvinylchloride (PVC) based potassium-selective membrane was placed between a gel electrolyte and the electrolyte of interest, separating the channel from the gate of the OECT. By increasing the concentration of the electrolyte, a decrease in the drain current which is proportional to the  $[K^+]$  is observed. This is attributed to the increase number of  $K^+$  ions penetrating the channel and de-doping it, or to the decrease of the electrolyte resistance. Figure 1.5e shows the calibration curve of drain current and effective membrane voltage versus ion concentration for pure KCl and NaCl solutions. The sensitivity to  $K^+$  ions is an order of magnitude higher than that of  $Na^+$  ions, and this confirms the ion selectivity of the membrane. In a similar configuration, Bernards *et al.*,<sup>53</sup> have placed a lipid bilayer with and without embedded proteins, in this case bacterial gramicidin ion pores, selective for monovalent cations, as a selective membrane instead of a polymeric one. In the absence of gramicidin no  $I_d$  modulation was observed when a gate potential was applied, whereas in the presence of gramicidin channels a clear modulation was observed in the presence of gramicidin, although only in the presence of KCl, not in the presence of  $CaCl_2$ , demonstrating the selectivity of the bilayer lipid membrane. A 1V pulse was demonstrated to disrupt the bilayer membrane, underlying the importance of operation at low voltages when interfacing with biological systems.

### 1.2.3. OECTs as enzymatic sensors

One of the first applications of the OECT for interfacing with biology was as an enzymatic sensor.<sup>60</sup> The operating principle of an OECT enzymatic sensor involves either a change in a local pH upon oxidation of species or transfer of electrons to the gate of the device (figure 1.6a). By measuring changes in pH Nishizawa *et al.*, have used polypyrrole based OECTs to sense penicillin.<sup>61</sup> They immobilized the enzyme penicillinase which catalyses the turnover of penicillin to penicilloic acid, on top of the channel and upon oxidation of the penicillin to penicilloic acid; the change of the local pH increased the conductivity of the polypyrrole. A major drawback, however, is that the conductivity of polypyrrole drops in physiological conditions, creating a mismatch between the device's operational regime and the optimal physiological environment of enzymes and proteins. In contrast, by measuring electron transfer, Zhu *et al.*,<sup>62</sup> demonstrated the use of a PEDOT: PSS based OECT for glucose sensing in a wide range of pH environments. The sensing mechanism is as follows: glucose oxidase catalyzes the conversion of glucose to gluconolactone in the presence of oxygen, forming hydrogen peroxide ( $H_2O_2$ ) as a byproduct. The  $H_2O_2$  in turn transfers an electron to the gate of the OECT (figure 1.6a(i)). In order for charge neutrality to be maintained in the electrolyte, a positive ion penetrates the OECT and compensates the PSS anion (figure 1.6a(ii)), which in turn causes a shift of the  $V_{g,eff}$  and thus a decrease of the source–drain current, proportional to the glucose concentration.<sup>63</sup> Pt has been extensively used as a gate in OECT-based glucose sensors<sup>64</sup> because of its good catalytic performance for the oxidation and reduction of  $H_2O_2$  and other biomolecules of interest such as dopamine and adrenaline.<sup>65-67</sup> The sensitivity of OECT devices, after optimization, can detect levels of glucose that exist in human saliva (as low as  $8\mu M$ ), and sweat ( $\sim 150\mu M$ ), leading to non – invasive measurement systems.<sup>64</sup>

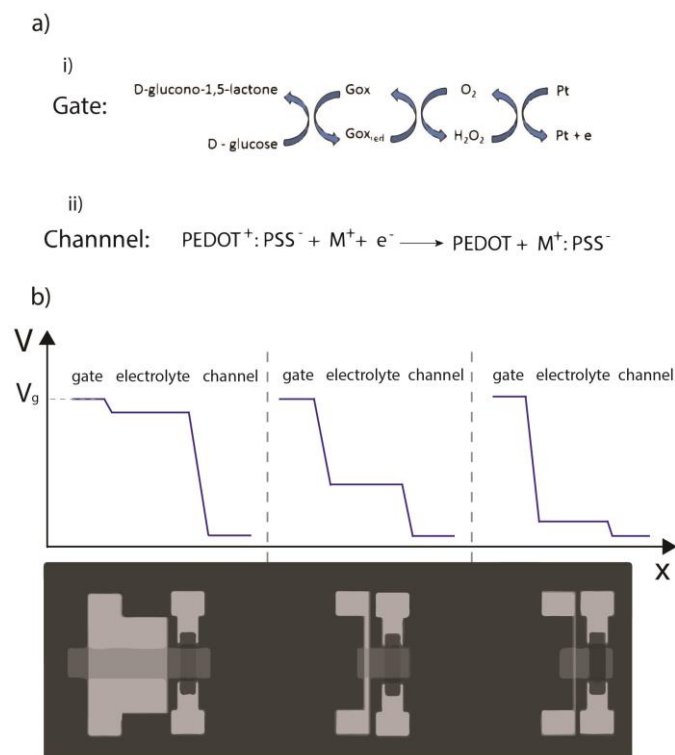


**Figure 1.6:** OECTs used as enzymatic sensors: a. i) transfer of electron from glucose to the gate through the biological reaction catalyzed by glucose oxidase ii) de-doping mechanism of PEDOT:PSS at the channel b. Drop of potential at the interfaces and its dependence on the gate/ channel size ratio. (b, is reproduced and modified from [68] with permission from [Wiley Online Library])

The geometry of an OECT-based enzymatic sensor affect its sensitivity and a systematic study has been performed by Cicoira *et al.*,<sup>68</sup> who measured the decomposition of  $\text{H}_2\text{O}_2$ , mentioned above as the byproduct of an enzymatic reaction, for devices with a constant channel area, but changing gate area (figure 1.6b). They showed that the sensitivity of the device increased as the gate size decreased. Such optimization is confirmed by modeling the behavior of the OECT and optimizing it for two types of applications: for electrochemical sensing and for ion to electron conversion.<sup>69,70</sup> This can be explained by the potential drop at the two interfaces: the gate/electrolyte and electrolyte/channel interface respectively (Figure 1.6b). Redox active molecules like  $\text{H}_2\text{O}_2$  which are produced in redox enzymatic reactions modulate the potential drop at the metal gate/electrolyte interface. In the case of a gate electrode which is much larger than the OECT channel, the potential drop vanishes at this interface as the overall electrode impedance is minimized, and electrochemical potential modulation cannot be detected. In case of smaller gate areas, the potential drop is maximized at the channel/electrolyte interface. In this situation, changes in the potential drop at the gate/electrolyte interface directly affect also the electrolyte/channel interface and thus modulate the OECT current.

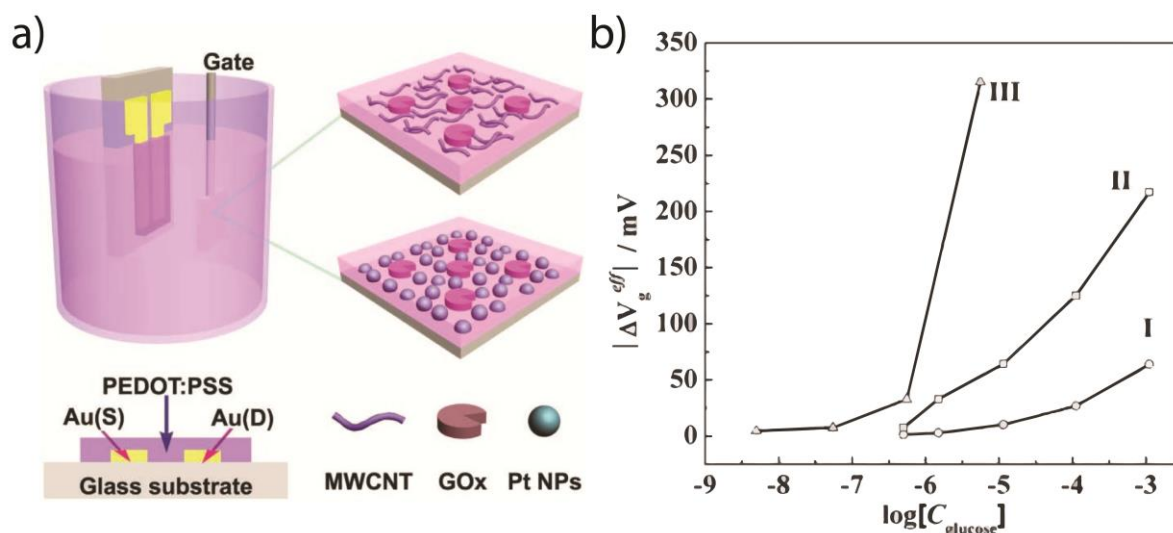


**Figure 1.7:** Schematic layout of an OEET glucose sensor with the gate modified with Pt - NPs, MWCTS and GOx d. the dependence of  $\Delta V_{g,eff}$  as a function of  $\log[C_{\text{glucose}}]$  for CHIT/GOx/Pt (line I), MWCNT-CHIT/GOx/Pt (line II) and CHIT/GOx/Pt-NPs/Pt (line III) gate electrodes. (c, d are reproduced from [71] with permission from [Wiley – VCH]).

The inherent amplification afforded by the OEET coupled with the optimization of the geometrical characteristics have resulted in highly sensitive enzymatic sensors. However, further modification of the gate with novel materials, such as Pt nanoparticles, has pushed the limit of detection to the nanomolar range. Tang *et al.*,<sup>71</sup> modified a Pt gate with Pt nanoparticles (Pt - NPs) and carbon nanotubes (figure 1.7a). Moreover, the enzyme was entrapped on the gate by a chitosan membrane. Owing to their high electrocatalytic activity and the high surface to volume ratio, the Pt - NP modified gate showed an increased sensitivity compared to the pristine Pt gate and the gate modified with carbon nanotubes, and increased the limit of detection for glucose to 10 nM (figure 1.7b). By using the same concept, Liao *et al.*,<sup>72</sup> used graphene and reduced graphene oxide flakes at the gate and pushed the sensitivity to a similar range while simultaneously improving the selectivity of sensing by adding a Nafion membrane. Negatively charged acids, such as ascorbic acid and uric acid commonly found in biological media, create interference in the measurements by direct oxidation at the gate. However, the use of a Nafion membrane or chitosan functionalization can repel and attract respectively these species while the neutral hydrogen peroxide can diffuse to the gate unimpeded. Finally, Kergoat *et al.*,<sup>73</sup> have blended Pt nanoparticles with PEDOT:PSS. By using the modified PEDOT:PSS:Pt-NPs, they have successfully fabricated OEETs in order to sense glutamate and acetylcholine, which are important neurotransmitters.

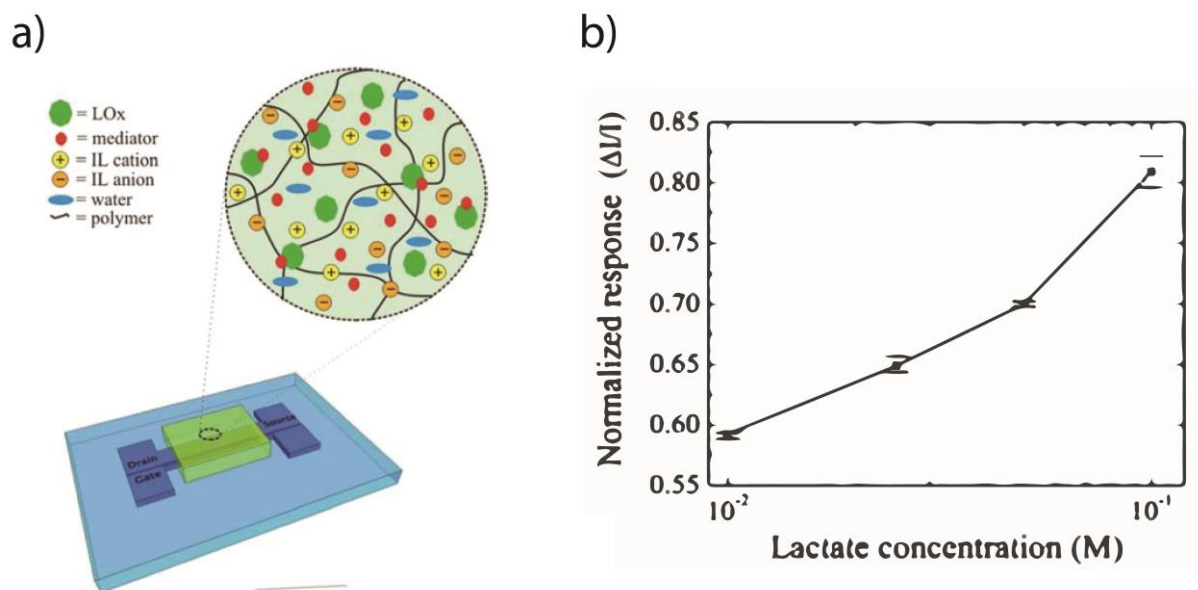


**Figure 1.8:** Schematic layout of an OECT lactate sensor with solid state ionogel electrolyte. *f.* normalized response of the OECT vs. lactate concentration. (a, b are reproduced from [74] with permission from [RSC Publishing]).

Apart from high sensitivity, the need for low cost and stable biosensors requires the use of alternative materials and simple fabrication techniques. Towards that goal, Shim *et al.*,<sup>22</sup> developed an all-PEDOT OECT for glucose sensing. PEDOT:PSS, however, exhibits low catalytic properties for the oxidation of  $H_2O_2$ . Therefore, owing to its low redox potential, ferrocene has been used as a mediator for the transfer of electrons to the gate. This facilitates a single step fabrication of low cost OECT based enzymatic sensors. Yang *et al.*,<sup>23</sup> have successfully demonstrated an all plastic OECT glucose sensor using room temperature ionic liquids (RTILs) as an electrolyte, thus solving issues related to long term stability of the OECTs for use in biosensing. Liquid electrolytes are unstable for long term applications, since they are susceptible to evaporation, and thus destabilization of ionic concentration. RTILs, molten salts at room temperature, have gained significant attention in electrochemistry as alternatives to aqueous electrolytes.<sup>75</sup> This is due to their desired characteristics, such as wide electrochemical window of operation, high ionic strength, low or zero evaporation rates, and for biological applications, stabilization of enzyme, conformation and function. For this application, Yang and co-workers dissolved both the mediator and the enzyme in the RTIL and drop casted on top of a hydrophobic virtual well. The glucose sensor showed sensitivities in the micromolar range. Subsequently, Khodagholy *et al.*,<sup>74</sup> combining ionic liquids with cross linkable polymers, developed an OECT lactate sensor integrated with a solid state electrolyte. The ionic liquid gel electrolyte included lactate oxidase and the ferrocene mediator for sensing, RTIL for its high ionic conductivity and for the stabilization of enzyme's conformation, and photo-cross-linkable monomer and photo-initiator for creating the solid state electrolyte

(figure 1.8a). Drop-casting and subsequent polymerization under UV resulted in a gel-like electrolyte. Figure 1.8b shows the normalized response of the OECT for a concentration range of lactate that exists in human sweat. This type of device was proposed as a wearable long term sensor for continuous monitoring of lactate levels in athletes. Finally, OECTs have been integrated with microfluidics for the fabrication of multi-analyte sensors: Yang *et al.*,<sup>26</sup> demonstrated surface directed microfluidic that uses capillarity forces to drive a sample consisting of glucose and lactate to an array of OECTs for simultaneous measurement of glucose and lactate.

#### 1.2.4. OECTs as Immunosensors / nucleotide sensors

OECTs can detect the presence of cells and biomolecules. Specifically, when a cell is in the proximity of an OECT channel, its membrane is polarized, resulting in an additional potential. The cause for the polarization of the cell is the potential difference between the channel and cell.<sup>76</sup> This additional potential shifts the effective gate voltage to lower values affecting the de-doping of the channel. Using this principle, He *et al.*,<sup>77</sup> have fabricated an OECT that detects the presence of the pathogenic bacteria *E. coli*. In more detail, an immobilization step of the anti-*E. Coli* antibody took place through biofunctionalization of the OECT channel (figure 1.9a). The *E. coli* bacteria were then captured through antibody antigen interactions. When the bacteria are in a low ionic concentration media, they exhibit a negative charge in their membrane, thus immobilized bacteria on top of the OECT channel form a negatively charged layer. Consequently, upon application of a gate voltage the negatively charged layer of bacteria attracts positive ions in the electrolyte, resulting in a shift of the  $V_{g,eff}$  to lower values (logarithmically proportional to the concentration), which means that fewer ions are de-doping the channel or a higher voltage has to be applied in order to de-dope the same magnitude of current in the absence of bacteria (figure 1.9b). The sensitivity of the device depends additionally on the ionic strength of the electrolyte, showing increasing sensitivity when the concentration of the electrolyte decreases.<sup>12</sup> This can limit the performance of the sensor in high ionic electrolytes. Similarly, Kim *et al.*,<sup>78</sup> fabricated an OECT based immunosensor for prostate specific antigen (PSA), by immobilizing a PSA specific antibody on the channel. The shift of the  $V_{g,eff}$  to the channel is proportional to the captured PSA antigen concentration. A secondary antibody conjugated with Au nanoparticles was then used in a typical sandwich-ELISA format, thereby resulting in an increased sensitivity, mostly likely due to the fact that Au-NPs are negatively charged in suspension.

Finally, an OECT DNA sensor has been developed by Lin *et al.*<sup>79</sup> Figure 1.9c shows the layout of the device, which consists of an OECT with integrated microfluidics on top of a flexible polyethylene terephthalate (PET) substrate. Single stranded DNA was immobilized on the gate, with a second gate was used as a control. Figure 1.9d shows a transfer curve, in which the gate voltage needed to de-dope the channel shifts to higher values after immobilization and hybridization of the complementary DNA strand. The mechanism of sensing is as described above; owing to its charge, the DNA affects the capacitance at the interface between gate and electrolyte, and thus shifts  $V_{g,eff}$ . A similar mechanism was also shown by Liao *et al.*, for the detection of diatoms, a type of algae found in sea water.<sup>80</sup> An interesting observation was that PEDOT:PSS appeared to promote diatom growth when compared with simple glass slides.

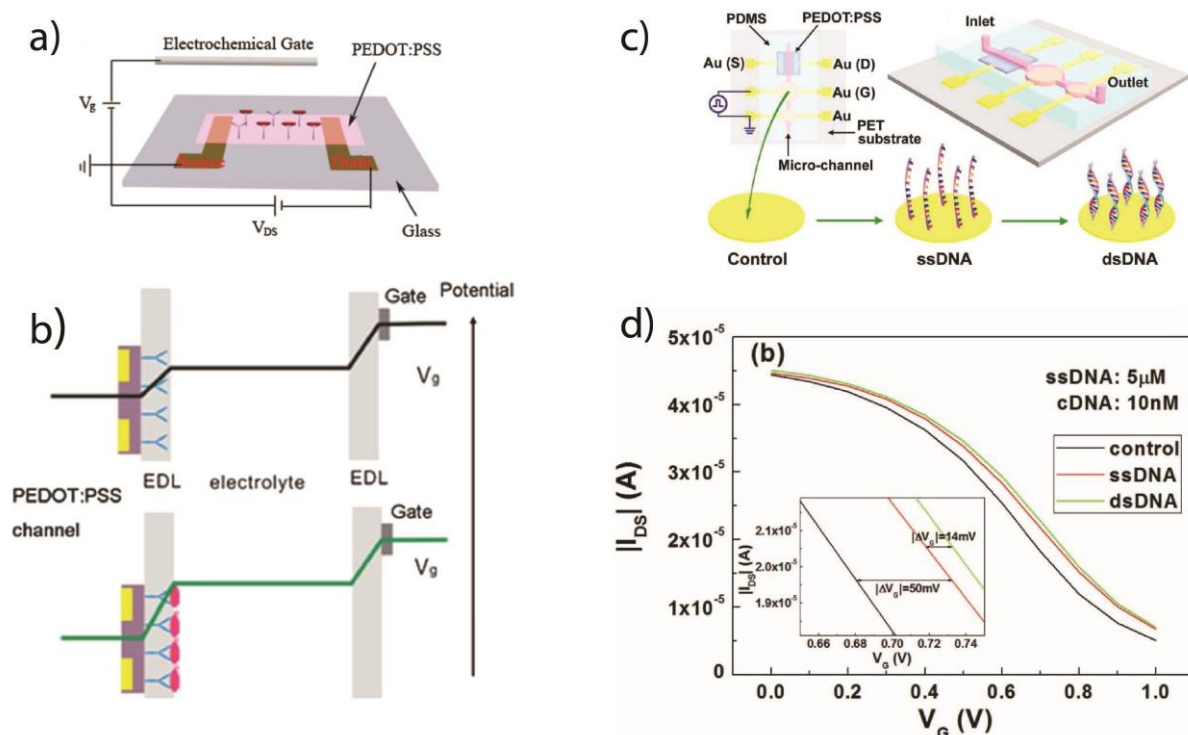


**Figure 1.9:** OECTs as Immunosensors and nucleotide sensors: a. Schematic of an *E. coli* O157:H7 sensor based on an OECT. b. Schematic diagram of potential drops in the electric double layers (EDL), including the channel/electrolyte and electrolyte/gate interfaces, in the OECT before and after the immobilization of *E. coli* O157:H7 on the PEDOT:PSS surface. (a, b, reproduced from [77], with permission from [RSC Publishing]) c. Schematic of an OECT integrated in a flexible microfluidic system, which is characterized before and after the modification and the hybridization of DNA on the surface of Au gate electrode. d. Transfer characteristics of OECTs measured in microfluidic channels before and after the immobilization and the hybridization of DNA on Au gate electrodes.  $V_{ds} =$

– 0.1 V. The inset shows the horizontal shifts of the transfer curves. (c, d, reproduced from [79], with permission from [Wiley Online Library])

### **1.3. OECT coupled with whole cells for electrophysiology**

In this section, work related to the coupling of OECTs with live mammalian cells will be discussed, rather than individual biomolecules or macromolecules as in the previous section. This section has been split into two subsections; integration with non-electrogenic cells for monitoring toxicology/diagnostics, and, integration with electrogenic cells such as cardiomyocytes and neurons. In the former case, the OECT is used to measure a ‘passive’ electrical property of the cells, whereas in the latter, the OECT is measuring active electrical properties of the cells, with applications both *in vitro* for toxicology/diagnostics, but also *in vivo* for potential therapeutics.

#### **1.3.1. Integration of OECTs with non-electrogenic cells**

The first report of OECTs with live mammalian cells was by Bolin *et al.*<sup>81</sup> MDCK (Madin Darby canine kidney) epithelial cells were seeded along the channel of an OECT and the device was used to bias the channel such that an electrochemical gradient was produced. Depending on the redox potential of discrete areas of the channel, differential cell adhesion was observed, illustrating the potential for conducting polymers with electrically tuneable surface properties in controlling adhesion of cells. A non-trivial issue associated with this work was the demonstration by the authors that live cells grow and proliferate on conducting polymer devices, indicating the biocompatibility of the materials used. Long term stability of these devices in cell culture media has also been demonstrated.<sup>21</sup> Subsequent integration of OECTs with live cells have focused on the sensitivity of the devices to changes in biological ion flux, a parameter which can be used for monitoring the integrity of mammalian cells, as the flow of ions is tightly regulated in tissues and dysregulation is often a sign of disease or dysfunction. In particular, OECTs have been used as an alternative technology for sensing barrier tissue integrity, monitoring variations in paracellular ion flux with state-of-the-art temporal resolution and high sensitivity. Barrier tissue is composed of epithelial or specialized endothelial cells whose role is to modulate ion flux between different bodily compartments. As this role is often compromised during

toxic events, monitoring of this tissue is very interesting for diagnostics/toxicology. In a first instance, Jimison *et al.*,<sup>82</sup> integrated epithelial cells grown on filter supports with the OECT, using a model of the gastrointestinal tract Caco-2 cell line which is established as a barrier tissue model (figure 1.10a). This configuration is compatible with existing barrier tissue characterization and toxicology methods and protocols which frequently use filter supports as they mimic the polarized nature of the cells *in vivo* where they separate different functional compartments (e.g. gastrointestinal tract from blood stream). The OECT ionic circuit on the addition of barrier tissue is shown schematically in figure 1.10b, with the cell layer represented as a resistor and capacitor in parallel. In this way, the OECT uses the ionic to electronic transduction to measure changes in the impedance of the ionic circuit. Application of a positive gate voltage  $V_g$  leads cations from the electrolyte, in this case cell culture media, into the conducting polymer channel thus de-doping it. The transient response, which gives the time of how fast the channel will be dedoped, can be quantified by the time constant ( $\tau = RC$ ). The  $\tau$  depends on the capacitance of the channel and the resistance of the electrolyte. The presence of the barrier tissue modifies the ionic flux, due to the addition of additional capacitor and resistor (figure 1.10b) and the drain current by inducing a slow response thus increase in the  $\tau$ .<sup>43</sup>

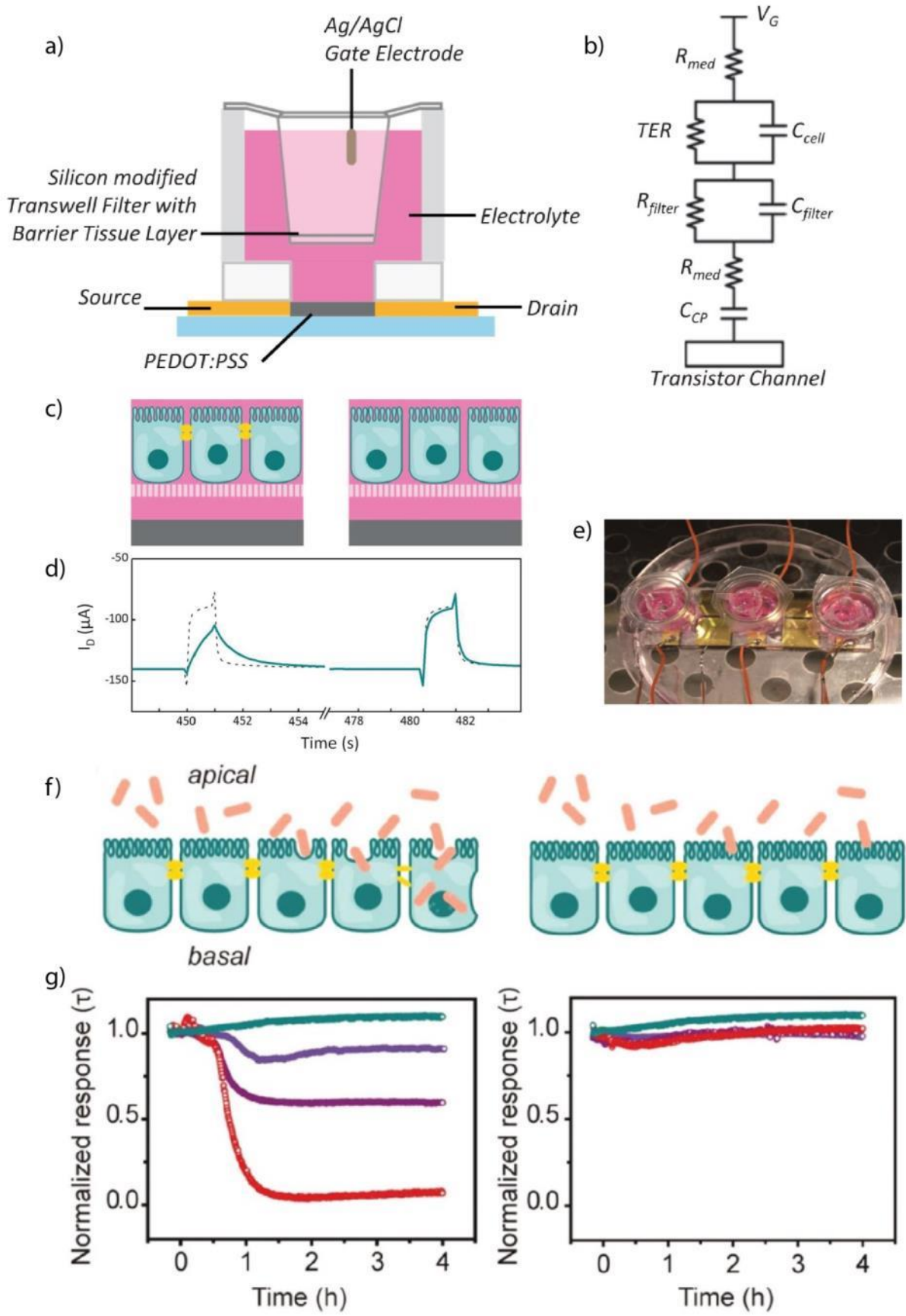


**Figure 1.10:** Barrier tissue integrity monitored with an OECT: a. layout of an OECT with an integrated barrier tissue b. equivalent circuit describing ionic

transport between gate electrode and transistor channel.  $TER$  refers to the transepithelial resistance of the cell layer,  $C_{cell}$  refers to the capacitance of the cell layer,  $R_{filter}$  and  $C_{filter}$  refer to the resistance and capacitance of the porous filter, respectively.  $R_{med}$  refers to the resistance of the media, and  $C_{cp}$  refers to the capacitance at the CP and electrolyte layer *c.* cartoon showing polarized Caco-2 cells with tight junctions (left) and without (right), sitting on a porous cell culture membrane, above a PEDOT:PSS transistor channel. Tight junctions are shown in yellow. *d.* OECT  $I_d$  transient response with cells before (left) and after (right) the addition of 100 mM  $H_2O_2$ , (solid lines). OECT  $I_d$  response in the absence of cells is overlaid (dashed lines) (*a, b, c, d*, reproduced from [82], with permission from [Wiley Online Library]) *e.* Picture of the multiplex device shown on a Petri dish inside the cell-culture incubator. The cell culture insert is shown suspended in the plastic holder affixed to the glass slide. The Ag/AgCl gate electrode is shown immersed in the apical media, while source and drain cables are attached to their respective positions on the glass slide *f.* cartoon illustrating infection with wildtype (WT) (left) and non-invasive *S. typhimurium* (right). *g.* mean normalized response ( $\tau$ ) of the OECT in the presence of WT (left) and non-invasive *S. typhimurium* (right) at different MOI over 4 h, bacteria were added at  $t = 0$ . Non-infected represents OECT + cells with no added bacteria. Non-infected cells are in cyan, MOI: 10 in blue, MOI: 100 in purple, and MOI: 1000 in red. (*e, f, g*, reproduced from [83], with permission from [Wiley Online Library])

The disruption of barrier tissue (illustrated schematically in figure 1.10c), related to the destruction of protein complexes between the cells, was also demonstrated upon addition of hydrogen peroxide ( $H_2O_2$ ), a known oxidant. Figure 1.10d illustrates the high temporal resolution of the OECT in monitoring barrier tissue disruption, from one pulse to the next. Monitoring of the  $I_d$  response to the gate voltage was normalized as a function of time in the presence of both  $H_2O_2$  and a second toxin, ethanol, and shown to have greater sensitivity than traditional methods. The effect of EGTA (Ethylene glycol-bis(beta-aminoethyl ether)-N,N,N',N'-tetra acetic acid) known to affect paracellular ion transport pathways and trans epithelial resistance of cells has also been demonstrated with the OECT.<sup>84</sup> Dose dependent responses to addition of EGTA were detected and validated against existing commercially available electrical impedance spectroscopy shown significant advantages of the OECT in terms of temporal resolution. A visual demonstration of the OECT fabrication and operation for monitoring barrier tissue disruption by EGTA has also been reported.<sup>83</sup>

For non-acute diagnostics applications, where time scales for readouts exceed minutes and may actually extend to days or even weeks, not only the stability of the sensor, but also the environmental conditions for measurement must be respected. To test the stability of the OECT and assess suitability for long term measurements of an OECT, Tria *et al.*, transitioned the device to a format

compatible with operation in physiological conditions, and to cope with the many varying parameters inherent to biological systems, the number of devices operated simultaneously was scaled-up (figure 1.10e).<sup>85</sup> This system was used to successfully monitor the kinetics of integrity of the same gastrointestinal model after infection with the pathogenic organism *Salmonella typhimurium* (illustrated in figure 1.10f), while a non-pathogenic *Salmonella* bacterium showed no response regardless of the concentration added (figure 1.10g). The experiment was also carried out in milk, a complex matrix containing many different compounds including proteins and fats; the OECT operation and detection of *Salmonella typhimurium* remained robust, unlike a leading commercially available alternative based on electrical impedance scanning using stainless steel electrodes.

OECTs show promise for applications requiring rapid and dynamic detection of variations in ion flow. The examples cited up until now have involved integration of the cells on a filter, physically separated from the device by the electrolyte, using a top-gate format. Another approach to measure the integrity of cells is to seed the cells directly on device, either with a top-gate format, or with a side-gate. This former principle was used by Lin *et al.*, and the device was shown to detect cell attachment and cell detachment by shifting the  $V_{g, eff}$  values, via a mechanism similar to that used by Yan and co-authors for detecting antibody/DNA binding.<sup>86</sup> Again, the stable operation of the OECT in cell culture medium was confirmed, as well as the ability to support cell growth, in this case two cell lines: human esophageal squamous epithelial cancer cells and fibroblasts. In a similar configuration, Yao *et al.*,<sup>87</sup> show the integration of human airway epithelial cells with the OECT. Cells were seeded directly on an OECT array and the cells directly above the PEDOT:PSS channel were postulated to be suspended over the channel with a gap formed below (figure 1.11a). The authors investigated the dose response of transepithelial ion transport to forskolin, an agonist which causes opening of the CFTR (cystic fibrosis transmembrane conductance regulator) channel (figure 1.11b), a major contributor to transcellular ion transport. The transport of  $\text{Na}^+$  ions from the basolateral compartment to the apical compartment resulted in a change in the channel current, which the authors converted to an effective gate voltage change. Ramuz *et al.*, combined optical and electronic sensing of epithelial cells using OECTs with both the gate and the channel in the same plane, both consisting of PEDOT:PSS.<sup>88</sup> This circumvents an issue for long-term operation of devices using Ag/AgCl electrodes which were demonstrated to be toxic to live cells for periods > 10 hours.<sup>85</sup> MDCK I cells were seeded directly over an area comprising both the channel and the gate. The authors demonstrated the possibility for continuous measurements of ion flow in epithelial cells coupled with optical imaging of the cell layer on the device, due to the transparent nature of the PEDOT:PSS film

(figure 1.11c). Further, the measured electrical signal is demonstrated to be due to tight junction-related barrier tissue formation and not due to simple cell coverage as the presence of cells on the active area of the OECT does not change the transistor response to gate pulse voltage unless the cells present barrier tissue properties. A corollary of this work is that high resolution imaging of cells is possible on PEDOT:PSS films, not only in bright field mode, but also for fluorescence imaging (figure 1.11d) and is highly valuable for definition of molecular mechanisms in biological systems.

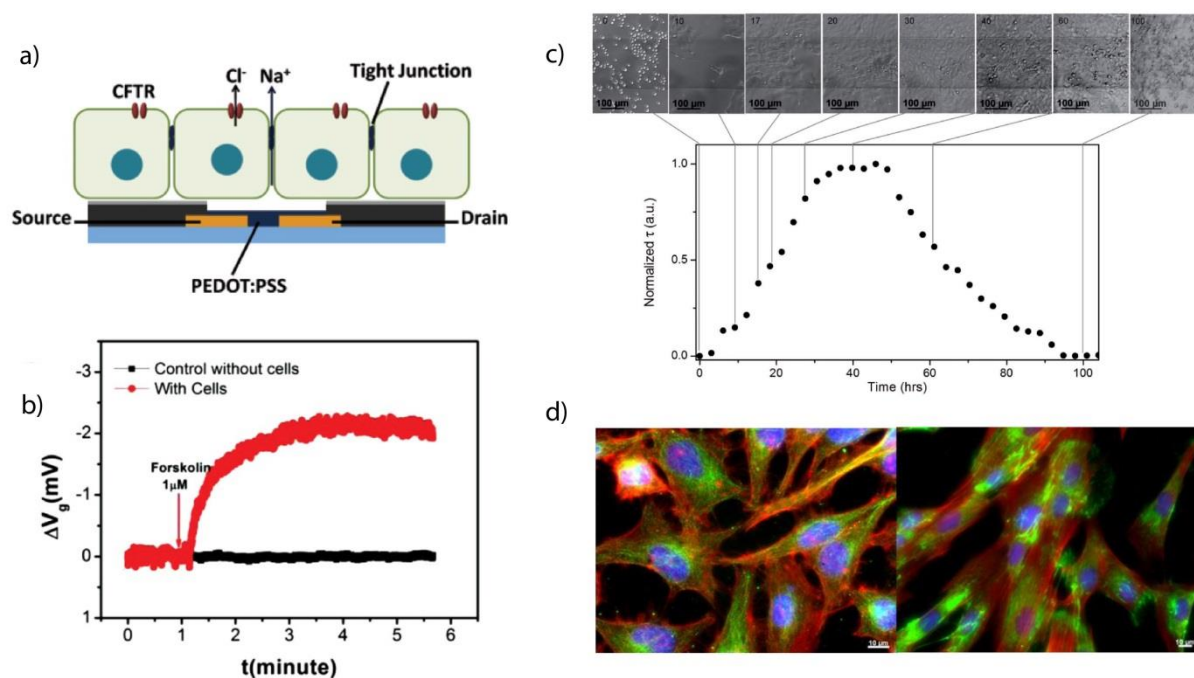


**Figure 1.11:** Non electrogenic cells in direct contact with OECTs: a. illustration of polarized Calu-3 cells with tight junction sitting on the PEDOT:PSS transistor channel of an OECT b. In situ OECT response with (red) and without (black) Calu-3 cells upon the addition of 1  $\mu$ M CFTR agonist forskolin. Transistor channel current change was converted to effective gate voltage change. (a, b reproduced from [87], with permission from [Wiley Online Library]). c. Micro-optical images of MDCK-I on top of the OECT channel area (the darker horizontal line in the middle of the picture corresponds to the PEDOT:PSS channel) and corresponding electrical characteristics with a measurement taken every 3h. d. Illustrative example of high resolution fluorescence imaging possible on PEDOT:PSS devices. HeLa cells (left) and immortalized human fibroblasts (right) (c, d, reproduced from [88], with permission from [Wiley Online Library]).

### 1.3.2. OECT for stimulation and recording of electrogenic cells

Electrical stimulation and recording of nerve tissue and neural activity have provided valuable information about physiological and pathological functions of the body and brain. Typically, these recordings are performed with metal electrodes.<sup>89</sup> For example, the main technique to record cardiac activity, electrocardiography (ECG), uses electrodes in contact with the skin which provide information about the normal function or abnormalities of the heart. OECTs include advantages that can overcome many limitations in electrophysiology. First of all, the low temperature fabrication of OECTs enables devices on flexible, biocompatible, and biodegradable substrates. Campana *et al.*,<sup>90</sup> fabricated OECTs on flexible, resorbable poly(L-lactide-co-glycolide) substrates for ECG recordings. Figure 1.12a shows the layout of the measurements and the raw signal compared to the theoretical heart pulse. In this work, the gate of the OECT was placed directly on skin close to the heart at a constant positive potential ( $V_g = 0.5 \text{ V}$ ) relative to the ground potential of the body, while the transistor channel was placed on the forearm at a negative potential ( $V_d = -0.3 \text{ V}$ ) relative to the ground. Every heartbeat creates an additional potential which modulates the  $V_{g,eff}$  seen by the channel and result in a clear de-doping of the channel. Conductive gels are usually used as an interface between the skin and channel in order to increase the adhesion for long-term measurements. Figure 1.12b shows how the fabrication of the device on a flexible substrate improves the contact with the skin which is desirable for recordings of freely moving subjects. Furthermore, the use of biodegradable materials can push to implantable devices that can be used for recording or stimulating electrogenic cells.

For the brain, there are three main electrophysiology recording techniques: electroencephalography (EEG) which utilizes electrodes in contact with the skin, electrocorticography (ECoG) which utilizes electrodes in contact with the surface of the brain, and stereoelectroencephalography (SEEG) which utilizes probes that penetrate deep in the brain.<sup>91</sup> Depending on the nature of the signal of interest, or the size of the neural population to be interrogated, or the invasiveness / goal of the measurement, EEG, ECG or SEEG may be selected. Most of the electrodes currently used are relatively inflexible, anchored in the skull, and do not follow the movements of the brain. Moreover, the recording quality usually deteriorates over time, due to the tissue injury and reaction of the immune system to the electrode.<sup>92</sup> A primary challenge is to form a good contact with the brain. This can

be achieved by using flexible electrodes that conform to the shape of the brain surface.<sup>28</sup> Other requirements are to obtain high quality and stable overtime recordings, *i.e* through the use of more biocompatible materials, and of course amplification of neuronal signals necessary to detect low magnitude signals of interest. As a proof of concept, Khodagholy *et al.*,<sup>51</sup> demonstrated implantable OEETs for ECoG recordings. A conformal device, consisting of integrated electrodes and OEETs array, was placed on the surface of the brain of an epileptic rat (figure 1.12c). The dimensions of the devices are on the order of few micrometers, fabricated on top of a 2  $\mu\text{m}$  polymer substrate. Figure 1.12d shows that the signal to noise ratio of the organic electrochemical transistor was far superior compared to the electrodes. Furthermore, the OEET could record low amplitude signals and fast signals from the interior of the brain that the electrodes were unable to detect, hitherto only recordable by depth probes (SEEG). Finally, a recent publication has demonstrated the use of an OEET to monitor cardiac rhythm, eye movement, and brain activity in a human volunteer (figure 1.12e-f).<sup>93</sup> The device showed a high transconductance operation at low gate voltage, which simplified the wiring, as it necessitated only one power supply to bias the drain.

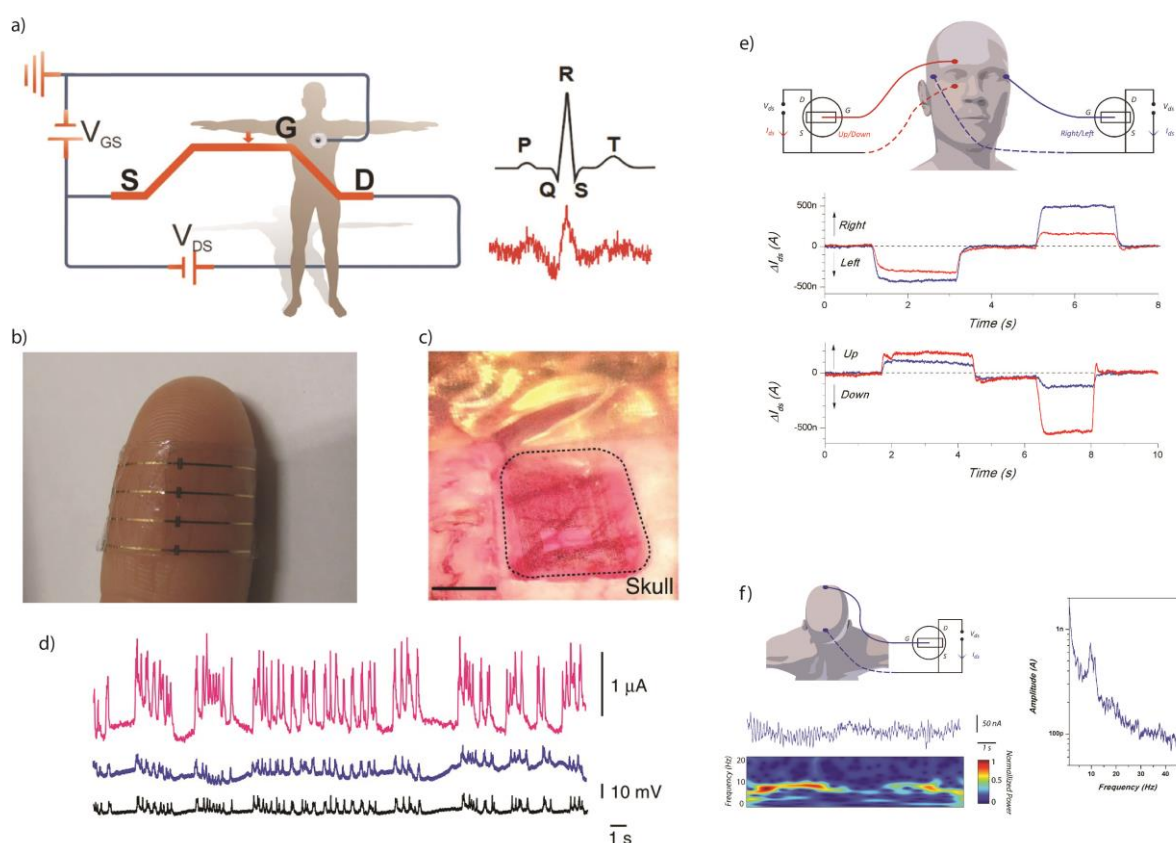


**Figure 1.12:** OEETs for measuring electrogenic cells: a. ECG recording with an OEET operated in direct contact with the skin. b. Photograph of the device showing its transparency and adaptability when attached to human skin. (a, b,

reproduced from [90], with permission from [Wiley Online Library]) c. Optical micrograph of the ECoG probe placed over the somatosensory cortex, with the craniotomy surrounded by dashed lines. Scale bar, 1mm d. Recordings from an OECT (pink), a PEDOT:PSS surface electrode (blue) and an Ir-penetrating electrode (black). The transistor was biased with  $V_d = -0.4$  V and  $V_g = 0.3$  V, and the scale of 10mV is for both surface and penetrating electrodes. Note the superior SNR of the OECT as compared with the surface electrode. (c, d, reproduced from [51], with permission from [Nature Publishing Group]). e. Wiring configuration chosen for the EOG measurement, recording of electrical activity during left/ right eyeball movements, recording of electrical activity during up/down eyeball movements. Both up/ down (red) and left/ right (blue) activities are measured. f. Wiring configuration used for the EEG measurement, along with recording of spontaneous brain activity (top) showing the alpha rhythm, and associated time-frequency spectrogram (bottom), Fourier analysis of a 3min recording. (e, f, reproduced from [93], with permission from [Wiley – VCH])

## 1.4. Conclusions

Bioelectronics is a growing interdisciplinary field which aims to interface electronics and biology, improving current biomedical tools. The particular niche for *organic* electronic materials in integration with biological materials or use in biomedical applications comes from a host of beneficial properties unique to these materials in contrast to traditional electronic materials. The underlying notion of amplification, a pre-requisite in biosensing, pushes towards active devices (transistors) rather than passive devices (electrodes). The organic electrochemical transistor lies at the heart of this field principally because of the intimate nature of the interface with biological components, where the biological milieu comprises an integral part of the device, and ions from this milieu are the key to the operation mechanism of the OECT. Improved signal transduction and amplification are common themes in the research cited above, demonstrated repeatedly for the OECT in a wide variety of formats and applications. Stability is a highly valued characteristic for biosensing, and the OECT has been shown to operate stably in a variety of different electrolytes, include complex cell media, seawater and even milk. Long term operation in these electrolytes on the scale of days to weeks has also been possible.

The OECT is a current to voltage transducer; small changes at the input ( $\Delta V_{g,eff}$ ) result in big changes at the output ( $\Delta I_d$ ). OECTs exhibit high transconductance values, essentially high gain, and by tuning the geometry and the size of the channel, the transconductance and the time response can be optimized. Different modes of operation depend on how the effective gate voltage ( $V_{g,eff}$ ) shifts. For

example, the  $V_{g,eff}$  can be modulated by changes in the resistance of the electrolyte, charge transfer to the gate, or sensing of an additional external  $\Delta V_g$  signal. Using this principle, OECTs have been used as ion-sensors, enzymatic sensors, DNA sensors, immunosensors, and pathogen sensors. Further, OECTs have been integrated with individual cells, tissues, and even whole organs. Application dependent tuning is a very important benefit of the use of conducting polymers, which are amenable to chemical modification, biofunctionalisation, and fabrication using a wide variety of techniques on different substrates. Compatibility with photolithographical techniques also facilitates fabrication of micron-scale devices, particularly interesting for monitoring of cells *in vitro* and *in vivo*, as well as for high-throughput device arrays.

Although considerable progress has been made in the past decade on the development of OECTs for biological applications, numerous challenges remain. These include the development and implementation of novel active materials (conducting polymers) with improved properties in terms of conductivity, stability, patterning, resorbability etc. Another significant challenge lies in the fabrication of circuits for integrating sensors with multiplex miniaturized arrays, as well as integration of circuits that will potentially power, record, and transmit the recordings. Future applications for OECTs are expected to further exploit the beneficial properties of these devices, with significant potential in tissue engineering for *in vivo* applications. However, more challenges are to be addressed such as integration of sensor-OECTs with measurement systems as well as further improving stability of the biological elements such as enzymes. Although, the first wave of industrial prototypes in the biomedical arena is anticipated imminently.

## 1.5. References

1. Berggren, M., and Richter-Dahlfors, A. (2007) Organic bioelectronics, *Adv. Mater.* **19**, 3201-3213.
2. Svennersten, K., Larsson, K. C., Berggren, M., and Richter-Dahlfors, A. (2011) Organic bioelectronics in nanomedicine, *Biochimica et biophysica acta* **1810**, 276-285.
3. Owens, R., Kjall, P., Richter-Dahlfors, A., and Cicoira, F. (2013) Organic bioelectronics - novel applications in biomedicine. Preface, *Biochimica et biophysica acta* **1830**, 4283-4285.
4. Owens, R. M., and Malliaras, G. G. (2010) Organic Electronics at the Interface with Biology, *MRS Bulletin* **35**, 449-456.
5. Buzsáki, G., Anastassiou, C. A., and Koch, C. (2012) The origin of extracellular fields and currents — EEG, ECoG, LFP and spikes, *Nat Rev Neurosci* **13**, 407-420.

6. Rivnay, J., and Malliaras, G. G. (2013) The Rise of Organic Bioelectronics.
7. Khodagholy, D., Rivnay, J., Sessolo, M., Gurfinkel, M., Leleux, P., Jimison, L. H., Stavriniidou, E., Herve, T., Sanaur, S., Owens, R. M., and Malliaras, G. G. (2013) High transconductance organic electrochemical transistors, *Nature communications* 4, 2133-2133.
8. Bernardis, D. a., and Malliaras, G. G. (2007) Steady-State and Transient Behavior of Organic Electrochemical Transistors, *Advanced Functional Materials* 17, 3538-3544.
9. White, H. S., Kittlesen, G. P., and Wrighton, M. S. (1984) Chemical Derivatization of an Array of Three Gold Microelectrodes with Polypyrrole: Fabrication of a Molecule-Based Transistor, 5375-5377.
10. Kim, S. H., Hong, K., Xie, W., Lee, K. H., Zhang, S., Lodge, T. P., and Frisbie, C. D. (2013) Electrolyte-gated transistors for organic and printed electronics, *Advanced materials (Deerfield Beach, Fla.)* 25, 1822-1846.
11. Crone, B., Dodabalapur, a., Gelperin, a., Torsi, L., Katz, H. E., Lovinger, a. J., and Bao, Z. (2001) Electronic sensing of vapors with organic transistors, *Applied Physics Letters* 78, 2229-2229.
12. Magliulo, M., Mallardi, A., Mulla, M. Y., Cotrone, S., Pistillo, B. R., Favia, P., Vikholm-Lundin, I., Palazzo, G., and Torsi, L. (2013) Electrolyte-gated organic field-effect transistor sensors based on supported biotinylated phospholipid bilayer, *Advanced materials (Deerfield Beach, Fla.)* 25, 2090-2094.
13. Hammock, M. L., Knopfmacher, O., Naab, B. D., Tok, J. B. H., and Bao, Z. (2013) Investigation of Protein Detection Parameters Using Nanofunctionalized Organic Field-Effect Transistors, *ACS Nano* 7, 3970-3980.
14. Torsi, L., Magliulo, M., Manoli, K., and Palazzo, G. (2013) Organic field-effect transistor sensors: a tutorial review, *Chemical Society Reviews* 42, 8612-8628.
15. Kergoat, L., Piro, B., Berggren, M., Horowitz, G., and Pham, M.-C. (2012) Advances in organic transistor-based biosensors: from organic electrochemical transistors to electrolyte-gated organic field-effect transistors, *Analytical and bioanalytical chemistry* 402, 1813-1826.
16. Blaudeck, T., Ersman, P. A., Sandberg, M., Heinz, S., Laiho, A., Liu, J., Engquist, I., Berggren, M., and Baumann, R. R. (2012) Simplified Large-Area Manufacturing of Organic Electrochemical Transistors Combining Printing and a Self-Aligning Laser Ablation Step, *Advanced Functional Materials* 22, 2939-2948.
17. Basiricò, L., Cosseddu, P., Fraboni, B., and Bonfiglio, A. (2011) Inkjet printing of transparent, flexible, organic transistors, *Thin Solid Films* 520, 1291-1294.
18. Basiricò, L., Cosseddu, P., Scidà, A., Fraboni, B., Malliaras, G. G., and Bonfiglio, A. (2012) Electrical characteristics of ink-jet printed, all-polymer electrochemical transistors, *Organic Electronics* 13, 244-248.
19. Kaihovirta, N., Mäkelä, T., He, X., Wikman, C.-j., Wilén, C.-e., and Österbacka, R. (2010) Printed all-polymer electrochemical transistors on patterned ion conducting membranes, *Organic Electronics* 11, 1207-1211.

20. Nilsson, D., Kugler, T., Svensson, P.-o., and Berggren, M. (2002) An all-organic sensor  $\pm$  transistor based on a novel electrochemical transducer concept printed electrochemical sensors on paper, *Sensors and Actuators B* **86**, 193-197.
21. Andersson Ersman, P., Nilsson, D., Kawahara, J., Gustafsson, G., and Berggren, M. (2013) Fast-switching all-printed organic electrochemical transistors, *Organic Electronics* **14**, 1276-1280.
22. Khodagholy, D., Doublet, T., Quilichini, P., Gurfinkel, M., Leleux, P., Ghestem, A., Ismailova, E., Hervé, T., Sanaur, S., Bernard, C., and Malliaras, G. G. (2013) In vivo recordings of brain activity using organic transistors, *Nature communications* **4**, 1575-1575.
23. Shim, N. Y., Bernardis, D. a., Macaya, D. J., DeFranco, J. a., Nikolou, M., Owens, R. M., and Malliaras, G. G. (2009) All-Plastic Electrochemical Transistor for Glucose Sensing Using a Ferrocene Mediator, *Sensors* **9**, 9896-9902.
24. Yang, S. Y., Cicoira, F., Byrne, R., Benito-Lopez, F., Diamond, D., Owens, R. M., and Malliaras, G. G. (2010) Electrochemical transistors with ionic liquids for enzymatic sensing, *Chemical communications (Cambridge, England)* **46**, 7972-7974.
25. Sessolo, M., Khodagholy, D., Rivnay, J., Maddalena, F., Gleyzes, M., Steidl, E., Buisson, B., and Malliaras, G. G. (2013) Easy-to-Fabricate Conducting Polymer Microelectrode Arrays, *Advanced Materials* **25**, 2135-2139.
26. Khodagholy, D., Gurfinkel, M., Stavrinidou, E., Leleux, P., Herve, T., Sanaur, S. b., and Malliaras, G. G. (2011) High speed and high density organic electrochemical transistor arrays, *Applied Physics Letters* **99**, 163304-163304.
27. Yang, S. Y., DeFranco, J. a., Sylvester, Y. a., Gobert, T. J., Macaya, D. J., Owens, R. M., and Malliaras, G. G. (2009) Integration of a surface-directed microfluidic system with an organic electrochemical transistor array for multi-analyte biosensors, *Lab on a chip* **9**, 704-708.
28. Mabeck, J. T., DeFranco, J. a., Bernardis, D. a., Malliaras, G. G., Hocdé, S., and Chase, C. J. (2005) Microfluidic gating of an organic electrochemical transistor, *Applied Physics Letters* **87**, 013503-013503.
29. Khodagholy, D., Doublet, T., Gurfinkel, M., Quilichini, P., Ismailova, E., Leleux, P., Herve, T., Sanaur, S., Bernard, C., and Malliaras, G. G. (2011) Highly Conformable Conducting Polymer Electrodes for In Vivo Recordings, *Advanced materials (Deerfield Beach, Fla.)*, 268-272.
30. Hamedi, M., Forchheimer, R., and Inganäs, O. (2007) Towards woven logic from organic electronic fibres, *Nature materials* **6**, 357-362.
31. Mattana, G., Cosseddu, P., Fraboni, B., Malliaras, G. G., Hinestroza, J. P., and Bonfiglio, A. (2011) Organic electronics on natural cotton fibres, *Organic Electronics* **12**, 2033-2039.
32. Muller, C., Hamedi, M., Karlsson, R., Jansson, R., Marcilla, R., Hedhammar, M., and Inganäs, O. (2011) Woven electrochemical transistors on silk fibers, *Adv Mater* **23**, 898-901.
33. Heeger, A. J. (2001) Semiconducting and Metallic Polymers: The Fourth Generation of Polymeric Materials†, *The Journal of Physical Chemistry B* **105**, 8475-8491.

34. Heeger, A. J., MacDiarmid, A. G., and Shirakawa, H. (2000) The Nobel Prize in chemistry, 2000: conductive polymers, *Stockholm, Sweden: Royal Swedish Academy of Sciences*.
35. Guimard, N. K., Gomez, N., and Schmidt, C. E. (2007) Conducting polymers in biomedical engineering, *Progress in Polymer Science* 32, 876-921.
36. Asplund, M., Nyberg, T., and Inganas, O. (2010) Electroactive polymers for neural interfaces, *Polym Chem-Uk* 1, 1374-1391.
37. Thompson, B. C., Winther-Jensen, O., Vongsvivut, J., Winther-Jensen, B., and MacFarlane, D. R. (2010) Conducting Polymer Enzyme Alloys: Electromaterials Exhibiting Direct Electron Transfer, *Macromolecular Rapid Communications* 31, 1293-1297.
38. Heller, A. (1992) Electrical connection of enzyme redox centers to electrodes, *The Journal of Physical Chemistry* 96, 3579-3587.
39. McQuade, D. T., Pullen, A. E., and Swager, T. M. (2000) Conjugated Polymer-Based Chemical Sensors, *Chemical Reviews* 100, 2537-2574.
40. Owens, R. M., and Malliaras, G. G. (2010) Organic Electronics at the Interface with Biology, *Mrs Bull* 35, 449-456.
41. Jimison, L. H., Rivnay, J., and Owens, R. M. (2013) Conducting Polymers to Control and Monitor Cells.
42. Bongo, M., Winther-Jensen, O., Himmelberger, S., Strakosas, X., Ramuz, M., Hama, A., Stavrinidou, E., Malliaras, G. G., Salleo, A., Winther-Jensen, B., and Owens, R. M. (2013) PEDOT:gelatin composites mediate brain endothelial cell adhesion, *Journal of Materials Chemistry B* 1, 3860-3860.
43. Jimison, L. H., Hama, A., Strakosas, X., Armel, V., Khodagholy, D., Ismailova, E., Malliaras, G. G., Winther-Jensen, B., and Owens, R. M. (2012) PEDOT:TOS with PEG: a biofunctional surface with improved electronic characteristics, *Journal of Materials Chemistry* 22, 19498-19498.
44. Strakosas, X., Sessolo, M., Hama, A., Rivnay, J., Stavrinidou, E., Malliaras, G. G., and Owens, R. M. (2014) A facile biofunctionalisation route for solution processable conducting polymer devices, *Journal of Materials Chemistry B* 2, 2537-2537.
45. Jimison, L. H., Rivnay, J., and Owens, R. M. (2013) Conducting Polymers to Control and Monitor Cells, In *Organic Electronics*, pp 27-67, Wiley-VCH Verlag GmbH & Co. KGaA, Weinheim, Germany
46. Stavrinidou, E., Leleux, P., Rajaona, H., Khodagholy, D., Rivnay, J., Lindau, M., Saur, S., and Malliaras, G. G. (2013) Direct measurement of ion mobility in a conducting polymer, *Advanced materials (Deerfield Beach, Fla.)* 25, 4488-4493.
47. Simon, D. T., Kurup, S., Larsson, K. C., Hori, R., Tybrandt, K., Gojny, M., Jager, E. W. H., Berggren, M., Canlon, B., and Richter-Dahlfors, A. (2009) Organic electronics for precise delivery of neurotransmitters to modulate mammalian sensory function, *Nat Mater* 8, 742-746.
48. Isaksson, J., Kjall, P., Nilsson, D., Robinson, N., Berggren, M., and Richter-Dahlfors, A. (2007) Electronic control of Ca<sup>2+</sup> signalling in neuronal cells using an organic electronic ion pump, *Nat Mater* 6, 673-679.

49. Tybrandt, K., Forchheimer, R., and Berggren, M. (2012) Logic gates based on ion transistors, *Nat Commun* 3, 871.
50. Rivnay, J., Leleux, P., Sessolo, M., Khodagholy, D., Hervé, T., Fiocchi, M., and Malliaras, G. G. (2013) Organic electrochemical transistors with maximum transconductance at zero gate bias, *Advanced materials (Deerfield Beach, Fla.)* 25, 7010-7014.
51. Bernards, D. a., Malliaras, G. G., Toombes, G. E. S., and Gruner, S. M. (2006) Gating of an organic transistor through a bilayer lipid membrane with ion channels, *Applied Physics Letters* 89, 053505-053505.
52. Lin, P., Yan, F., and Chan, H. L. W. (2010) Ion-sensitive properties of organic electrochemical transistors, *ACS applied materials & interfaces* 2, 1637-1641.
53. Tarabella, G., Balducci, A. G., Coppedè, N., Marasso, S., D'Angelo, P., Barbieri, S., Cocuzza, M., Colombo, P., Sonvico, F., Mosca, R., and Iannotta, S. (2013) Liposome sensing and monitoring by organic electrochemical transistors integrated in microfluidics, *Biochimica et biophysica acta* 1830, 4374-4380.
54. Tarabella, G., Nanda, G., Villani, M., Coppedè, N., Mosca, R., Malliaras, G. G., Santato, C., Iannotta, S., and Cicoira, F. (2012) Organic electrochemical transistors monitoring micelle formation, *Chemical Science* 3, 3432-3432.
55. Svensson, P.-O., Nilsson, D., Forchheimer, R., and Berggren, M. (2008) A sensor circuit using reference-based conductance switching in organic electrochemical transistors, *Applied Physics Letters* 93, 203301-203301-203303.
56. Sessolo, M., Rivnay, J., Bandiello, E., Malliaras, G. G., and Bolink, H. J. (2014) Ion-Selective Organic Electrochemical Transistors, *Advanced Materials* 26, 4803-4807.
57. Mousavi, Z., Ekholm, A., Bobacka, J., and Ivaska, A. (2009) Ion-Selective Organic Electrochemical Junction Transistors Based on Poly(3,4-ethylenedioxythiophene) Doped with Poly(styrene sulfonate), *Electroanalysis* 21, 472-479.
58. Lin, P., and Yan, F. (2012) Organic thin-film transistors for chemical and biological sensing, *Advanced materials (Deerfield Beach, Fla.)* 24, 34-51.
59. Nishizawa, M., Matsue, T., and Uchida, I. (1992) Penicillin sensor based on a microarray electrode coated with pH-responsive polypyrrole, *Analytical Chemistry* 64, 2642-2644.
60. Zhu, Z.-T., Mabeck, J. T., Zhu, C., Cady, N. C., Batt, C. A., and Malliaras, G. G. (2004) A simple poly(3,4-ethylene dioxythiophene)/poly(styrene sulfonic acid) transistor for glucose sensing at neutral pH, *Chemical Communications*, 1556-1557.
61. Bernards, D. a., Macaya, D. J., Nikolou, M., DeFranco, J. a., Takamatsu, S., and Malliaras, G. G. (2008) Enzymatic sensing with organic electrochemical transistors, *Journal of Materials Chemistry* 18, 116-116.
62. Macaya, D. J., Nikolou, M., Takamatsu, S., Mabeck, J. T., Owens, R. M., and Malliaras, G. G. (2007) Simple glucose sensors with micromolar sensitivity based on organic electrochemical transistors, *Sensors and Actuators B: Chemical* 123, 374-378.

63. Tang, H., Lin, P., Chan, H. L. W., and Yan, F. (2011) Highly sensitive dopamine biosensors based on organic electrochemical transistors, *Biosensors & bioelectronics* **26**, 4559-4563.
64. Tarabella, G., Pezzella, A., Romeo, A., D'Angelo, P., Coppedè, N., Calicchio, M., d'Ischia, M., Mosca, R., and Iannotta, S. (2013) Irreversible evolution of eumelanin redox states detected by an organic electrochemical transistor: en route to bioelectronics and biosensing, *Journal of Materials Chemistry B* **1**, 3843-3843.
65. Coppede, N., Tarabella, G., Villani, M., Calestani, D., Iannotta, S., and Zappettini, A. (2014) Human stress monitoring through an organic cotton-fiber biosensor, *Journal of Materials Chemistry B* **2**, 5620-5626.
66. Cicoira, F., Sessolo, M., Yaghmazadeh, O., DeFranco, J. a., Yang, S. Y., and Malliaras, G. G. (2010) Influence of device geometry on sensor characteristics of planar organic electrochemical transistors, *Advanced materials (Deerfield Beach, Fla.)* **22**, 1012-1016.
67. Tarabella, G., Santato, C., Yang, S. Y., Iannotta, S., Malliaras, G. G., and Cicoira, F. (2010) Effect of the gate electrode on the response of organic electrochemical transistors, *Applied Physics Letters* **97**, 123304-123304.
68. Yaghmazadeh, O., Cicoira, F., Bernards, D. A., Yang, S. Y., Bonnassieux, Y., and Malliaras, G. G. (2011) Optimization of organic electrochemical transistors for sensor applications, *Journal of Polymer Science Part B: Polymer Physics* **49**, 34-39.
69. Tang, H., Yan, F., Lin, P., Xu, J., and Chan, H. L. W. (2011) Highly Sensitive Glucose Biosensors Based on Organic Electrochemical Transistors Using Platinum Gate Electrodes Modified with Enzyme and Nanomaterials, *Advanced Functional Materials* **21**, 2264-2272.
70. Liao, C., Zhang, M., Niu, L., Zheng, Z., and Yan, F. (2013) Highly selective and sensitive glucose sensors based on organic electrochemical transistors with graphene-modified gate electrodes, *Journal of Materials Chemistry B* **1**, 3820-3820.
71. Kergoat, L., Piro, B., Simon, D. T., Pham, M.-C., Noël, V., and Berggren, M. (2014) Detection of Glutamate and Acetylcholine with Organic Electrochemical Transistors Based on Conducting Polymer/Platinum Nanoparticle Composites, *Advanced materials (Deerfield Beach, Fla.)*, 1-7.
72. Khodagholy, D., Curto, V. F., Fraser, K. J., Gurfinkel, M., Byrne, R., Diamond, D., Malliaras, G. G., Benito-Lopez, F., and Owens, R. M. (2012) Organic electrochemical transistor incorporating an ionogel as a solid state electrolyte for lactate sensing, *J. Mater. Chem.* **22**, 4440-4443.
73. Lee, K. H., Kang, M. S., Zhang, S., Gu, Y., Lodge, T. P., and Frisbie, C. D. (2012) "Cut and stick" rubbery ion gels as high capacitance gate dielectrics, *Advanced materials (Deerfield Beach, Fla.)* **24**, 4457-4462.
74. Lin, P., Yan, F., Yu, J., Chan, H. L., and Yang, M. (2010) The application of organic electrochemical transistors in cell-based biosensors, *Adv Mater* **22**, 3655-3660.
75. He, R.-X., Zhang, M., Tan, F., Leung, P. H. M., Zhao, X.-Z., Chan, H. L. W., Yang, M., and Yan, F. (2012) Detection of bacteria with organic electrochemical transistors, *Journal of Materials Chemistry* **22**, 22072-22072.

76. Kim, D.-J., Lee, N.-E., Park, J.-S., Park, I.-J., Kim, J.-G., and Cho, H. J. (2010) Organic electrochemical transistor based immunosensor for prostate specific antigen (PSA) detection using gold nanoparticles for signal amplification, *Biosensors & bioelectronics* *25*, 2477-2482.
77. Lin, P., Luo, X., Hsing, I. M., and Yan, F. (2011) Organic electrochemical transistors integrated in flexible microfluidic systems and used for label-free DNA sensing, *Advanced materials (Deerfield Beach, Fla.)* *23*, 4035-4040.
78. Liao, J., Lin, S., Liu, K., Yang, Y., Zhang, R., Du, W., and Li, X. (2014) Organic electrochemical transistor based biosensor for detecting marine diatoms in seawater medium, *Sensors and Actuators B: Chemical* *203*, 677-682.
79. Bolin, M. H., Svennersten, K., Nilsson, D., Sawatdee, A., Jager, E. W. H., Richter-Dahlfors, A., and Berggren, M. (2009) Active Control of Epithelial Cell-Density Gradients Grown Along the Channel of an Organic Electrochemical Transistor, *Adv. Mater.* *21*, 4379-+.
80. Khodagholy, D., Doublet, T., Quilichini, P., Gurfinkel, M., Leleux, P., Ghestem, A., Ismailova, E., Herve, T., Sanaur, S., Bernard, C., and Malliaras, G. G. (2013) In vivo recordings of brain activity using organic transistors, *Nat Commun* *4*, 1575.
81. Jimison, L. H., Tria, S. A., Khodagholy, D., Gurfinkel, M., Lanzarini, E., Hama, A., Malliaras, G. G., and Owens, R. M. (2012) Measurement of barrier tissue integrity with an organic electrochemical transistor, *Adv Mater* *24*, 5919-5923.
82. Tria, S. A., Ramuz, M., Huerta, M., Leleux, P., Rivnay, J., Jimison, L. H., Hama, A., Malliaras, G. G., and Owens, R. M. (2014) Dynamic monitoring of Salmonella typhimurium infection of polarized epithelia using organic transistors, *Adv Healthc Mater* *3*, 1053-1060.
83. Tria, S., Jimison, L. H., Hama, A., Bongo, M., and Owens, R. M. (2013) Sensing of EGTA Mediated Barrier Tissue Disruption with an Organic Transistor, *Biosensors* *3*, 44-57.
84. Tria, S. A., Ramuz, M., Jimison, L. H., Hama, A., and Owens, R. M. (2014) Sensing of barrier tissue disruption with an organic electrochemical transistor, *Journal of visualized experiments : JoVE*, e51102.
85. Lin, P., Yan, F., Yu, J. J., Chan, H. L. W., and Yang, M. (2010) The Application of Organic Electrochemical Transistors in Cell-Based Biosensors, *Adv. Mater.* *22*, 3655-+.
86. Yao, C., Xie, C., Lin, P., Yan, F., Huang, P., and Hsing, I. M. (2013) Organic Electrochemical Transistor Array for Recording Transepithelial Ion Transport of Human Airway Epithelial Cells, *Advanced Materials* *25*, 6575-6580.
87. Ramuz, M., Hama, A., Huerta, M., Rivnay, J., Leleux, P., and Owens, R. M. (2014) Combined optical and electronic sensing of epithelial cells using planar organic transistors, *Adv Mater* *26*, 7083-7090.
88. Campana, A., Cramer, T., Simon, D. T., Berggren, M., and Biscarini, F. (2014) Electrocardiographic recording with conformable organic electrochemical transistor fabricated on resorbable bioscaffold, *Advanced materials (Deerfield Beach, Fla.)* *26*, 3874-3878.

89. Jasper, H. H., Arfel-Capdeville, G., and Rasmussen, T. (1961) Evaluation of EEG and cortical electrographic studies for prognosis of seizures following surgical excision of epileptogenic lesions, *Epilepsia* 2, 130-137.
90. Gilletti, A., and Muthuswamy, J. (2006) Brain micromotion around implants in the rodent somatosensory cortex, *Journal of neural engineering* 3, 189-195.
91. Leleux, P., Rivnay, J., Lonjaret, T., Badier, J. M., Benar, C., Herve, T., Chauvel, P., and Malliaras, G. G. (2015) Organic electrochemical transistors for clinical applications, *Adv Healthc Mater* 4, 142-147.

# Chapter 2

---

## **2. Biofunctionalization of PEDOT:TOS and exploration of enzyme wiring for realization of 3<sup>rd</sup> generation enzymatic sensors**

### **2.1. PEDOT :TOS :PEG with increased conductivity and surface functionality.**

Conducting polymers discovered in the 1970s<sup>1</sup> have shown widespread promise in their use as electrically active materials at the interface with biology. The significant rise in the use of conducting polymers in biomedical and bioengineering applications is due to inherent properties that make these materials ideal for interfacing with biological systems<sup>2</sup>. The ‘soft’ nature of conducting polymers assures compatibility with flexible substrates, and allows for good mechanical matching with delicate biological tissue. The unique ability of organic electronic materials to conduct ions, in addition to electrons and holes, facilitates their communication with biological systems, which rely heavily on ion fluxes. Furthermore, as Van der Waals bonded solids, these materials are capable of forming ideal interfaces with electrolytes, without disruptive dangling bonds or oxides and leading to improved electronic sensitivity and reduced noise. Finally, the ability to chemically tune both molecular architecture and film microstructure allows for significant flexibility when optimizing materials for a specific application.

There exist many examples of conducting polymers in contact with mammalian cells for applications in tissue engineering<sup>3</sup>. The bulk of the literature has focused on the relatively passive use of conducting polymers as coating materials for interface optimisation<sup>4-8</sup>. Recent applications have exploited the unique attributes of conducting polymers to realise new devices with novel capabilities.

Smart conducting polymer surfaces can be used to control cell adhesion, proliferation and migration<sup>9-11</sup>. Organic electronic ion pumps (OEIPs) that can precisely control the flow of ions have been used to deliver neurotransmitters in the inner ear of a guinea pig<sup>12-14</sup>. The organic electrochemical transistor (OECT), first introduced in 1984<sup>15</sup> has proven to be an extremely versatile device for interfacing with biological systems<sup>16</sup>. OECTs are being developed for a variety of biosensing applications, including ion detection<sup>17, 18</sup> enzymatic sensing<sup>19-21</sup> and whole cell sensing.<sup>22</sup>

The vast majority of OECTs are fabricated from poly(3,4-ethylenedioxythiophene) (PEDOT). This semiconducting polymer is degenerately p-type doped and rendered conducting with negative dopant ions, which stabilize positive holes on the conjugated backbone and balance overall charge. Common dopants include poly(styrenesulfonate) (PSS) and the tosylate anion (TOS). PEDOT doped with either PSS or TOS has shown considerable promise with respect to electrical properties, biocompatibility, and film stability and are therefore appropriate for applications in biological interfacing.

In order to further improve the material/tissue interface, there is a concerted effort to add increased biofunctionality by incorporating bioactive species into the conducting polymer. Such additives can include peptides and proteins for the purpose of encouraging cell adhesion<sup>23-26</sup> and directing axon growth<sup>27</sup> or enzymes for the purpose of bactericidal properties or sensing capabilities<sup>28</sup>. The bioactive species can be incorporated into the conducting polymer film in a number of ways. A commonly used method is to add the desired species to the electrolyte solution during electropolymerisation<sup>29</sup>. In this way, the bioactive species are entrapped in the conducting polymer films during growth, and often serve as a dopant or co-dopant. However, bulky biochemical molecules can have a disruptive effect on the final film. The incorporation of neural growth factor with ligands into PEDOT films via electropolymerization has been shown to result in both decreased electroactivity and poor mechanical properties<sup>30, 31</sup>, attributed to the change in polymerisation rate upon the addition of the biomolecule. Similarly, while the incorporation of hyaluronic acid (HA) into Polypyrrole (Ppy) via electropolymerization was found to encourage angiogenesis, the resulting composite film was brittle and conductivity was reduced by four orders of magnitude<sup>27</sup>. An alternative to molecular entrapment is to employ covalent tethering of the bioactive species to the semiconducting polymer using carboxylic acid ligand binding. For this purpose, films of Ppy with carboxylic acid functional groups, Ppy(COOH) were electropolymerised<sup>32</sup>. However, along with increasing functionality, Ppy(COOH) was shown to have a slightly lower doping level and drastically lower conductivity compared to Ppy. The degradation in electrical properties was attributed to the decrease in the polymerization rate and

disruption of the Ppy molecular planarity caused by the additional functional group.

Enhancement of the CP-tissue interface will allow for more stable, reliable and functional bioelectronics materials. However, this improvement should not come at the cost of electronic performance. Ideally, the electronic properties of a conducting polymer should be maintained, or even better, *improved*, on addition of the bioactive species. Vapour phase polymerisation (VPP) is an *in situ* polymerisation technique, in which an oxidant is used to coat a surface on which the EDOT monomer is then sourced, leading to the formation of a conducting polymer film<sup>33</sup>. This simple technique lends itself well to the incorporation of various additives to the conducting polymer film. Recent studies have demonstrated that mixing other molecules with the oxidant results in composite films, in which the additive is intimately incorporated in the conducting PEDOT matrix<sup>34-36</sup>. Moreover, a correctly chosen additive can serve to enhance the microstructure and electronic properties of the CP. In this study, we show that on addition of PEG to PEDOT:TOS, electroactivity is maintained and the conductivity is improved. OECTs were fabricated with the composite films, and modulation was identical compared to neat PEDOT:TOS films. PEG is a biocompatible material often used in tissue engineering applications, whose alcohol groups can be readily activated for subsequent functionalization of bioactive species<sup>37</sup>. The incorporation of PEG into PEDOT:TOS films provides a means to achieve specific binding of a bioactive species, without negatively affecting the conducting polymer microstructure or electronic structure. In this approach, the protein is introduced after film fabrication, and is therefore not exposed to the harsh temperatures and solvents associated with *in-situ* polymerisation techniques. We believe the PEDOT:TOS-PEG composites in this work can act as an ideal platform for interfacing organic electronics and biological systems.

## 2.2. Vapor Phase Polymerization (VPP)

PEDOT:TOS, PEDOT:TOS:PEG and PEDOT:TOS:PEG(COOH) composites were fabricated by vapor phase polymerization (VPP) according to a previously published protocol (figure 2.1)<sup>35</sup>. Briefly, a solution consisting of Fe(III) tosylate dissolved in butanol was used as the oxidant for the polymerization of EDOT, with pyridine as a weak base in order to stabilize the polymerization. Poly(ethylene glycol) was dissolved in a small amount of water before being added to the oxidant solution. The ratio of PEG to PEDOT was estimated on the basis that it requires 2.25 moles of Fe(III) to produce 1 mole of PEDOT<sup>38</sup>. The amount of PEG added to each oxidant solution was chosen in order to achieve

films with 30%, 50% and 70% PEG content as compared to PEDOT. For purposes of lowering final film thickness, the oxidant solutions were diluted with ethanol. To promote adhesion between the final PEDOT film and the substrate, glass slides were coated with plasma polymerised maleic anhydride<sup>39</sup> prior to deposition of the oxidant solution. The oxidant solution was spun onto the substrates at 1500 rpm for 30 sec and placed directly in the vapour phase polymerisation chamber without a drying step. The vaporisation chamber, containing EDOT monomer (was kept in an oven at 70°C, at ambient pressure. EDOT was allowed to polymerise on the coated substrates for 30-40 minutes, at which point samples were removed from the polymerisation chamber and rinsed twice in ethanol to remove excess Fe(III)Tos and unpolymerised EDOT monomer.

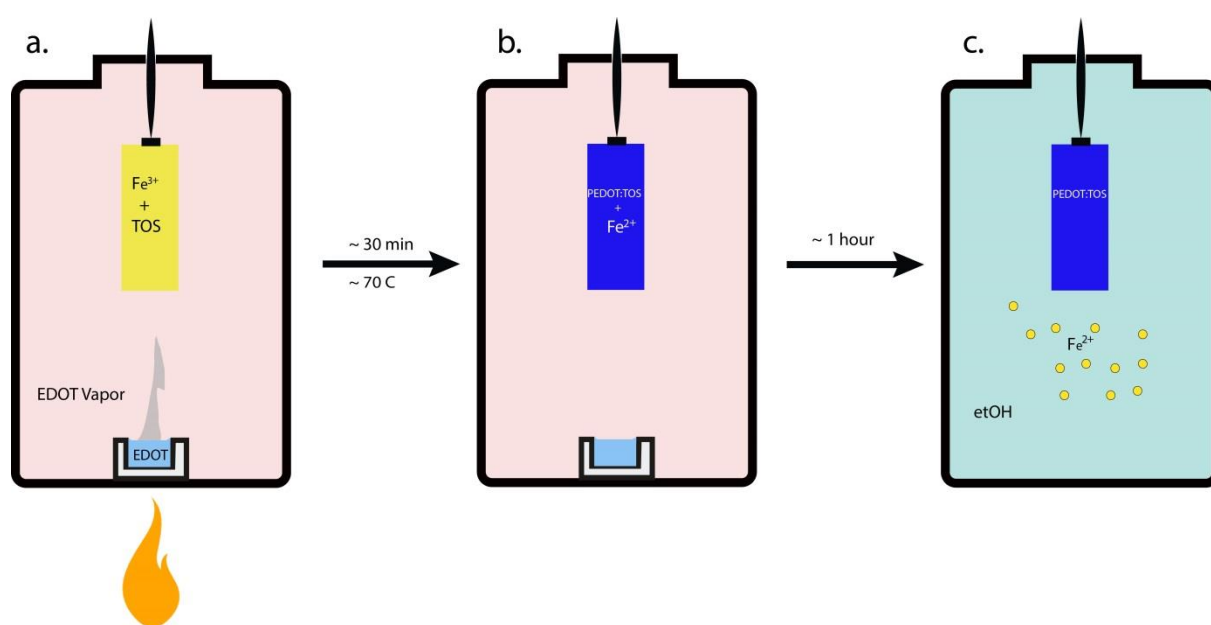


**Figure 2.1:** Vapor phase polymerization of PEDOT:TOS (a) exposure of iron(III) tosylate in a desiccator with EDOT vapor. (b) Polymerization of EDOT to PEDOT:TOS on the sample. (c) Stringent soaking in ethanol in order to remove the iron(II) and excess of tosylate.

### 2.2.1. Characterization of films and devices

To further investigate electrical performance, composite films of PEDOT:TOS and PEG were prepared with various PEG to PEDOT ratios: 0% PEG, 30% PEG, 50% PEG and 70% PEG (referred to as PEDOT:TOS, PEDOT:TOS-30PEG, PEDOT:TOS-50PEG and PEDOT:TOS-70PEG, respectively). For the range of PEG content measured in this study, the film conductivity was found to increase with increasing PEG concentration (figure 2.2a). These data confirm previous

observations of increasing PEDOT conductivity on the addition of PEG<sup>35, 36</sup>, and similar non-conducting materials<sup>40-43</sup>. This effect has been attributed to a number of factors relating to film microstructure and energetics. As observed previously, we saw that the addition of PEG suppresses the formation of  $\mu$ -scale domains (figure S2.1), presumably providing a smoother energetic landscape for charge transport. Perhaps the most important factor for the increase in conductivity is the decrease of the solid-solid phase transition temperature by as much as 70°C observed for PEDOT-PEG blends compared to PEDOT alone<sup>35</sup>. This strongly implies that the order of PEDOT in the blended materials is maintained, but the energy required to disrupt this order is significantly reduced. Thus, the composite materials are more suitable for undergoing the necessary conformational changes along the conjugated backbone required for efficient charge transfer.

Having established an increase in the conductivity, we wanted to validate the potential of PEDOT:TOS-PEG as the active material in an OECT. As mentioned in the introduction, OECTs are an important device in the field of bioelectronics, used for biosensing and ionic signal transduction. OECTs are comprised of a conducting polymer film acting as the transistor channel, with metallic source and drain electrodes. The CP, in this case PEDOT:TOS or PEDOT:TOS-PEG, is in direct contact with an electrolyte, and a gate electrode is submersed in the electrolyte. The application of a positive gate-source bias encourages migration of ions: tosylate anions leave the polymer film as cations from the electrolyte enter the polymer film. Both of these actions serve to de-dope the CP. As the number of mobile holes is reduced, the drain current decreases. In this way, the OECT translates changes in ion flux to a change in electrical current, making it an ideal platform for the integration of electronics and biological systems.

We fabricated OECTs with PEDOT:TOS and PEDOT:TOS:PEG. The transient response of the OECT drain current to a square gate voltage pulse for films with different PEG to PEDOT ratios is shown in figure 2.2b. As discussed above, the addition of PEG results in an increase in film conductivity. This is manifest as a shift in the steady state drain current of the device on the addition of PEG. On application of the positive gate voltage, all devices show efficient de-doping, as evidenced by rapid decrease in drain current. Upon removal of this voltage, the drain current recovers to the original steady state value. The surface plot in figure 2.2c illustrates the effect of both applied gate voltage and film composition on the transistor response (defined as the change in drain current on application of a positive gate voltage, normalised by the baseline current). In all films, an increase of the gate voltage results in an increase of the normalised modulation, while the PEG content has a negligible effect.

It has been demonstrated previously that OECT behaviour can be modelled as a

combination of an electronic circuit, which accounts for hole transport in the polymer channel, and an ionic circuit, which accounts for the ionic transport from the electrolyte to the polymer channel<sup>44</sup>. As a simple approximation, the behaviour of the ionic circuit resembles that of an RC circuit, with R determined by the resistance of the electrolyte and C being an effective capacitance of the channel/electrolyte interface (in the case where a Ag/AgCl electrode is used as the gate). The time response of the device to a square voltage pulse on the gate is related to charging of that “effective” capacitor, and it is related to the ability of the polymer channel to store charge. Data shown in figure 2.2b and 2.2c shows that the addition of PEG does not alter the RC time. From a physical perspective, this implies that the PEG content presents no additional barrier for ion migration both into and out of the film during the de-doping/doping process. The efficiency of the doping and de-doping process is further evidenced by the very high transconductance (average of 768  $\mu\text{S}$ , or 274  $\mu\text{S}/\text{mm}$  when normalised for channel width) measured in the OECTs, which is an order of magnitude greater than that of typical organic field effect transistors<sup>45</sup>.

The data presented here assures that the addition of PEG is not harmful to device performance, and in fact, improves conductivity. Since our efforts are directed towards organic electronic devices for biological applications, it is also necessary to determine the biocompatibility of these composite films. It has been observed previously that unpolymerised EDOT monomers can be toxic to cells<sup>46</sup>, but once polymerised, PEDOT is generally accepted to be cytocompatible.

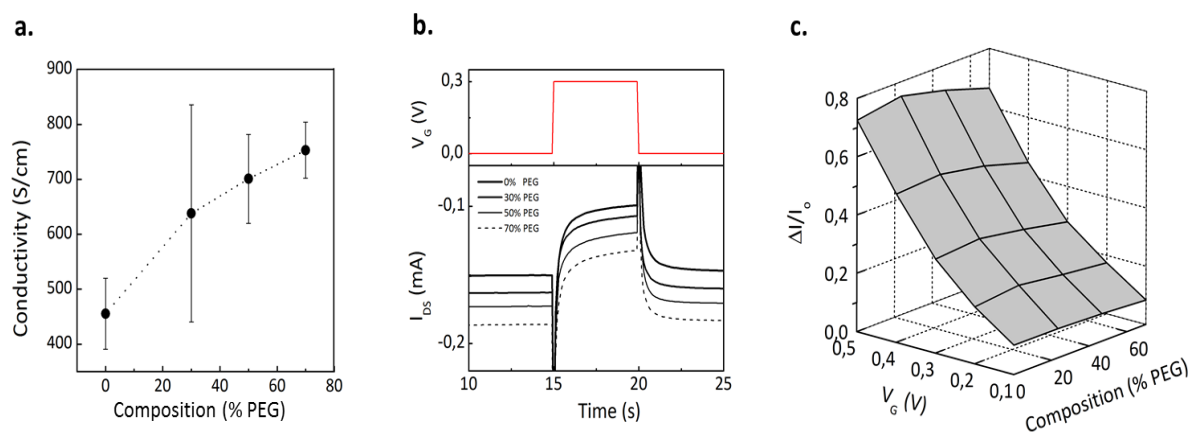


**Figure 2.2:** a. Conductivity as a function of PEG content. Error bars represent standard deviation from the mean b. Transient OECT response for films with varying PEG content, c. Normalised OECT response as a function of gate voltage and film composition (PEG content.)

## 2.2.2. Biofunctionalization of the films

To address the need for conducting polymer surfaces with specifically covalently incorporated proteins we carried out preliminary work to biofunctionalise the surface of our composite materials by taking advantage of the readily activated alcohol groups on the PEG. Namely, composites comprised of PEDOT:TOS and a carboxylic acid functionalised PEG, referred to as PEG(COOH), were made. XPS data confirms that incorporation of 70% PEG into PEDOT:TOS films (both PEG-COOH and PEG) results in a surface layer of approximately 18-20% PEG. In the PEDOT:TOS:PEG(COOH) composite, approximately 2% of the total carbon can be attributed to the COOH groups. EDC/NHS (EDC: N-(3-Dimethylaminopropyl)-N'-ethylcarbodiimide hydrochloride/ NHS: N-hydroxysuccinimide) chemistry was used to incorporate fluorescent proteins onto these surfaces via the carboxyl groups present in the functionalised PEG. EDC reacts with carboxylic acid groups in the presence of NHS to form a stable amide bond between the carboxyl group and ubiquitous primary amines found in all proteins. Subsequent stringent wash steps were included (3X PBS washes, one wash with PBS containing detergent, followed by a wash step with 0.5M NaCl) in attempt to exclude the possibility of electrostatic binding of proteins to the surfaces tested. A standard curve carried out using the fluorescent antibody serially diluted and quantitated for fluorescence in solution, in an identical well, on a PEDOT:TOS coated film – data not shown) was used to approximate the protein bound, with the maximum amount found to correspond to approximately 1 $\mu$ g of protein. The amount of protein coupled is low; however, this is something that may be optimised for future experiments.

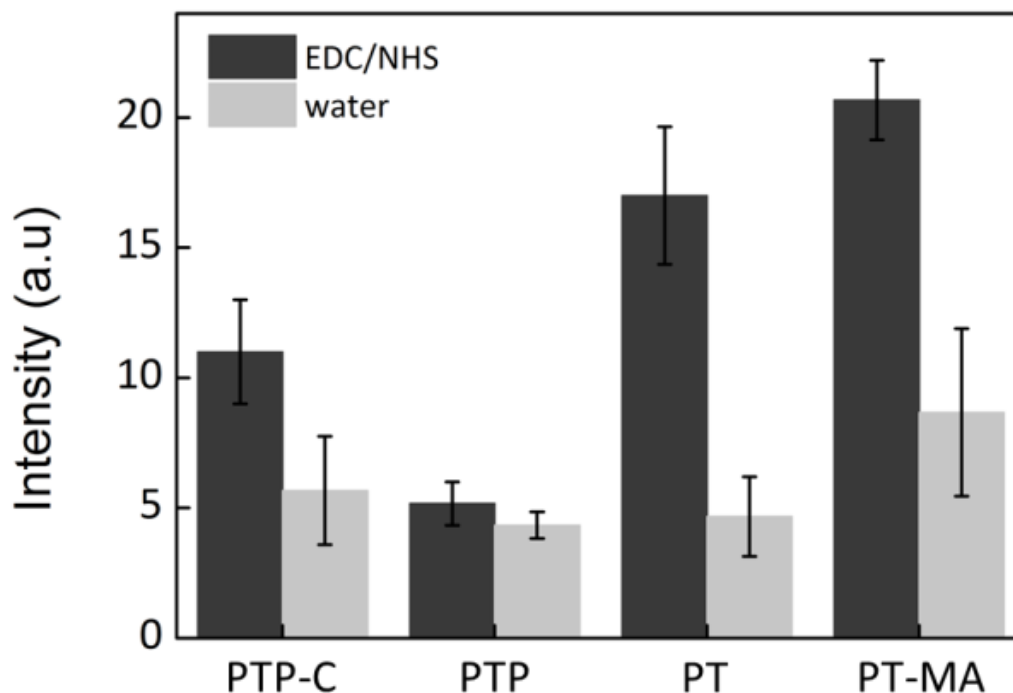


**Figure 2.3:** Biofunctionalisation of conducting polymer surfaces. Data shown is the mean fluorescence of 8 mm<sup>2</sup> diameter wells on a variety of CP surfaces, each carried out in triplicate. Error bars represent standard deviation from the mean. Samples from left to right: PEDOT:TOS:70PEG(COOH) (**PTP-C**), PEDOT:TOS:70PEG (**PTP**), PEDOT:TOS (**PT**), and PEDOT:TOS treated with a plasma coating of maleic anhydride (**PT-MA**)

The data shown in figure 2.3 show the fluorescence intensity of four different surfaces: PEDOT:TOS-PEG with COOH (PTP-C), PEDOT:TOS-PEG without COOH (PTP), PEDOT:TOS alone (PT), and PEDOT:TOS coated with plasma polymerised maleic anhydride (PT-MA). It can be seen that the PEDOT:TOS:PEG(COOH) surface has a low level of specific binding of protein, which does not occur in the absence of the EDC/NHS treatment. In contrast, the PEDOT:TOS-PEG surface does not show any difference between the control or the EDC/NHS treated surface. Interestingly, a PEDOT:TOS surface, tested as a control, showed specific binding of protein in the presence of EDC/NHS treatment, but not without this treatment. As an additional control, we coated a PEDOT:TOS:PEG surface with plasma polymerised maleic anhydride, which has been shown to result in high concentrations of carboxyl groups on the surface<sup>39</sup>. Indeed, this sample exhibited the highest fluorescent intensity, indicating that –COOH groups are covalently bound with the protein. We believe that both PEDOT, and -COOH groups on the PEG are participating in the EDC/NHS

chemistry, forming specific linkage with the protein. While further elucidation of this reaction mechanism is necessary, we are currently presented with at least directions to proceed. First, we could substitute the functional group on the PEG and use orthogonal chemistry that does not interfere with the PEDOT. Second, we could specifically block the PEDOT functional groups before proceeding with the PEG functionalization. Finally, we could take advantage of the unexpected specific binding allowed with EDC/NHS chemistry, and functionalize the PEDOT itself.

## 2.3. Discussion

In this work we have demonstrated that composite materials comprised of the conducting polymer PEDOT:TOS and the nonconducting polymer PEG show electrical properties equal or superior to PEDOT:TOS alone. We showed that these composite materials are biocompatible through rigorous direct and indirect tests and that the degree of biocompatibility is not dependent on the concentration of PEG. Furthermore, we have demonstrated the potential of the incorporated PEG to provide an avenue for the specific incorporation of biomolecules onto PEDOT:TOS surfaces in a manner that is compatible with the sensitive nature of most of these moieties. We believe the development of PEDOT:TOS:PEG biofunctional materials can lead to the improvement of biomaterials and bioelectronic devices.

## 2.4. Experimental section

*Vapor Phase Polymerisation of PEDOT:TOS composites:* PEDOT:TOS, PEDOT:TOS:PEG and PEDOT:TOS:PEG(COOH) composites were fabricated according to a previously published protocol<sup>35</sup>. Prior to VPP, an oxidant solution was prepared. Fe(III)tosylate (40 wt% in solution with butanol, Yacoo Chemical Company) was used as the oxidant, with pyridine (Sigma; used as received) as a weak base in all solutions. Poly(ethylene glycol) and PEG(COOH) (PEG,  $M_n = 20000$ , and PEG(COOH),  $M_n = 600$ , Sigma Aldrich) were dissolved in a small amount of water before being added to the oxidant solution. The amount of PEG added to each oxidant solution was chosen in order to achieve films with 30%, 50% and 70% PEG content as compared to PEDOT. For purposes of lowering final film thickness, the oxidant solutions were diluted with ethanol. To promote adhesion between the final PEDOT film and the substrate, glass slides were coated with plasma polymerised maleic anhydride<sup>39</sup> prior to deposition of the

oxidant solution. The oxidant solution was spun onto the substrates at 1500 rpm for 30 sec and placed directly in the vapour phase polymerisation chamber without a drying step. The vaporisation chamber, containing EDOT monomer (HD Stark or Yacoo Chemical Company) was kept in an oven at 70°C, at ambient pressure. EDOT was allowed to polymerise on the coated substrates for 30-40 minutes, at which point samples were removed from the polymerisation chamber and rinsed twice in ethanol to remove excess Fe(III)Tos and unpolymersed EDOT monomer.

*Conductivity Measurements:* Conductivity measurements were performed by measuring the resistance across PEDOT:TOS and PEDOT:TOS:PEG samples of defined length and width. The thicknesses of the films were measured using profilometry and final film thickness values used in calculations were averaged from at least three measurements. Conductivity values shown were averaged over at least 5 separate samples.

*OECT Fabrication and Characterisation:* OECT fabrication consisted of first defining a conducting polymer channel on a glass substrate. Polymethylsiloxane (PDMS) was used to define the well (active channel area: ca. 16 mm<sup>2</sup>.) Phosphate buffered saline (PBS) was used as the electrolyte. Ag/AgCl was used as the gate electrode. Transistor characteristics were measured using a Keithley 2612A Sourcemeter and customised Labview software. Transient measurements were carried out in two ways. In the first method, the drain-source voltage ( $V_{DS}$ ) was kept at -0.2 V, while a square voltage pulse of 0.3 V for a duration of 5 sec was applied to the gate ( $V_{GS}$ ), allowing 10 sec recovery periods. In a second measurement, the gate voltage was stepped from 0.1 to 0.5 V in intervals of 0.1 V, while maintaining a drain voltage of -0.2 V and the same duty cycle as the previous measurement. Transconductance values were extracted from the maximum of the derivative of the steady state transfer curves, at a drain voltage of -0.6 V.

*Biofunctionalisation:* A sixteen well incubation chamber was affixed to PEDOT:TOS and PEDOT:TOS:PEG composite films on glass substrates. An alexa-fluor labeled Donkey Anti-Rabbit igG Antibody was used for coupling experiments (Aex578 nm/Aem 603 nm) (Invitrogen; 2 mg/ml). **A solution of EDC** (Sigma; 0.4M in DI water) and NHS (Sigma; 0.1M in DI water) was prepared and 100  $\mu$ l was added to each well (8mm<sup>2</sup>), with three replicates for each condition. 100  $\mu$ l of DI water was used as a control in an additional three wells. Reactions were allowed to proceed at room temperature for 1 hour. EDC/NHS was then removed and samples were rinsed once with 1X PBS. Next, 100  $\mu$ l of protein solution at 0.1 mg/ml were added inside the wells. The samples were covered with aluminum foil and left to incubate for two hours at room temperature. The antibody was then removed and the samples were rinsed three times with PBS,

followed by a rinse with PBS-T (0.05% Tween-20). Finally, samples were rinsed with PBS with NaCl adjusted to 0.5M. Fluorescence measurements were performed using a spectrofluorimeter (Tecan Infinite® M1000).

## **2.5. Stuffing of biomolecules and enzyme in PEDOT:TOS for enhanced cell adhesion and for 3<sup>rd</sup> generation enzymatic sensors**

Cellular adhesion is an important process, both for adhesion to substrates and adhesion to adjacent cells. Interactions between cells and their support generate contractile forces which are transmitted through the substrate by mechanotransduction<sup>47,48</sup>. The surface of the substrate can also change the interactions and induce an internal reorganization of cellular architecture. The behaviour of cells on surfaces of varying rigidity or 'hardness' can be indicative of a particular phenotype: for example, the growth of cells on "soft" gels is now used as a means to identify cancer cells<sup>49</sup>. Cell-cell interactions are mediated by tight contacts and are crucial for cell morphology, function and growth. However, this adhesion is dependent on the interaction between cells and extracellular matrix (ECM) proteins which are known to support cell attachment and growth<sup>50</sup>. ECM proteins include fibronectin, laminin and collagen. Gelatin is a derivative of collagen, one of the most well-known ECM proteins.

One cell type known to require gelatin for adhesion are capillary endothelial cells of the blood brain barrier (BBB). The BBB is a dynamic, physiological and metabolic barrier separating the blood from the central nervous system and is essential for maintaining brain homeostasis and enabling proper neuronal function. The BBB consists of endothelial cells lining the blood vessels (or capillaries) in the brain<sup>51</sup>. This barrier is very selective and impermeable. However when this barrier is altered, diseases such as Alzheimer's, Parkinson's, and other neurodegenerative disorders can occur<sup>52</sup>. A limitation of current treatments in the field of neurology is an understanding of the complex functioning of the central nervous system and its interaction with the BBB. Thus, as in other tissue engineering strategies, the ability to develop an *in vitro* BBB model environment becomes a key element for successful tissue engineering<sup>53</sup>.

A wide variety of bio-materials are used in tissue engineering and it is known that the choice of materials can influence the behavior of cells<sup>54</sup>. CPs have frequently been studied as a potential new material in tissue engineering due to their ability to conduct ions and electrons, with potential applications in

electrically controlled drug release<sup>55</sup>, release of cells from surfaces<sup>56</sup>, controlled alignment of muscle fibres<sup>57</sup> and many more<sup>3</sup>. For example, Schmidt et al. demonstrated that the CP polypyrrole created topographical cues for neuronal cells and had an effect on axon orientation<sup>58</sup>. Several groups have made composites between CPs and biomolecules, frequently via electropolymerisation, through incorporation of the desired species in the electrolyte solution.<sup>29</sup> Often, the goal for incorporation of the biospecies is to improve the interface with the CP. Although certain cell types have been demonstrated to grow directly on CPs including epithelial cells<sup>55</sup>, endothelial cells<sup>59</sup>, human breast cancer cells and fibroblasts<sup>10</sup>, often ECM proteins are coated onto the substrates to enhance adhesion. Certain cells adhere very poorly even to tissue culture treated plastic substrates, a surface that has been specially treated (by a corona discharge) to encourage cell growth, therefore necessitating the addition of an exogenously added ECM protein. When adding biospecies to CPs, two concerns must be addressed. First, the functionality of the biospecies should not be damaged during the polymerization process, nor during subsequent processing steps. Second, the electrical properties of the CP should not suffer due to the incorporation of the biomolecule. Previous incorporation of proteins such as growth factors or ECM proteins into PEDOT films via electropolymerisation has been shown to result in both decreased electroactivity and poor mechanical properties<sup>30, 31</sup> attributed to changes in rate of polymerisation. Incorporation of the ECM component hyaluronic acid (HA) into polypyrrole by electropolymerisation encouraged angiogenesis, but the resulting film was brittle with a four orders of magnitude lower conductivity<sup>27</sup>.

In this study, we set out to determine if CP composites can be a suitable substrate for bovine brain capillary endothelial cell (BBCEC) adhesion, for future use in an *in vitro* model of the BBB with integrated organic electronic devices for measuring the integrity of this tissue layer. To improve the interface between CPs and biorecognition elements, we adopted a previously described procedure to incorporate biomolecules by vapour phase polymerisation (VPP)<sup>31</sup>. We previously described the use of VPP to make PEDOT(TOS):PEG composites, in a manner that not only did not decrease the electrical properties of the CP, but actually increased the conductivity. A particular difficulty to overcome, when using iron(III) as oxidant for PEDOT VPP in combination with a hydrophilic polymer with a large amount of active groups, is to avoid the coordination of Fe(III) to these groups and thereby avoiding the formation of a gel during the mixing of the VPP precursors. This was overcome by changing the solvent system to a combination of water and acetic acid, where the acetic acid preferably coordinate to Fe(III) and thereby prevent gelation. As acetic acid is a weak acid, it was thought to be a good choice to avoid denaturation of biomolecules included in the oxidant solution. In the current study we use this new generic method to show

the feasibility of PEDOT:TOS to be combined with the biomolecule gelatin to promote BBCEC adhesion and growth on composite films. The method was designed to not only maintain the electrical properties of the CP, but also to retain the functionality of the biomolecule. Furthermore, we used an alternative approach in the incorporation of enzymes to PEDOT:TOS and PEDOT:TOS:gelatin that takes place after the VPP process. By using these methods we, first of all, avoid exposure of the enzyme to high temperatures that can result denaturation of the protein and thereby loss of activity, and secondly, immobilize the protein directly into the polymer, something that potentially will result in wiring of the enzyme with the CP and fabrication of third generation biosensors.

### 2.5.1. Characterization of PEDOT:TOS:Gelatin.

To fully characterise PEDOT:TOS:Gelatin composites, a variety of substrates were prepared, including **PEDOT:TOS**, PEDOT:TOS overlays (coated) with either Gelatin or a control protein bovine serum albumin (BSA): **PEDOT:TOS + Gelatin**, **PEDOT:TOS + BSA**, and PEDOT:TOS polymer composites with either gelatin or BSA: **PEDOT:TOS:Gelatin** and **PEDOT:TOS:BSA**. For cell culture experiments, films or proteins alone were coated onto 96-well tissue culture plates and therefore an additional control was included of the plastic well alone (**Well**).

Gelatin is a polypeptide that consists of different protein fractions resulting from the degradation of the inter- and intra-molecular hydrogen bonds that constitute collagen molecules. The particular type of gelatin used was from porcine skin, prepared from acid cured tissue, with an estimated molecular weight of 50-100 kDa. The molecular weight of the EDOT monomer is 142 Da. To verify the presence of gelatin in the composite films, X-ray Photoelectron Spectroscopy (XPS) was performed. Representative traces from XPS are shown in figure 2.4. The appearance of a Nitrogen peak, present in the multiple amine groups of gelatin is obvious in the PEDOT:TOS:Gelatin trace, but absent in the PEDOT:TOS trace. The percentage of the individual elements taken from multiple spots on the composite films is shown in Table S1 in the supplemental information. The average percentages in the PEDOT:TOS film were 28%, 64%, and 7% for Oxygen, Carbon, and Sulphur respectively, with negligible Nitrogen present. The average percentages in the PEDOT:TOS:Gelatin films were 28%, 62%, 4% and 5% for Oxygen, Carbon, Sulphur and Nitrogen respectively.

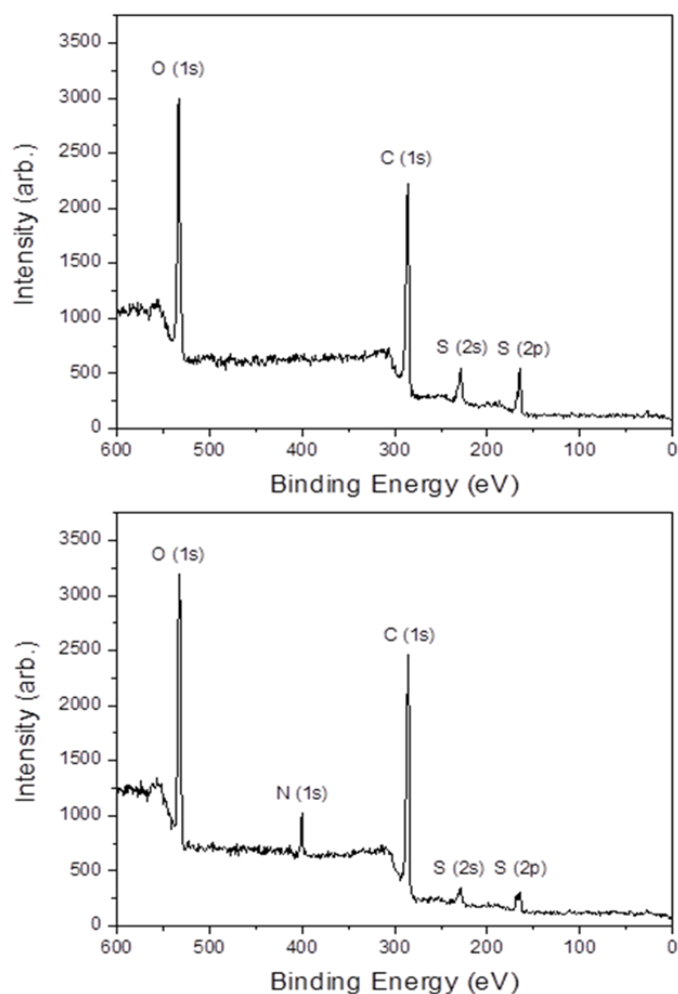


**Figure 2.4:** XPS of PEDOT:TOS top, and PEDOT:TOS:Gelatin (bottom) films.

An evaluation of the electrochemical properties of the films was carried out to ensure that there was no adverse effect on the CP through the introduction of the Gelatin protein. CVs of PEDOT:TOS:Gelatin 1:1 and 1:2 (figure 2.5) showed typical electrochemical characteristics for PEDOT indicating that the incorporation of Gelatin, for these ratios, did not significantly change the electrochemical properties of PEDOT. Conductivity of PEDOT:TOS:Gelatin 1:1 was in the same range as the PEDOT:TOS which was about 310 S/cm. The dilution effect was obvious with PEDOT:TOS:Gelatin 1:2 where the conductivity was about 200 S/cm. This trend is apparently different from PEDOT:TOS:poly(ethylene glycol) (PEDOT:TOS:PEG) where the conductivity increased with higher quantities of PEG in the composites. This is probably due to different interactions between PEDOT-PEG and PEDOT-Gelatin which is being investigated and will be reported elsewhere.

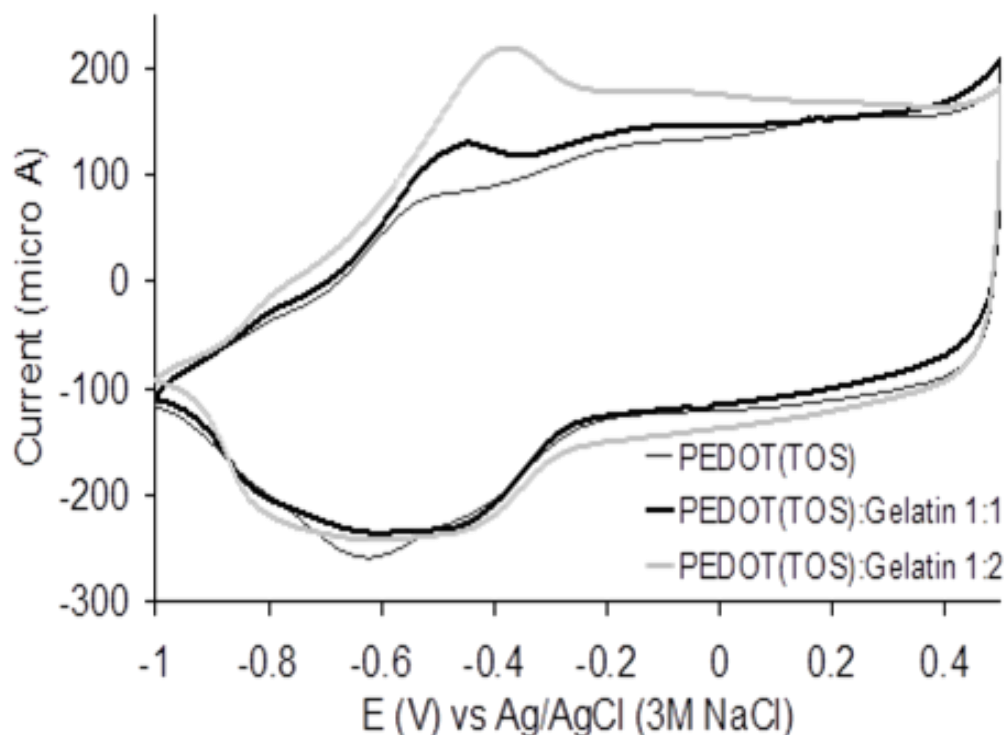


**Figure 2.5:** CVs of PEDOT:TOS, PEDOT:TOS:Gelatin 1:1 and PEDOT:TOS:Gelatin 1:2 in 0.05 M NaTOS pH 6.9 at 20 mV/s.

### 2.5.2. Adhesion of BBB cells

To address the biocompatibility of the prepared composite films, bovine brain capillary endothelial cells (BBCEC) were observed 3 hours after cell seeding (figure 2.6 (1)). On all substrates, the cell seeding concentration was identical. The numbers of cells in each well was relatively constant; cells were isolated and well distributed. We observed a difference in cell morphology depending on the coating used. In the case of the wells alone or coated with gelatin, PEDOT:TOS + gelatin or PEDOT:TOS:Gelatin, the cells are elongated which is a good indicator for initial adhesion, a necessary step for future proliferation. In the case of all other wells, cells remained round and non-elongated, indicating poor adhesion to the substrate. To determine the viability of the BBCEC on the polymer composites, a calcein-AM/propidium iodide assay was carried out (figure 2.6 (2)). Calcein-AM stains the live cells in green and propidium iodide stains the dead cells in red. Again to control rigorously for effects that might be due to a non-specific protein interaction, BSA was included as a control. It is clear from figure 2.6 that BSA does not support cell adhesion and therefore cell viability. In all wells containing BSA, either coated directly on the well (D), overlaid on PEDOT:TOS (F) or in a composite with PEDOT:TOS (H), cells died and formed

clusters. This result was expected, as there is no evidence to suggest that BSA can support the adhesion of cells. In the case of the control well and the PEDOT:TOS films either with overlaid gelatin or with gelatin as a composite, cells were alive and evenly spread out. PEDOT:TOS alone was also unable to support cell growth. This result shows a similar trend to the initial adhesion data. Although exogenously added ECM proteins are thought to be important specifically during the adhesion process, after which cells usually produce their own adhesion proteins, the stability of the gelatin within the film was also determined by a QCM swelling experiment. The results show that the composite films had a water uptake in the same level as PEDOT:TOS and PEDOT:TOS:PEG and confirm that PEDOT:TOS:Gelatin films are not disintegrating over the testing period.

The MTT assay reflects the level of cell metabolism<sup>60</sup>. The results for the MTT assay for viability of growth of BBECs on the tested films are shown with the relative cell growth rates (figure 2.6). As described previously, the MTT is used as an indirect measurement to ensure that despite multiple wash steps in both ethanol and PBS, that compounds are not released into the cell medium over time. The indirect test was designed to investigate changes in cell metabolism caused by substances that may leach out of the PEDOT:TOS films (such as gelatin fragments, tosylate ions and unpolymerised EDOT monomers). The viability for the growth rate of BBECs is determined by measuring the absorbance of the formazan solution. Substrates coated with PEDOT:TOS +/- biomolecules were submerged in media for one week. This exposed medium was then used to culture BBCEC, previously seeded and cultured in unexposed media. Results shown in figure 2.6 indicate that although the wells alone (tissue culture treated plastic (2)) supports growth of BBCEC cells, wells coated with gelatin (1) have a greater relative growth rate. In addition, when gelatin was added to PEDOT:TOS either by overlaying (5) or in a composite (7), viability of cells cultured using the exposed media was decreased only slightly compared to that of control cells cultured with unexposed media. However as was noted for the adhesion and viability assays in figure 2.6 2, BSA was unable to support cell growth either coated directly onto the well, nor integrated with PEDOT:TOS as an overlay or as a composite. As before, PEDOT:TOS alone did not support cell growth.

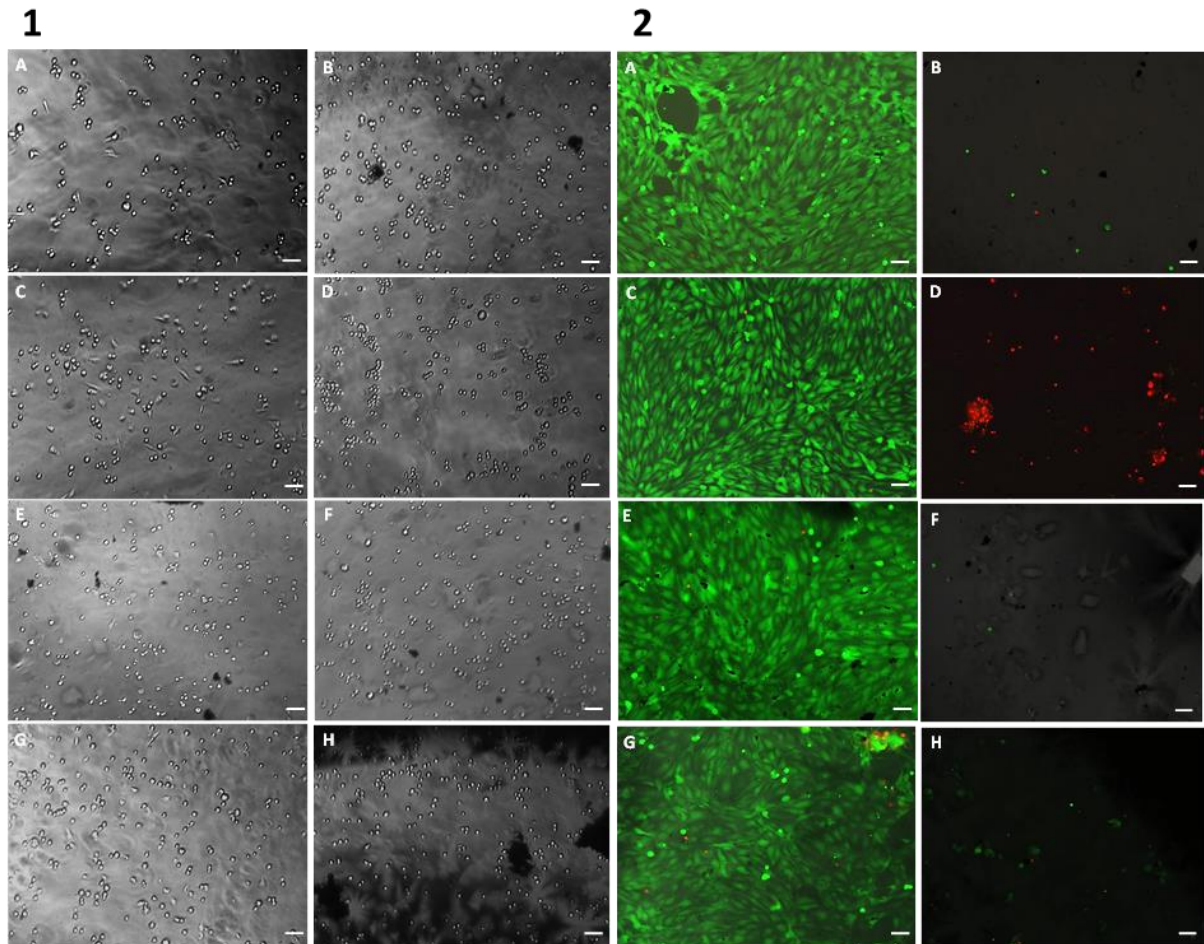


**Figure 2.6:** Initial adhesion (1) and viability (2) of BBCEC observed 3 hours and 5 days after seeding on 96-well plates +/- polymer composite coating. Wells are as follows: A) Well, B) PEDOT:TOS, C) Gelatin, D) BSA, E) PEDOT:TOS+Gelatin, F) PEDOT:TOS+BSA, G) PEDOT:TOS:Gelatin, H) PEDOT:TOS:BSA. For initial adhesion study images were taken by phase contrast microscopy. For viability assay cells live cells stained with calcein-AM (green) and dead cells with propidium iodide (red). Scale bar = 50 $\mu$ m.

### 2.5.3. Stuffing of enzymes in PEDOT:TOS

Another type of applications in which CPs have been extensively used are as enzymatic sensors. A well-known example is a glucose sensor. The electrochemical glucose sensor developed by Clark *and Lyons* consisted of an enzyme, glucose oxidase (GOx), entrapped by a semipermeable membrane on top of an oxygen electrode<sup>61</sup>. GOx catalyzes the conversion of glucose to hydrogen peroxide in the presence of oxygen through redox reactions, and in turn the hydrogen peroxide is reduced into water at the negatively charged Pt electrode cathode or oxidized again back to oxygen if the potential of the Pt electrode is positive. The use of Pt is necessary because of its high catalytic properties in the decomposition of hydrogen peroxide. These types of biosensors, due to the consumption of oxygen to water in the reduction process, limit the stability and accuracy of the sensor. Additionally, the need of large scale production of glucose sensor necessitated the replacement of Pt, owing to its high cost. To overcome such limitations redox active species such as ferrocene, were employed as mediators. Owing to their low oxidation potentials these mediators allowed the fabrication of biosensors using as electrodes alternative to Pt metals. Thus, by using fabrication processes such as screen printing large scale production of glucose sensors with entrapped enzymes and mediators on top of electrodes have been realized. Since, however, these redox active species are small molecules and they are immobilized by entrapment on top of the electrodes, the utilization of these sensor sort-term measurements. Furthermore, binding these redox active species into polymers and wiring the active site of the enzyme has realized direct electron transfer and these type of biosensors is called mediator-less or 3<sup>rd</sup> generation biosensors. Heller *et al.*, demonstrated electrical connection of the active site of the GOx with a redox active polymer based on osmium complexes, and by covalently binding the enzyme to the polymer resulted stable glucose sensors<sup>62</sup>. Additionally, alternative materials such as carbon nanotubes have been used for wiring with enzymes. CPs, because of their semi-metallic properties, can be used as alternative materials to metals for the fabrication of electrodes. Electro polymerized PEDOT has been shown to decrease the impedance of electrodes by increasing the surface area, and thus increasing signal quality. In the case of enzymatic sensors, furthermore, wiring of the enzyme with the conducting polymer has not been explored thoroughly.

To insure no degradation of the enzyme during the VPP process, which includes high temperatures and organic solvents, the immobilization of these fragile biomolecules into PEDOT:TOS was carried out in the rinsing step, after polymerizing the film. Specifically, The VPP polymerization results in films with

thicknesses in the order of 20  $\mu\text{m}$ , owing to the remaining iron(II) and un-polymerized EDOT crystals. During the rinsing step, the iron(II) crystals were washed away in the presence of mild organic solvents such as ethanol. Thus, the film collapses, resulting in thickness of the final film in the order of 200 nm. Alternatively, if the rinsing solution contains biomolecules, they can be entrapped into the polymer during the film's collapsing step. Figure 2.7a-b shows SEM plane view images of pristine (a) PEDOT:TOS and (b) PEDOT:TOS:GOx, which means that the first film was washed with phosphate buffer and the second one with phosphate buffer containing an enzyme (glucose oxidase), respectively. In order to ensure complete removal of the iron(II) oxidant crystals, the rinsing process was carried out for one hour and repeated at least three times. After the immobilisation of the enzymes, the films were rinsed with buffer to remove loosely bound enzymes. In both figures 2.7a and 2.7b we observe the creation of salt crystals on top of the film. In figure 2.7a we also observe the creation of cracks in the film, which are created during the formation of the salt crystals, highlighting the fragility of the film during the fabrication process. On the other hand, the presence of enzymes during the rinsing step of the film improves its stability and integrity (figure 2.7b) and no cracks are observed. Figure 2.7c shows a cross-section of the PEDOT:TOS film after the rinsing step. The thickness of the polymer is 500 nm and the surface is smooth. On the other hand, in figure 2.7d, which is a cross-section of PEDOT:TOS:GOx, we observe blobs of enzymes on top of the film with thicknesses at around 500 nm. This validates the presence of enzymes after thorough rinsing, and thus a successful immobilization.

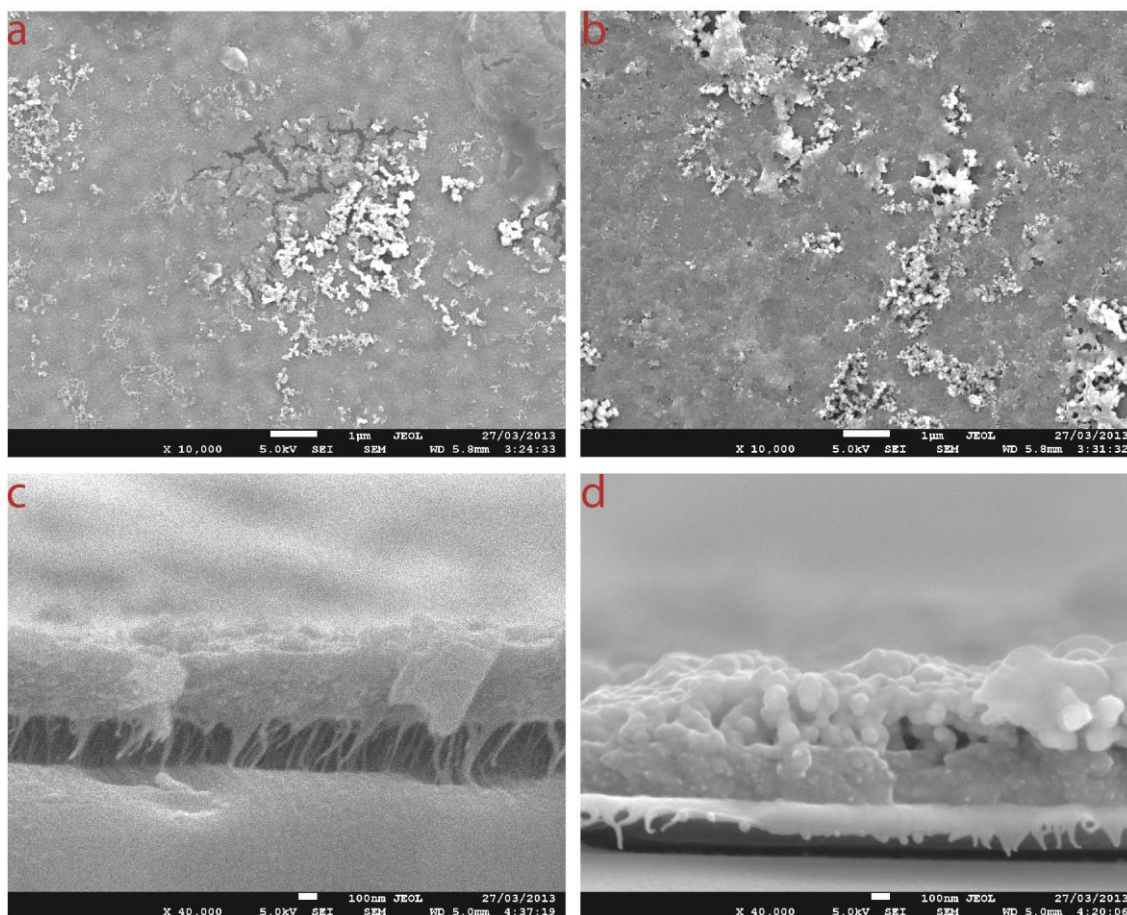


**Figure 2.7:** SEM images of stuffing enzyme to PEDOT:TOS (a-b) plane view of pedot:tos and pedot:tos:gox scale bar 1  $\mu\text{m}$ . (c-d) cross section of pedot:tos and pedot:tos:gox scale bar 100 nm.

Apart from their presence in the conducting polymer, an important parameter of the functionalization is the wiring of the enzyme to the conducting polymer. In order to test the direct electron transfer from the active site of the enzyme to the electrode, VPP PEDOT:TOS and PEDOT:TOS:GOx were coated on top of a gold electrode and a cyclic voltammetry was performed in phosphate buffer. Figure 2.8 shows a CV of PEDOT:TOS and PEDOT:TOS:GOx. In the case of PEDOT:TOS:GOx, a reduction and oxidation peak is observed at the negative potential  $V = -0.5$  vs Ag/AgCl. The redox peaks are not observable in the case of PEDOT:TOS electrodes. More analytically, the reduction peak at the negative potential shows that the active site of the enzyme called Flavin adenine dinucleotide (FAD) accepts an electron from the electrode and by its turn returns the electron back to the electrode when the potential of the electrode is in more positive potentials than  $-0.5$  V vs Ag/AgCl. Importantly, no mediator has been used in the electrolyte and because the enzyme is stuffed or is in the close

proximity with the CP, a direct electron transfer is observed. This shows that the FAD of the enzyme is wired to the PEDOT:TOS and can possibly result a mediator-less glucose sensor.

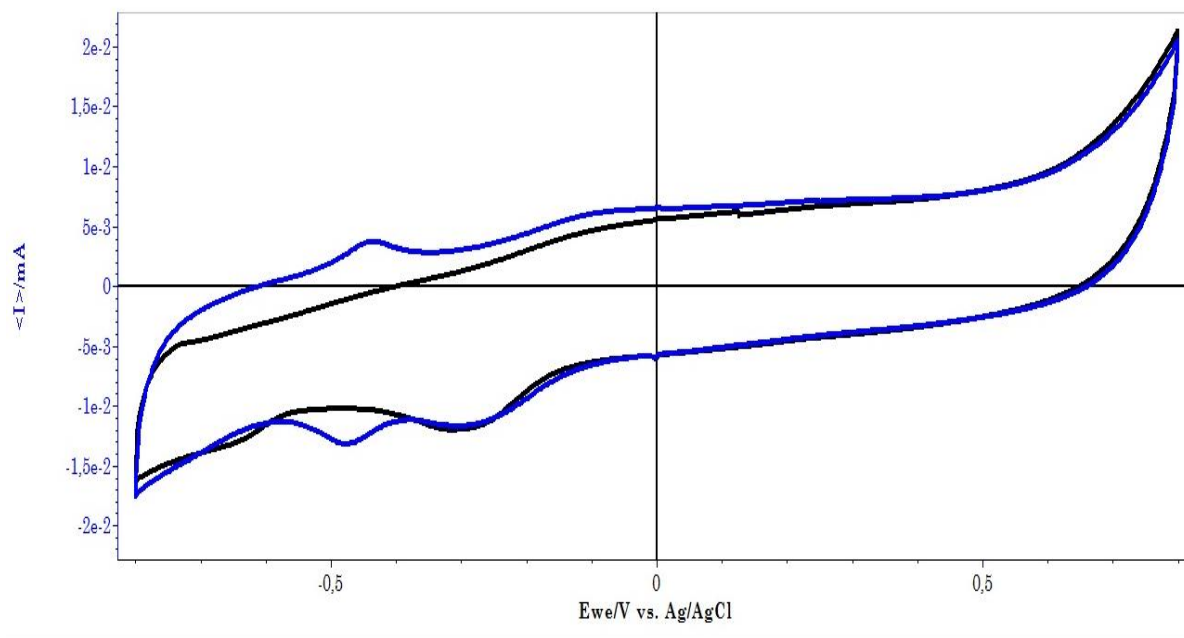


**Figure 2.8:** CV of PEDOT:TOS (black line) and PEDOT:TOS:GOx (blue line) in phosphate buffer. The cycling potential is between -0.8 and +0.8 V vs Ag/AgCl.

In order to test the functionality of the enzyme to the oxidation of the corresponding substrate, for example in the case of GOx in the presence of glucose, a CV of the functionalized electrode was performed. Figure 2.9 shows a CV of PEDOT:TOS:GOx in phosphate buffer, and after extensive flow of N<sub>2</sub> to remove O<sub>2</sub>, in the presence and absence of glucose. No difference is observed between the two curves indicating that the enzyme is not active. Possible reasons are the following: First, due to the stuffing process, the conformation of the enzyme can change; thereby affecting its catalytic activity. Second, a conformational change can be caused by the local acidity of the iron(II) tosylate. In order to protect the enzyme conformation when the collapse of the film takes place, gelatin was employed to the VPP process. The incorporation of the enzyme in PEDOT:TOS:Gelatin took place and a further CV in the absence and presence of glucose was carried out. Unfortunately, no glucose oxidation was observed in this case either as showed.

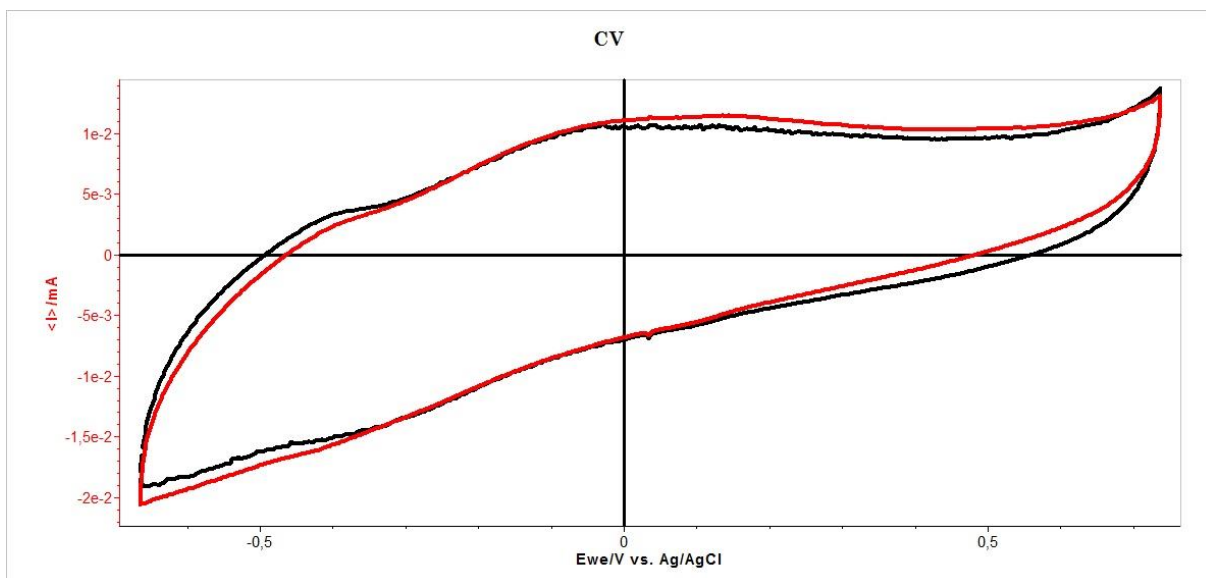


**Figure 2.9:** CV of PEDOT:TOS:GOx in the absence (black curve) and presence (red curve) of glucose at concentration of 10 mM in phosphate buffer. The cycling potential is between -0.7 and + 0.7 V vs Ag/AgCl.

## 2.6. Discussion

Our results show that PEDOT:TOS:Gelatin composites maintain not only electrochemical properties of the CP, but also retain the functionality of the incorporated biomolecule. We demonstrate that the gelatin composite materials had relatively little change in their characteristics with respect to the morphology of PEDOT:TOS. The PEDOT:TOS:Gelatin composite materials allowed the growth of BBECs while the PEDOT:TOS films did not. The cell growth on PEDOT:TOS:Gelatin composite films was shown to be specific to the gelatin protein, as PEDOT:TOS:BSA films that were used as a control could not support cell growth. This demonstrates that the mediation of cell adhesion was as a result of the specific functionality of the gelatin protein, and not a non-specific protein effect, implying that the VPP method used was non-destructive to the protein. Although a complete characterization of molecular interactions between the cells and the polymer surface is warranted, our results support the use of CP composites in tissue engineering and open the possibility of controlling cell behavior electrically using such composites.

Furthermore, we carried out the incorporation of redox active enzymes into the conducting polymer in order to facilitate wiring of the enzyme's active site to the electrode. The functionalization of the enzyme took place after the polymerization process, during the rinsing step of the film. A direct electron transfer from the

enzyme to the electrode and vice versa was observed, a promising step for the potential to fabricate 3<sup>rd</sup> generation enzymatic sensors or biofuel cell applications. In the first case, the enzyme shows no catalytic activities upon addition of the substrate, probably because the process is affecting its conformation, or the active site is not accessible. Further research is necessary in order to lead to the fabrication of a reliable mediator-free enzymatic sensor.

## 2.7. Experimental section

*Vapor phase polymerisation of PEDOT:TOS and PEDOT:TOS composite films:* To promote adhesion between the final PEDOT film and the substrate, glass slides were coated with plasma polymerised maleic anhydride prior to deposition of the oxidant solution. PEDOT:TOS:Gelatin composites were prepared by dissolving 419 mg Fe(III)TOS in 0.80 ml of 1:1.67 water:acetic acid (v/v) mixture in a vial and 24  $\mu$ l pyridine was added and vigorously stirred. In a separate vial, gelatin (35.4 mg and 70 mg for PEDOT:TOS:Gelatin 1:1 and 1:2 ratios, respectively) was dissolved in 0.625 ml of 1:1.5 water:acetic acid (v/v). Gelatin was used at 1:1 and 1:2 for the CV experiments but otherwise the ratio was maintained at 1:1 throughout. The gelatin was omitted for PEDOT:TOS. The oxidant mixture was then added to the gelatin solution and stirred to mix thoroughly. The oxidant solution was spun onto the substrates (either glass slides or 96-well tissue culture treated plastic plates) at 1500 rpm for 30 s and placed directly in the vapor phase polymerization chamber without a drying step. The vaporization chamber, containing an EDOT monomer (HD Stark or Yacoo Chemical Co.,Ltd.), was kept in an oven at 70 °C, at ambient pressure. EDOT was allowed to polymerize on the coated substrates for 30 min to about an hour. After polymerisation the film was cooled to room temperature and washed with ethanol three times to remove Fe(II)Tos, excess Fe(III)Tos and unpolymerized EDOT monomer. Protein coated substrates were prepared by depositing gelatin (2  $\mu$ g/ml in water) or BSA (5  $\mu$ g/ml in water) onto substrates (either glass slides or 96-well tissue culture treated plastic plates or already prepared PEDOT(TOS) films) and incubating for 1 hour at 37 °C. For contact angle experiments alternative samples were prepared by spin-coating the protein samples on the substrate and then baking at 70°C for 30 minutes.

*XPS:* PEDOT:TOS or PEDOT:TOS:Gelatin 1:1 composites were coated on glass slides. XPS measurements were carried out on a SSI S-Probe XPS Spectrometer. *Cyclic Voltammetry (CV):* PEDOT:TOS or PEDOT:TOS:Gelatin coated Au mylar was scanned in 0.05 M NaTOS pH 6.9 (bubbled with nitrogen for about 10 min prior to scanning) at 20 mV/s. Ag/AgCl (3M NaCl) and Pt wire were used as

reference and counter electrodes, respectively.

*Cell culture and characterisation of cell growth and proliferation:* Bovine Brain Endothelial Cell (BBECs) were a kind gift of the University Lille Nord de France, U. Artois, BBB Laboratory (LBHE). The BBECs were cultured at 37°C in 5% CO<sub>2</sub> humidified incubators, in DMEM supplemented with 10% heat inactivated newborn calf serum (CS) (Invitrogen) and 10% heat inactivated horse serum (HS) (Invitrogen), 2 mM Glutamine (Glutamax™-1, Invitrogen), 50 µg/ml gentamicin and 1 ng/ml basic fibroblast growth factor (bFGF) (Sigma Aldrich). Cells were detached by trypsinization (0.05% trypsin–EDTA 1X, Invitrogen) and numbers were determined by a cell counter (Scepter handheld automated cell counter, Millipore).

*Cell adhesion and proliferation tests:* A 96-well cell culture dish (approximate area: 0.3 cm<sup>2</sup>) was coated with the CP composites according to the procedure described above. Each coated substrate was sterilized for 20 min in 70% ethanol, rinsed twice in PBS. Cells were seeded at a concentration of 10<sup>3</sup> cells per well. An additional 0.4 mL of DMEM was added to each well. Cell adhesion was observed 3 hours after seeding (Primovert, Carl Zeiss). Adhesion and proliferation were evaluated after 4 days. A calcein-AM/propidium iodide assay was carried out to determine the cell viability (calcein-AM, Sigma) at 1 mg mL<sup>-1</sup> and propidium iodide (propidium iodide solution, Sigma) at 2 mg mL<sup>-1</sup>. To perform these tests, media in the dishes were discarded and the cells were gently rinsed two times with PBS. 0.3 mL of the calcein-AM–PI mixture was added to each well and incubated for 30 min at 37 °C. Fluorescence images were taken (Axio Observer Z1, Carl Zeiss, calcein AM 485 nm/ 535 nm, PI 530 nm/620 nm) and cells were counted to determine viability.

*MTT assay:* The MTT assay (MTT Cell Proliferation Assay Kit, Cayman Chemical) was carried out according to the manufacturer's instructions. Four replicates were evaluated. After 4 days, the media was aspirated and replaced firstly with 100 µl of fresh media supplemented with 10 µl of MTT reagent and the plate was incubated at 37°C for 3 hours. Then 100 µl of crystal dissolving reagent was added to dissolve formazan crystals and the absorbance (A<sub>570nm</sub>) was measured with a spectrophotometer (Infinite, M1000, Tecan). For comparison, the absorbance of formazan solution measured from Gelatin was assigned as a control group. The ratio of the differences in absorbance of the formazan solution between the several groups and the Gelatin control was defined as the relative cell growth rate.

*Immunofluorescence assay:* To investigate the distribution of gelatin throughout the film and surface availability, an anti-gelatin antibody was used. The blocking step was done with PBS-T (0.05% Tween 20 in PBS), 5% non-fat dry milk during

30 min at room temperature. A rabbit polyclonal anti-Gelatin antibody (Mybiosource) was used in PBS for 1 h at room temperature and then Alexa Fluor 568 goat anti-rabbit (Molecular Probes) was added for 1 h at room temperature. Finally, samples were examined with a fluorescent microscope (Axio Observer Z1 Carl Zeiss).

*Scanning Electron Microscopy:* To assess the film morphology, a scanning electron microscopy (SEM, Ultra 55, Carl Zeiss) was involved.

## 2.8. Supplementary Information

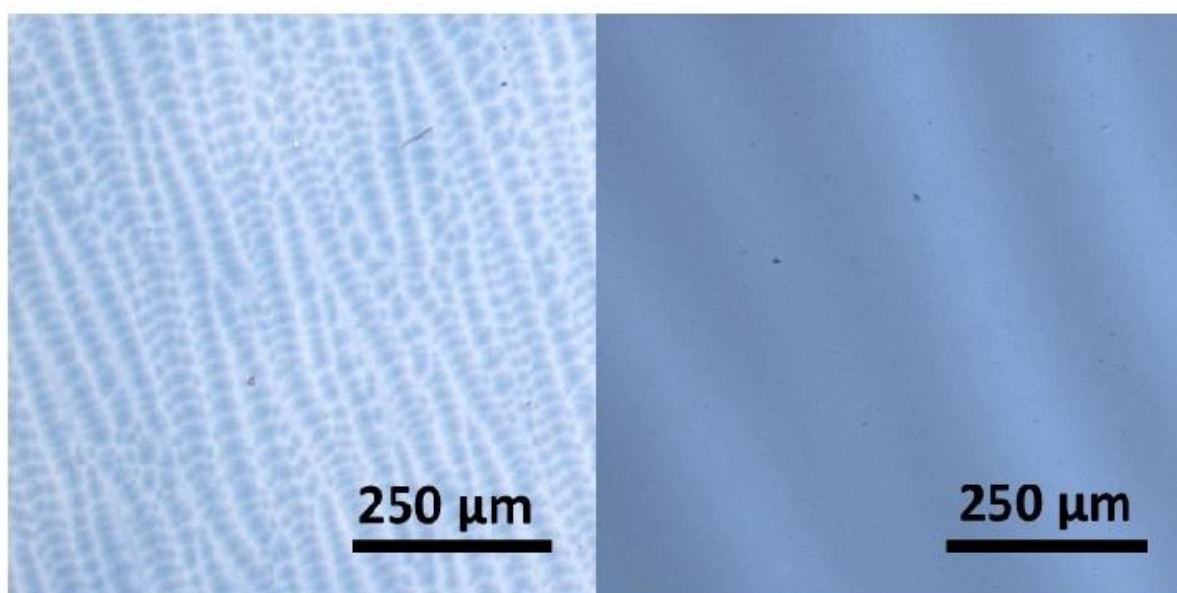


**Figure S2.1:** Image from optical microscope PEDOT:TOS-0PEG (left), PEDOT:TOS-70PEG (right).

## 2.9. References

1. Shirakawa, H., Louis, E. J., Macdiarmid, A. G., Chiang, C. K., and Heeger, A. J. (1977) Synthesis of Electrically Conducting Organic Polymers - Halogen Derivatives of Polyacetylene, (Ch)X, *J Chem Soc Chem Comm*, 578-580.
2. Owens, R. M., and Malliaras, G. G. (2010) Organic Electronics at the Interface with Biology, *Mrs Bull* 35, 449-456.
3. Guimard, N. K., Gomez, N., and Schmidt, C. E. (2007) Conducting polymers in biomedical engineering, *Progress in Polymer Science* 32, 876-921.
4. Kim D. H., A. M. R. R.-B. S., Povlich S., Spanninga S., Hendricks J., Martin D. C. (2007) Soft, fuzzy, and bioactive conducting polymers for improving the chronic performance of neural prosthetic devices, In *Indwelling neural implants: Strategies for contending with the in vivo environment. CRC Press (2008)*. (M., R. W., Ed.), CRC Press, Durham, North Carolina.
5. Kim, D. H., Wiler, J. A., Anderson, D. J., Kipke, D. R., and Martin, D. C. (2010) Conducting polymers on hydrogel-coated neural electrode provide sensitive neural recordings in auditory cortex, *Acta Biomaterialia* 6, 57-62.
6. Abidian, M. R., Corey, J. M., Kipke, D. R., and Martin, D. C. (2010) Conducting-Polymer Nanotubes Improve Electrical Properties, Mechanical Adhesion, Neural Attachment, and Neurite Outgrowth of Neural Electrodes, *Small* 6, 421-429.
7. Kim, D. H., Richardson-Burns, S. M., Hendricks, J. L., Sequera, C., and Martin, D. C. (2007) Effect of immobilized nerve growth factor on conductive polymers: Electrical properties and cellular response, *Adv. Funct. Mater.* 17, 79-86.
8. Poole-Warren, L., Lovell, N., Baek, S., and Green, R. (2010) Development of bioactive conducting polymers for neural interfaces, *Expert Review of Medical Devices* 7, 35-49.
9. Wong, J. Y., Langer, R., and Ingber, D. E. (1994) Electrically conducting polymers can noninvasively control the shape and growth of mammalian cells, *Proc Natl Acad Sci U S A* 91, 3201-3204.
10. Wan, A. M. D., Brooks, D. J., Gumus, A., Fischbach, C., and Malliaras, G. G. (2009) Electrical control of cell density gradients on a conducting polymer surface, *Chemical Communications*, 5278-5280.
11. Salto, C., Saindon, E., Bolin, M., Kancierzewska, A., Fahlman, M., Jager, E. W. H., Tengvall, P., Arenas, E., and Berggren, M. (2008) Control of Neural Stem Cell Adhesion and Density by an Electronic Polymer Surface Switch, *Langmuir* 24, 14133-14138.
12. Simon, D. T., Kurup, S., Larsson, K. C., Hori, R., Tybrandt, K., Goiny, M., Jager, E. H., Berggren, M., Canlon, B., and Richter-Dahlfors, A. (2009) Organic electronics for precise delivery of neurotransmitters to modulate mammalian sensory function, *Nature Materials* 8, 742-746.

13. Isaksson, J., Kjall, P., Nilsson, D., Robinson, N. D., Berggren, M., and Richter-Dahlfors, A. (2007) Electronic control of Ca<sup>2+</sup> signalling in neuronal cells using an organic electronic ion pump, *Nature Materials* 6, 673-679.
14. Tybrandt, K., Larsson, K. C., Richter-Dahlfors, A., and Berggren, M. (2010) Ion bipolar junction transistors, *Proceedings of the National Academy of Sciences of the United States of America* 107, 9929-9932.
15. Kittlesen, G. P., White, H. S., and Wrighton, M. S. (1984) Chemical Derivatization of Microelectrode Arrays by Oxidation of Pyrrole and N-Methylpyrrole - Fabrication of Molecule-Based Electronic Devices, *J. Am. Chem. Soc.* 106, 7389-7396.
16. White, H. S., Kittlesen, G. P., and Wrighton, M. S. (1984) Chemical Derivatization of an Array of 3 Gold Microelectrodes with Polypyrrole - Fabrication of a Molecule-Based Transistor, *J. Am. Chem. Soc.* 106, 5375-5377.
17. Mabeck, J. T., and Malliaras, G. G. (2006) Chemical and biological sensors based on organic thin-film transistors, *Anal. Bioanal. Chem.* 384, 343-353.
18. Bernards, D. A., Malliaras, G. G., Toombes, G. E. S., and Gruner, S. M. (2006) Gating of an organic transistor through a bilayer lipid membrane with ion channels, *Appl Phys Lett* 89, -.
19. Yang, S. Y., Cicoira, F., Byrne, R., Benito-Lopez, F., Diamond, D., Owens, R. M., and Malliaras, G. G. (2010) Electrochemical transistors with ionic liquids for enzymatic sensing, *Chem Commun (Camb)* 46, 7972-7974.
20. Yang S.Y., C. F., Byrne R., Benito-Lopez F., Diamond D., Owens R.M., Malliaras G. (2010) Integration of organic electrochemical transistors with ionic liquids for enzymatic sensing.
21. Green, J. M., Pritchett, R. C., Tucker, D. C., Crews, T. R., and McLester, J. R. (2004) Sweat lactate response during cycling at 30 degrees C and 18 degrees C WBGT, *J Sports Sci* 22, 321-327.
22. Lin, P., Yan, F., Yu, J. J., Chan, H. L. W., and Yang, M. (2010) The Application of Organic Electrochemical Transistors in Cell-Based Biosensors, *Adv. Mater.* 22, 3655-+.
23. Zhang, L., Stauffer, W. R., Jane, E. P., Sammak, P. J., and Cui, X. Y. T. (2010) Enhanced Differentiation of Embryonic and Neural Stem Cells to Neuronal Fates on Laminin Peptides Doped Polypyrrole, *Macromolecular Bioscience* 10, 1456-1464.
24. Teixeira-Dias, B., del Valle, L. J., Estrany, F., Mano, J. F., Reis, R. L., and Alemán, C. (2011) Dextrin- and Conducting-Polymer-Containing Biocomposites: Properties and Behavior as Cellular Matrix, *Macromol Mater Eng*, 359-368.
25. Xiao, Y., Li, C. M., Wang, S., Shi, J., and Ooi, C. P. (2010) Incorporation of collagen in poly(3,4-ethylenedioxythiophene) for a bifunctional film with high bio- and electrochemical activity, *Journal of Biomedical Materials Research Part A* 92A, 766-772.
26. Stauffer, W. R., and Cui, X. T. (2006) Polypyrrole doped with 2 peptide sequences from laminin, *Biomaterials* 27, 2405-2413.
27. Collier, J. H., Camp, J. P., Hudson, T. W., and Schmidt, C. E. (2000) Synthesis and characterization of polypyrrole-hyaluronic acid composite

- biomaterials for tissue engineering applications, *Journal of Biomedical Materials Research* 50, 574-584.
28. Teixeira-Dias, B., del Valle, L. J., Aradilla, D., Estrany, F., and Alemán, C. (2011) A Conducting Polymer/Protein Composite with Bactericidal and Electroactive Properties, *Macromol Mater Eng*, 427-436.
  29. Cosnier, S. (1999) Biomolecule immobilization on electrode surfaces by entrapment or attachment to electrochemically polymerized films. A review, *Biosens. Bioelectron.* 14, 443-456.
  30. Asplund, M. L. M., Thaning, E. M., Nyberg, T. A., Inganas, O. W., and von Hoist, H. (2010) Stability of Poly(3,4-ethylene dioxothiophene) Materials Intended for Implants, *Journal of Biomedical Materials Research Part B-Applied Biomaterials* 93B, 407-415.
  31. Green, R. A., Lovell, N. H., and Poole-Warren, L. A. (2010) Impact of co-incorporating laminin peptide dopants and neurotrophic growth factors on conducting polymer properties, *Acta Biomaterialia* 6, 63-71.
  32. Lee, J. W., Serna, F., Nickels, J., and Schmidt, C. E. (2006) Carboxylic acid-functionalized conductive polypyrrole as a bioactive platform for cell adhesion, *Biomacromolecules* 7, 1692-1695.
  33. Winther-Jensen, B., Chen, J., West, K., and Wallace, G. (2004) Vapor phase polymerization of pyrrole and thiophene using iron(III) sulfonates as oxidizing agents, *Macromolecules* 37, 5930-5935.
  34. Fabretto, M., Jariego-Moncunill, C., Autere, J.-P., Michelmore, A., Short, R. D., and Murphy, P. (2011) High conductivity PEDOT resulting from glycol/oxidant complex and glycol/polymer intercalation during vacuum vapour phase polymerisation, *Polymer* 52, 1725-1730.
  35. Winther-Jensen, B., Fraser, K., Ong, C., Forsyth, M., and MacFarlane, D. R. (2010) Conducting Polymer Composite Materials for Hydrogen Generation, *Adv Mater* 22, 1727-1730.
  36. Winther-Jensen, B., Knecht, T., Ong, C., Vongsvivut, J., and Clark, N. (2011) Inhomogeneity Effects in Vapor Phase Polymerized PEDOT: A Tool to Influence Conductivity, *Macromol Mater Eng* 296, 185-189.
  37. Cha, T., Guo, A., Jun, Y., Pei, D., and Zhu, X.-Y. (2004) Immobilization of oriented protein molecules on poly(ethylene glycol)-coated Si(111), *PROTEOMICS* 4, 1965-1976.
  38. Wu, X. Y., Xie, Q. A., He, Z. G., and Wang, D. X. (2008) Free and forced Rossby waves in the western South China Sea inferred from Jason-1 satellite altimetry data, *Sensors-Basel* 8, 3633-3642.
  39. Ademovic, Z., Wei, J., Winther-Jensen, B., Hou, X., and Kingshott, P. (2005) Surface Modification of PET Films Using Pulsed AC Plasma Polymerisation Aimed at Preventing Protein Adsorption, *Plasma Processes and Polymers* 2, 53-63.
  40. Fabretto, M., Mueller, M., Zuber, K., and Murphy, P. (2009) Influence of PEG-ran-PPG Surfactant on Vapour Phase Polymerised PEDOT Thin Films, *Macromol Rapid Comm* 30, 1846-1851.
  41. Fabretto, M., Autere, J.-P., Hoglinger, D., Field, S., and Murphy, P. (2011) Vacuum vapour phase polymerised poly(3,4-ethylenedioxythiophene) thin films for use in large-scale electrochromic devices, *Thin Solid Films* 519, 2544-2549.

42. Zuber, K., Fabretto, M., Hall, C., and Murphy, P. (2008) Improved PEDOT conductivity via suppression of crystallite formation in Fe(III) tosylate during vapor phase polymerization, *Macromol Rapid Comm* **29**, 1503-1508.
43. Winther-Jensen, B., Breiby, D. W., and West, K. (2005) Base inhibited oxidative polymerization of 3,4-ethylenedioxythiophene with iron(III)tosylate, *Synthetic Met* **152**, 1-4.
44. Bernardis, D. A., and Malliaras, G. G. (2007) Steady-state and transient behavior of organic electrochemical transistors, *Adv. Funct. Mater.* **17**, 3538-3544.
45. Wang, Y. S., Weinacker, H., and Koch, B. (2008) A Lidar point cloud based procedure for vertical canopy structure analysis and 3D single tree modelling in forest, *Sensors-Basel* **8**, 3938-3951.
46. del Valle, L. J., Aradilla, D., Oliver, R., Sepulcre, F., Gamez, A., Armelin, E., Aleman, C., and Estrany, F. (2007) Cellular adhesion and proliferation on poly(3,4-ethylenedioxythiophene): Benefits in the electroactivity of the conducting polymer, *Eur Polym J* **43**, 2342-2349.
47. Hynes, R. O. (2002) Integrins: bidirectional, allosteric signaling machines, *Cell* **110**, 673-687.
48. Lim, J. Y., Dreiss, A. D., Zhou, Z. Y., Hansen, J. C., Siedlecki, C. A., Hengstebeck, R. W., Cheng, J., Winograd, N., and Donahue, H. J. (2007) The regulation of integrin-mediated osteoblast focal adhesion and focal adhesion kinase expression by nanoscale topography, *Biomaterials* **28**, 1787-1797.
49. Discher, D. E., Janmey, P., and Wang, Y. L. (2005) Tissue cells feel and respond to the stiffness of their substrate, *Science* **310**, 1139-1143.
50. Engler, A. J., Sen, S., Sweeney, H. L., and Discher, D. E. (2006) Matrix elasticity directs stem cell lineage specification, *Cell* **126**, 677-689.
51. Bernacki, J., Dobrowolska, A., Nierwinska, K., and Malecki, A. (2008) Physiology and pharmacological role of the blood-brain barrier, *Pharmacological reports : PR* **60**, 600-622.
52. Saha, A., Sarkar, C., Singh, S. P., Zhang, Z. J., Munasinghe, J., Peng, S. Y., Chandra, G., Kong, E. Y., and Mukherjee, A. B. (2012) The blood-brain barrier is disrupted in a mouse model of infantile neuronal ceroid lipofuscinosis: amelioration by resveratrol, *Human Molecular Genetics* **21**, 2233-2244.
53. Ma, S. H., Lepak, L. A., Hussain, R. J., Shain, W., and Shuler, M. L. (2005) An endothelial and astrocyte co-culture model of the blood-brain barrier utilizing an ultra-thin, nanofabricated silicon nitride membrane, *Lab on a chip* **5**, 74-85.
54. Svennersten, K., Bolin, M. H., Jager, E. W., Berggren, M., and Richter-Dahlfors, A. (2009) Electrochemical modulation of epithelia formation using conducting polymers, *Biomaterials* **30**, 6257-6264.
55. Abidian, M. R., Kim, D. H., and Martin, D. C. (2006) Conducting-polymer nanotubes for controlled drug release, *Adv. Mater.* **18**, 405-+.
56. Persson, K. M., Karlsson, R., Svennersten, K., Loffler, S., Jager, E. W., Richter-Dahlfors, A., Konradsson, P., and Berggren, M. (2011) Electronic control of cell detachment using a self-doped conducting polymer, *Adv Mater* **23**, 4403-4408.

57. Gilmore, K. J., Kita, M., Han, Y., Gelmi, A., Higgins, M. J., Moulton, S. E., Clark, G. M., Kapsa, R., and Wallace, G. G. (2009) Skeletal muscle cell proliferation and differentiation on polypyrrole substrates doped with extracellular matrix components, *Biomaterials* 30, 5292-5304.
58. Nickels, J. D., and Schmidt, C. E. (2012) Surface modification of the conducting polymer, polypyrrole, via affinity peptide, *Journal of biomedical materials research. Part A*.
59. Gumus, A., Califano, J. P., Wan, A. M. D., Huynh, J., Reinhart-King, C. A., and Malliaras, G. G. (2010) Control of cell migration using a conducting polymer device, *Soft Matter* 6, 5138-5142.
60. HuveneersOorsprong, M. B. M., Hoogenboom, L. A. P., and Kuiper, H. A. (1997) The use of the MTT test for determining the cytotoxicity of veterinary drugs in pig hepatocytes, *Toxicology in Vitro* 11, 385-392.
61. Wang, J. (2008) Electrochemical Glucose Biosensors, *Chemical Reviews* 108, 814-825.
62. Heller, A. (1992) Electrical Connection of Enzyme Redox Centers to Electrodes, *J Phys Chem-Us* 96, 3579-3587.

## Chapter 3

---

### 3. A novel biofunctionalization route for solution processed PEDOT:PSS based devices.

Biofunctionalization is an essential step in the fabrication of a biosensor or biomedical device. For biosensor operation, the so-called 'biorecognition element' is usually immobilized on the active area of the transducer in order for the target molecule to be captured and for signal transduction to occur. For biomedical devices, active areas are increasingly being coated or functionalized with biomolecules to improve biocompatibility and facilitate integration with living systems for both *in vitro* and *in vivo* applications. A variety of methods such as passive adhesion and electrostatic interactions may be used, however for longer lifetime and better control of immobilisation, covalent interactions are preferable. For traditional electronic materials such as silicon or metal electrodes, a variety of covalent functionalization methods have been developed ranging from silanization, thiolation and the ubiquitous EDC/NHS chemistry for coupling of the commonly found biological amine and carboxyl functional groups<sup>1, 2</sup>.

A rapidly emerging area of research in bioelectronics is the use of conducting polymers (CPs) as an alternative to traditional electronic materials. The field of organic bioelectronics has gained tremendous momentum in the past decade<sup>3, 4</sup>. In particular, the use of (CPs) to interface with biology has been shown to be advantageous for numerous reasons including potential low cost of the materials, mechanical flexibility, mixed electronic/ionic conductivity, improved interfaces and tunability of the materials due to their organic nature<sup>5, 6</sup>. Applications for organic electronic devices in biology have ranged from relatively simple biosensing<sup>7, 8</sup> to more complex applications for use in drug delivery<sup>9</sup>, neurotransmitter delivery<sup>10</sup>, toxicology<sup>11</sup>, and neural probes<sup>12, 13</sup>. Devices of particular interest in biosensing are organic electrochemical transistors (OECTs) which take advantage of the mixed electronic/ionic conductivity of CPs, in order to achieve efficient ion-to-electron transduction<sup>6</sup>.

The polythiophene PEDOT doped with the water dispersible polystyrene sulfonate (PSS) or with the tosylate anion (TOS), is currently the most commonly used conducting polymer in organic bioelectronic applications. This is due to a combination of factors including good thermal, electrochemical stability, relatively high conductivity<sup>14</sup>, and demonstrated biocompatibility<sup>15, 16</sup>, compared with other CPs based on polypyrrole and polyaniline. A number of different methods exist for deposition of PEDOT films; solution deposition, electropolymerization, and vapor phase polymerization. Previous work on incorporation of biomolecules into either the bulk or onto the surface of PEDOT has employed the latter techniques, for example, incorporating biomolecules as dopants in the electrolyte solution during polymerization<sup>17, 18</sup>. We recently reported a novel method for incorporation of gelatin into films of vapor phase polymerised PEDOT doped with tosylate (TOS), maintaining both the electrochemical properties of the conducting polymer, and also the functionality of the biomolecule. A recent study on PEDOT, showed the use of a modified dopant (PSS-maleic acid) could generate films with good electrical performance but also with sufficient carboxyl groups for subsequent biofunctionalization<sup>19</sup>. PEDOT:PSS is often chosen because it is commercially available as a liquid dispersion suitable for solution-based deposition methods such as spin coating and inkjet printing<sup>20, 21</sup>. One disadvantage of the commercially available formulation of PEDOT:PSS is that it is difficult to perform chemistry on an already cured film, moreover, since the PSS is in excess with respect to the PEDOT<sup>22</sup>, commonly targeted chemical modification of PEDOT would lead to inhomogeneous functionalization and disruption of conductivity. The most desirable approach for biofunctionalization is for the biomolecule to be added after film processing steps in order to avoid exposure to solvents or high temperatures that are required during fabrication, but may cause biomolecule denaturation.

Herein we demonstrate the an easy-to-use method for the covalent linkage of biomolecules to films of PEDOT:PSS deposited from commercially available dispersion. We show the successful, large area functionalization of PEDOT:PSS films with different biomolecule types: the enzyme glucose oxidase (GOx) and the extracellular matrix derived polypeptide poly-L-lysine (PLL). We demonstrate that the resulting conducting polymer devices maintain excellent electrical properties. Finally, we show not only the functionality of these immobilized biomolecules, but also applications for the functionalized films.

### 3.1.1. Biofunctionalization strategy using PVA and silane

Silanization is a widely used functionalization technique for glass or metal oxide surfaces. A silane reagent can form a covalent linkage with free hydroxyl groups on the surface via a condensation reaction. The most useful silanization reagents are heterobifunctional, containing an alkoxy silane as well as an organic functional group that can selectively bind a second organic molecule. Different examples of silanization reagents include aminosilanes (such as APTES (3-aminopropyltriethoxysilane)) and glycidoxysilanes such as GOPS, which yield amine and epoxy functional groups respectively, for subsequent linkage to a secondary organic molecule<sup>2</sup>. The lack of hydroxyl groups on polythiophenes such as PEDOT, would appear to rule out this method of biofunctionalization for films or devices made from these polymers. Therefore, we sought to add a hydroxyl containing polymer to solutions of commercially available PEDOT:PSS, that could later be used for biofunctionalizing the films via silanization, but would not cause deleterious effects to the film forming poorly soluble in aqueous solutions, and the polyanion PSS is used as a means to generate an aqueous dispersion that has good film forming properties and high conductivity<sup>23</sup>. One disadvantage of the PEDOT:PSS solution however, is that it is generally considered a finely balanced solution which can be disturbed by addition of extraneous additives or solvents. Nevertheless, several reports have been published on addition of compounds to PEDOT:PSS to enhance properties such as conductivity for application in a variety of device types including solar cells and displays. Additives to PEDOT:PSS include diols, such as ethylene glycol, diethylene glycol, or poly(ethylene glycol) (PEG), where addition to PEDOT:PSS emulsions before spin-coating increases the conductivity of the resultant thin films<sup>24 25 26</sup>. Addition of the sugar alcohol sorbitol is also known to enhance the conductivity of PEDOT:PSS thin films by three orders of magnitude<sup>27</sup>.

Given that alcohol containing polymers have often been used as additives for improving conductivity, we decided to incorporate Polyvinyl alcohol (PVA) as a handle for subsequent silanization of PEDOT:PSS. The proposed reaction scheme is outlined in Figure 3.1. The polyalcohol is mixed with the PEDOT:PSS in solution, after which the film is cast and cured. Following curing, GOPS is added by chemical vapour deposition to the film whereupon a condensation reaction occurs and the silane reagent is bonded to the polymer. Subsequent addition of amine containing polypeptides/proteins under basic conditions allows formation of a secondary amine bond with the biomolecule.

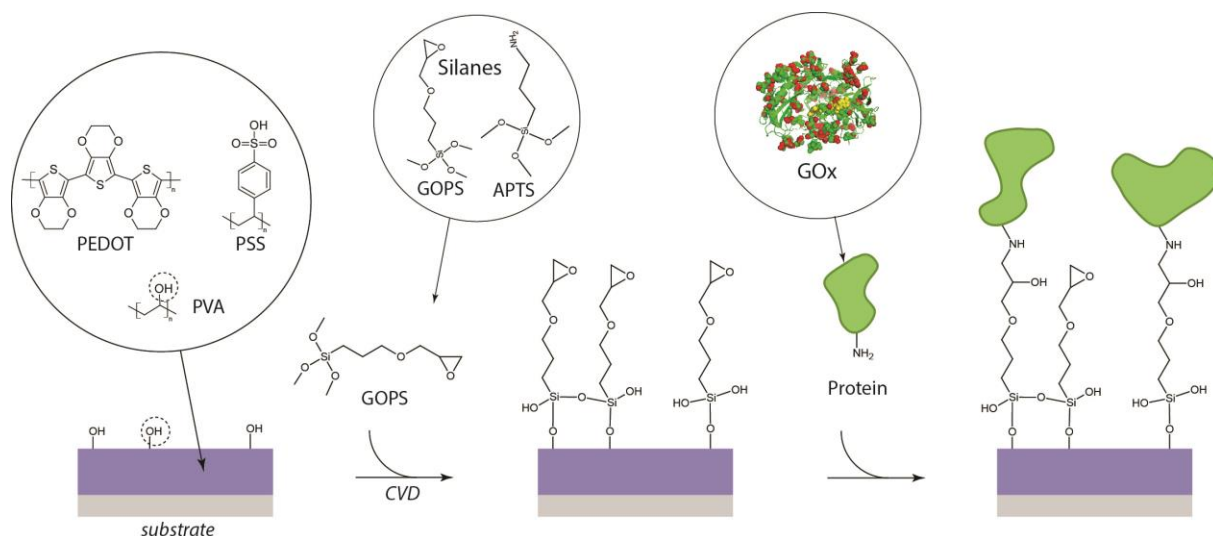


**Figure 3.1:** Reaction scheme for biofunctionalization of PEDOT:PSS by incorporation of PVA.

### 3.1.2. Efficiency of the biofunctionalization

In order to estimate the degree of biofunctionalization of PEDOT:PSS films using the above method, we immobilized a FITC-labelled Poly-L-Lysine on a photolithographically defined pattern. Figure 3.2a shows fluorescence images of the biofunctionalized pattern. Different amounts of PVA were added to the PEDOT:PSS dispersion (in concentrations ranging from 0 to 50 wt%) and we observed more homogeneous and brightest fluorescence (and thus biofunctionalization) for PVA concentrations around 20-25 wt%. High PVA loading wt50% resulted in more aggregated fluorescence morphology. It should be noted that the films were stringently washed first with PBS, and then with a high concentration salt solution (0.1 M NaCl) and finally with deionised water to remove any non-specific or electrostatically bound polypeptide, and thus making sure that the remaining polypeptide is covalently linked to the conducting polymer. In addition, the absence of fluorescent label on the 0 wt% PVA sample indicates that the PVA is necessary for the binding of the polypeptide to the surface, and that GOPS does not react with the PEDOT:PSS film or the Parylene C. The same procedure was attempted with PEG, however the patterning obtained with PEDOT:PSS:PEG were less homogenous and showed some evidence of aggregation or phase separation (Supplementary Figure 3.1b). The optimal concentration of PVA (25 wt%) was used to functionalise additional patterns as shown in Figure 3.2b.

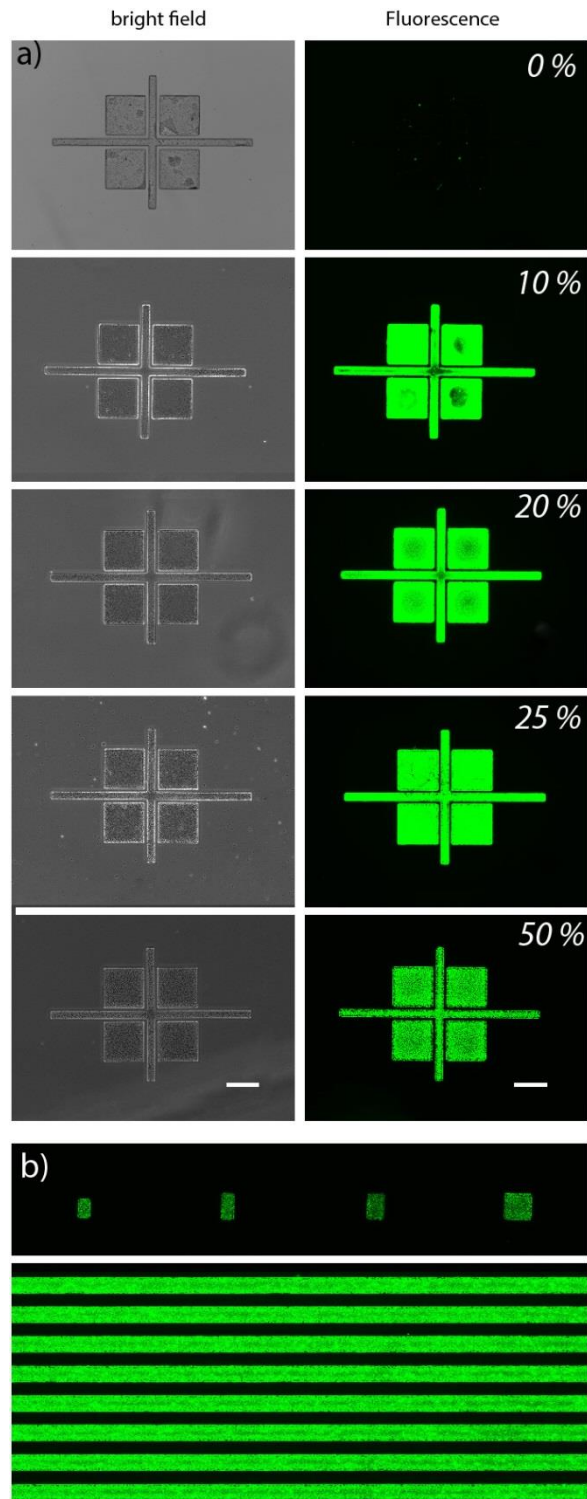


**Figure 3.2:** Biofunctionalization of FITC - PLL on PEDOT:PSS:PVA films. **(a)** Different concentrations of PVA added to PEDOT:PSS; 0, 10, 20, 25 and 50 wt% PVA. Scale bar 100  $\mu\text{m}$  **(b)** different patterns of FITC-PLL on PEDOT:PSS:PVA 25 wt%.

### 3.1.3. Electrical properties of PEDOT:PSS:PVA as active material on OECTs

An important consideration when adding compounds to conducting polymers which will later be used in devices, is that the electrical characteristics of the films remain unchanged. The conductivity of a range of different concentrations of PVA into PEDOT:PSS was measured (Figure 3.3a). The conductivity of the 25 wt% PVA sample remained high, within 10% of the neat PEDOT:PSS sample. Unlike addition of polymers such as PEG to PEDOT:TOS via vapor phase polymerization<sup>28, 29</sup>, addition of PVA did not enhance conductivity. A similar result was shown with addition of PEG to PEDOT:PSS (Supplementary Figure 3.1a). Previous studies have reported the combination of PVA with PEDOT:PSS for a variety of purposes: for example taking advantage of increased mechanical flexibility in free standing films of PEDOT:PSS:PVA films<sup>30</sup> and for preparation of conducting nanofibers<sup>31, 32</sup>. Reynolds and co-workers showed increases in conductivity upon addition of PVA to PEDOT:PSS but with maximum reported conductivity of 1 S/cm. Addition of polymers such as PEG and PVA to PEDOT:TOS most likely induce significant morphological rearrangements resulting in concurrent improvements in conductivity<sup>28, 33</sup>, however addition of such polymers to already highly conducting PEDOT:PSS solutions would appear to have merely a dilution effect after a certain point. It should be noted that we routinely add EG to improve conductivity of films. In order to test both electronic and electrochemical properties of PEDOT:PSS:PVA blends, they were used as active materials in OECTs. The organic electrochemical transistor (OECT) is a device which has been used by a number of groups in a variety of different biosensing applications. The geometry of the OECT device varies considerably depending on the particular application. In certain cases, e.g. for applications for neural probes *in vivo* very fast transistors are required. We demonstrate the successful employment of PVA modified PEDOT:PSS films as the channel in an OECT (channel dimensions: 10  $\mu\text{m}$  width and 5  $\mu\text{m}$  length) (Figure 3.3). Since the devices compared have the same channel dimensions, and are spun under the same conditions, direct comparison of transistor parameters allows for elucidation of the added effect of PVA in an OECT. Here we measure average transconductance values of 1.86 and 1.59 mS for devices of PEDOT:PSS:PVA 25 wt% and PEDOT:PSS+GOPS 1 wt.% in solution respectively. The latter is a typical formulation for stable high performance OECTs used *in vivo*, and achieves a transconductance similar to that previously reported<sup>34</sup>. The response times to a constant gate voltage pulse,  $\tau$ , (measured with an exponential fit) also compare favourably. PEDOT:PSS:PVA results in a  $\tau$  of 20.4  $\mu\text{s}$  compared to 27.5  $\mu\text{s}$  for PEDOT:PSS+GOPS 1 wt.% when a gate pulse of  $V_G = 0.6$  V is applied. The slight enhancement in response time with the addition of PVA is likely related to

the trend in ion mobility reported above.

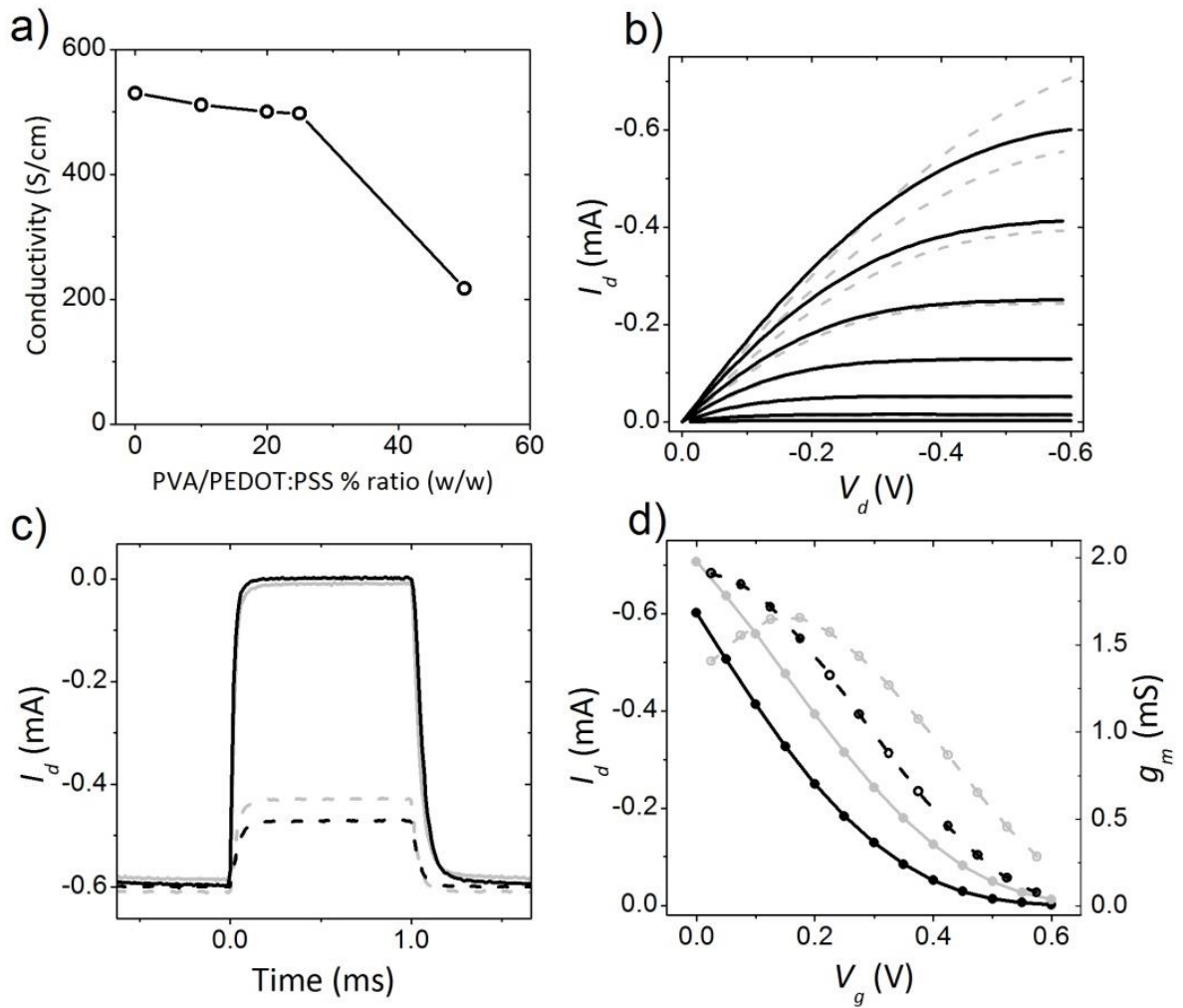


**Figure 3.3:** (a) Effect of different concentrations of PVA on PEDOT:PSS film conductivity. (b), (c) and (d) Electrical characterization of OECTs prepared with either PEDOT:PSS+PVA(25%) (black), or PEDOT:PSS+GOPS (grey). (b) Output IV curves for  $V_g=0-0.6V$ . (c) Time response of device in response to a  $V_g=0.1V$  (dashed), and  $V_g=0.6V$  (solid) square pulse. (d) Corresponding transfer curves (solid line/symbols), and transconductance,  $g_m$ , dashed line/open symbols.

## 3.2. Applications

### 3.2.1. Glucose sensing using biofunctionalized transistors

A second relevant test of the effectiveness of this biofunctionalization method was the immobilization of the enzyme Glucose oxidase (GOx) on PEDOT:PSS:PVA films for development of a glucose sensor as a proof of principle. To verify the immobilization of GOx onto PEDOT:PSS:PVA 25 wt% we monitored the binding and the stability of the enzyme with QCM. A thin film was deposited onto a quartz crystal sensor, where frequency is inversely proportional to the mass of the film. As we introduce enzyme to the cell (Figure 3.4a), we see a fast drop of the vibration frequency with a subsequent slow stabilization, which indicates interactions between the polymer and the enzyme, resulting in an increase in the mass of the polymer. However, after introducing deionized water to the chamber as a rinsing step, the film loses mass until is stabilized to a higher frequency value, which implies the removal of weakly bonded enzyme. In the frequency scan, the difference between the starting value and the value after washing  $\Delta f_b$  can be attributed to the presence of enzyme immobilized on the surface. The use of the OECT as a glucose sensor has previously been demonstrated by a number of groups, however with the GOx immobilized on a Pt gate electrode <sup>35</sup>.

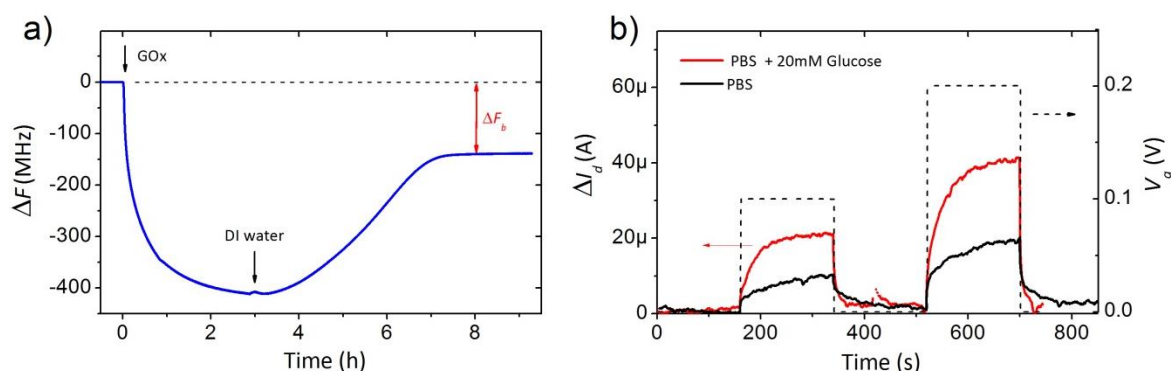


**Figure 3.4:** GOx functionalized PEDOT:PSS:PVA (a) QCM monitoring of GOx deposition on PEDOT:PSS:PVA films (b) Sensing of glucose with OECT,  $V_d = -0.4V$

Here, we demonstrate the operation of GOx functionalized PEDOT:PSS:PVA OECTs (Figure 3.4b). It should be noted that in contrast to the OECTs characterized in the preceding section, the OECTs developed for glucose sensing require significantly different geometry, with the conducting polymer channel

area significantly greater than that of the gate electrode. This has been described in detail elsewhere<sup>36, 37</sup>, along with the mechanism of the OECT for glucose sensing<sup>38</sup>. In this case a Pt gate electrode was used to avoid the necessity of adding a redox mediator<sup>7</sup>. The dimensions of the device used here were 1 cm width and 1 mm length. Additionally, the gate area was selected such that the ratio of the gate area to the channel area was  $< 1/10$ . Glucose was added, and a substantial increase in the modulation of the source-drain current was observed. Despite the limited amount of GOx immobilized on the surface (compared to experiments where the enzyme is present in solution) a clear difference is observed upon addition of glucose, compared to PBS for different values of gate voltage (Figure 3.4b). The successful operation of the OECT suggests that the enzyme is properly immobilized, and that biological activity of the enzyme is maintained. Conducting polymer devices have shown great potential for use in devices integrated with living cells.

### 3.2.2. Patterning of cells on active materials

The ability to pattern cells or cell-networks is advantageous for a number of applications, for example controlling the growth and connectivity of neurons for studies of artificial neuronal networks. PEDOT:PSS and PEDOT:TOS have been used as simple electrode coatings, but also as active materials for controlling cell adhesion<sup>39-41</sup>, proliferation<sup>42, 43</sup> or migration<sup>44, 45</sup>. Improving the interface by coating with proteins such as extracellular matrix components can have advantages for biocompatibility and may be essential in *in vivo* applications for avoiding rejection of implants by tissue<sup>46, 47</sup>. Examples include multielectrode arrays<sup>48</sup>, and biosensors for toxicology<sup>11, 49</sup>. Although a variety of methods exist for coating active surfaces, as mentioned above, covalent linkage of biomolecules offers gains in terms of stability and control of binding.

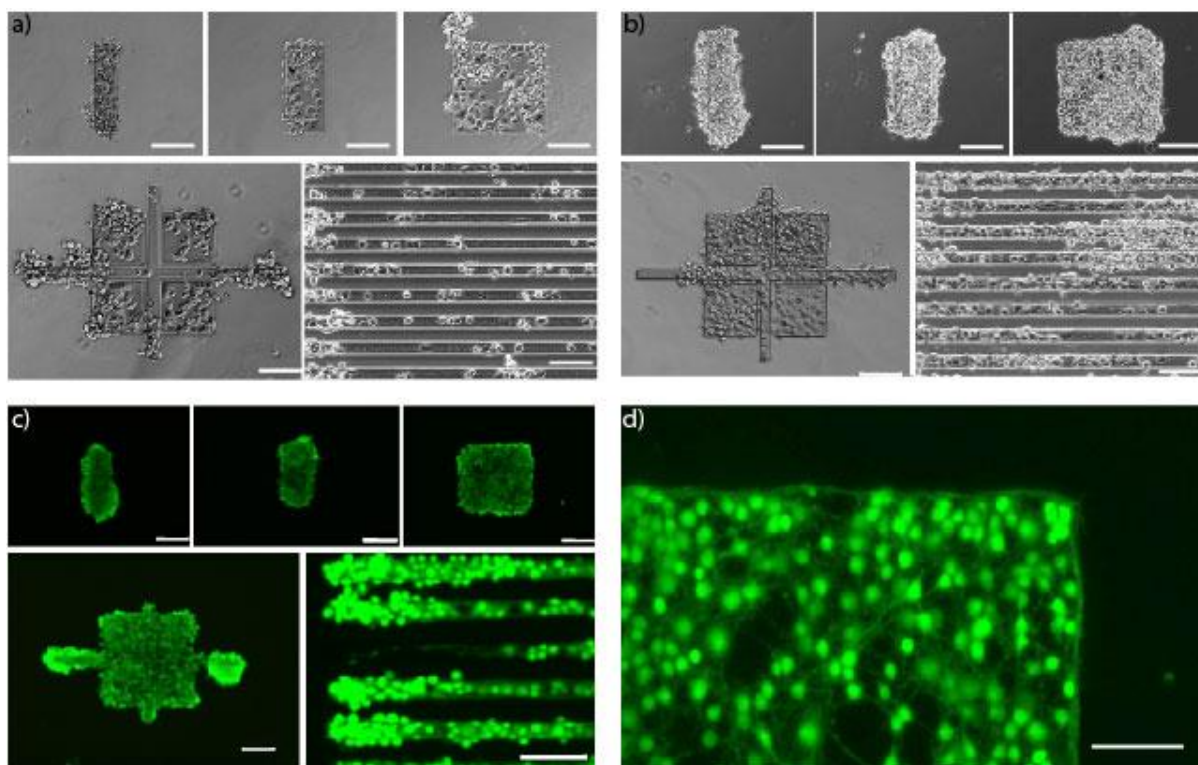


**Figure 3.5:** Growth and differentiation of PC12 cells on PLL functionalized PEDOT:PSS:PVA patterns. **(a)** Optical micrograph of PC12 cells 1 day after seeding. **(b)** Optical micrograph of PC12 cells 5 days after seeding. **(c)** Fluorescence imaging of live (green) /dead (red) stained of PC12 cells 5 days after seeding on PEDOT:PSS:PVA patterns. **(d)** Differentiation of PC12 cells on PEDOT:PSS:PVA pattern. Scale bars are 100  $\mu\text{m}$  for all the panels.

Figure 3.5 shows micron-scale patterning of PEDOT:PSS:PVA 25 wt.% on glass slides which were subsequently seeded with PC12 cells, a cell line which is often used as a model for neuronal differentiation. Figure 3.5a shows optical micrographs of PLL patterned surfaces with PC12 cells seeded at Day 1, illustrating an excellent confinement of the cells to the patterned PEDOT:PSS:PVA. The same pattern is shown with cells 5 days after differentiation, demonstrating maintenance of the pattern (Figure 3.5b). A live/dead cell staining assay was performed on PC12 cells grown on the patterns for 5 days, and confirms that the cells are alive and that the PEDOT:PSS:PVA material is biocompatible for this application and duration (Figure 3.5c). A close-up of one of the patterned areas from the same samples reveals connections formed between individual cells on the pattern, demonstrating that this functionality of the cells is also maintained (Figure 3.5d).

### 3.3. Discussion

We have demonstrated an easy-to-use, novel biofunctionalization method that is compatible with solution based processing of PEDOT:PSS films and devices. The method involves modification of the existing method for preparation of PEDOT:PSS films in three simple steps: 1. addition of a polyalcohol into the CP solution before film casting, 2. chemical vapor deposition of a silane reagent onto the cast film, and 3. addition of biomolecule. This method can therefore be easily incorporated into existing device preparation schemes, with the major advantage that the biomolecule is added after film preparation, meaning that it will not undergo denaturation due to harsh processing conditions such as high temperature and presence of solvents. We conclusively demonstrate a high-degree of biofunctionalization and demonstrate in two different applications that the biofunctionality of these molecules is maintained. Further we demonstrate that the conductivity is only negligibly changed, and that devices made from the mix of PVA with PEDOT:PSS have comparable performance to PEDOT:PSS with 1% gops devices used for *in vivo* applications. Future work will include more in-depth studies of different polyalcohols and silane reagents, as well as studies on functionalizing within the bulk of the conducting polymer to facilitate direct interactions between biomolecules and CPs.

### 3.4. Experimental section

*Preparation of conducting polymer (CP) films:* PEDOT:PSS (Heraeus, Clevios PH 1000) was used as the conducting polymer active layer. Dodecylbenzenesulfonic acid (DBSA) (0.5  $\mu\text{L}/\text{mL}$ ) and Ethylene glycol (Sigma Aldrich) (50  $\mu\text{L}/\text{mL}$ ) were added to the PEDOT:PSS dispersion to improve film formation and to increase conductivity. The formulation was sonicated and filtered to avoid aggregates. A stock solution of 5 wt% PVA (average  $M_w$  130,000) was prepared; heating for  $\sim 30\text{s}$  in a microwave oven assisted dissolution until a clear solution was obtained. The amount of PVA added to the solution was calculated according to the mass of PEDOT:PSS. Four different PEDOT:PSS:PVA composite solutions (10, 20, 25, 50 wt% ) were made, mixed thoroughly, and filtered before deposition. Following PEDOT:PSS:PVA spin - coating, samples were baked for 30 minutes at 140  $^{\circ}\text{C}$  under atmospheric conditions.

*Conductivity measurement:* PEDOT:PSS and PEDOT:PSS:PVA composites were coated onto glass slides which were cleaned by sonication in acetone, isopropyl alcohol, and DI water, followed by a drying step with nitrogen and brief exposure

to oxygen plasma. Sheet resistance was measured using Jandel four point probe device. The thicknesses of the films were measured using an ambios XP2 150 Profilometer. The conductivity was calculated from the measured sheet resistance and thickness.

*Electrochemical transistor fabrication and operation:* The fabrication process, similar to that reported previously<sup>34</sup> included the deposition and patterning of gold, parylene, and PEDOT:PSS:PVA. Source/drain contacts were patterned by a lift-off process, using S1813 photoresist, exposed to UV light through a SUSS MBJ4 contact aligner, and developed using MF-26 developer. 5 nm of chromium and 100 nm of gold were subsequently deposited using a metal evaporator, and metal lift-off was carried out in acetone. Metal interconnects and pads were insulated by depositing 2  $\mu\text{m}$  of parylene C using an SCS Labcoater 2, with a silane adhesion promoter. A dilute solution of industrial cleaner (Micro-90) was subsequently spin coated to act as an anti-adhesive for a second, sacrificial 2  $\mu\text{m}$  parylene C film. Samples were subsequently patterned with a 5  $\mu\text{m}$  thick layer of AZ9260 photoresist and AZ developer (AZ Electronic Materials). The patterned areas were opened by reactive ion etching with an oxygen plasma using an Oxford 80 Plasmalab plus. PEDOT:PSS:PVA 25 wt% and PEDOT:PSS + 1 wt% GOPS in solution, the usual formulation for *in vivo* applications, were spin coated at 3000 rpm, and baked for 90 sec in 100 °C. The second layer of parylene was peeled off with a subsequent rinsing in DI water and baking at 140 °C for 30 min. All characterization was done using a 100 mM NaCl solution in DI water as the electrolyte and a Ag/AgCl wire (Warner Instruments) as the gate electrode. The measurements were performed using a National Instruments PXIe-1062Q system. The channel of the OECT was biased using one channel of a source-measurement unit NI PXIe-4145. The gate voltage was applied using a NI PXI-6289 modular instrument. In the case of the IV-characteristics and transconductance characterization, the drain current was measured using the SMU channel used for the bias. Concerning the time response characterization of the OECT, one NI-PXI-4071 digital multimeter measured drain current, and a channel of the NI PXI-6289 equipment measured gate voltage. All the measurements were triggered through the built-in PXI architecture.

*Measurement of ion mobility in PEDOT:PSS:PVA films:* Ionic mobility was measured as previously described<sup>50</sup>. Briefly, a PEDOT:PSS:PVA film, deposited on a parylene-coated glass substrate, was coated with a layer of SU-8 serving as an ion barrier. Using photolithography, a well was created in the SU8/PEDOT:PSS stack and filled with an electrolyte, forming a planar junction with an area  $A$  of 16 mm. An Ag/AgCl counter electrode was immersed into the electrolyte, and an Au pad provided contact with the conducting polymer composite film, positioned at a distance  $L = 32$  mm from the electrolyte interface. The experiment was carried out by applying a positive bias at the Ag/AgCl

electrode while simultaneously measuring the current flow in the device and recording the electrochromic changes associated with the propagation of the dedoping front using an inverted Carl Zeiss Axio Observer Z1, in the bright field mode with 1X objective. We used 10 mM KCl electrolyte in order to measure the mobility of potassium.

*Silanization and fluorescence imaging of patterned films:* To investigate the distribution of the fluorescence we prepared patterns with PEDOT:PSS and PEDOT:PSS:PVA composites using photolithography and the parylene C peel-off technique. Prior to the peel-off, 3-glycidoxypropyltrimethoxysilane (GOPS) was deposited by vapor deposition at 90 °C for 45 minutes under vacuum. Fluorescein isothiocyanate labelled poly-L lysine (PLL), with concentration 50 µg/mL in phosphate buffered saline (PBS), adjusted to pH 8-9 by addition of 50 mM NaOH, was drop-cast on to the sample allowed to react for two hours at room temperature. The resulting films were thoroughly cleaned with 0.1 M PBS, 0.1 M NaCl, and DI water. Finally, samples were examined with a fluorescent microscope (Carl Zeiss Axio Observer Z1).

*Quartz crystal microbalance (QCM):* Glucose oxidase (GOx) immobilization monitoring was undertaken using a Q – sense E4 system. PEDOT:PSS:PVA 25 wt% was spin coated on top of quartz crystal sensors, with additional GOPS deposition as mentioned above. The samples were transferred to the QCM flow module part of the Q-sense E4 device and equilibrated in DI water for 60 min. GOx 50 µg/mL in PBS with 50 mM of NaOH was introduced to the axial flow sample chamber and a constant flow rate of 20 µL/min for 180 min and then rinsed with DI water at a constant rate of 60 µL/min.

*Glucose sensing assay using GOx functionalised OECTs:* All PEDOT:PSS:PVA 25 wt% transistors were patterned using a parylene peel-off technique, and functionalized with GOx (1 mg mL<sup>-1</sup> in PBS, pH adjusted to 8-9 with NaOH), both of which are described above. 20 mM glucose was prepared in PBS. Due to its hydrophobicity, parylene C served as a virtual well for the drop of the electrolyte. Finally, a platinum wire was immersed in the electrolyte from the top serving as a gate of the transistor. The measurements were recorded by a Keithley 2612A and customized Labview software.

*Cell culture:* PC12 cells from Health Protection Agency culture collections (Salisbury, UK) were cultured at 37°C, 5% CO<sub>2</sub> in humidified atmosphere. RPMI 1640 media supplemented with 10% horse serum (HS, Invitrogen), 5 % fetal bovine serum (FBS, Invitrogen), 2 mM glutamine (Glutamax™, Invitrogen), 25 U/mL penicillin-streptomycin (PenStrep, Invitrogen), 50 ng/mL gentamicin (Gentamicin, Invitrogen). During maintenance, the cells were cultivated in

suspension and numbers were determined by a cell counter (Scepter handheld automated cell counter, Millipore).

*Cell patterning using collagen and PLL functionalized conducting polymer films:*  
*Cell Adhesion and Differentiation Tests:* Patterned substrates (approximate area: 4.9 cm<sup>2</sup>) were coated with the conducting polymer PEDOT:PSS:PVA 25 wt% according to the procedure described above. Each coated substrate was sterilized for 20 minutes in 70% ethanol, rinsed twice in PBS, and placed in a separate 6-well plate. Cells were seeded at a concentration of 10<sup>5</sup> cells/well. The final volume of each well was 3 mL. Adhesion was evaluated after 24 h. A Calcein AM/Propidium Iodide assay 2 µg/mL was carried out to determine the cell viability (Calcein-AM, and Propidium Iodide, Sigma). To perform these tests, the media in the wells was discarded and the cells gently rinsed two times with PBS. 3 mL of the Calcein-AM/PI mixture was added to each well and incubated for 30 min at 37°C. Fluorescence images were then recorded (Axio Observer Z1, Carl Zeiss, Calcein AM 485 nm/535 nm, PI 530 nm/620 nm). After 24h of culture, the media was changed to discard the cells in suspension using differentiation media: RPMI 1640 supplemented with 1 % (v/v) HS, 2 mM glutamine, 50 ng/mL nerve growth factor (NGF, Sigma), 25 U/mL penicillin-streptomycin, and 50 ng/mL gentamicin. The media was changed every two days until the end of the experiment.

### 3.5. Supplementary information

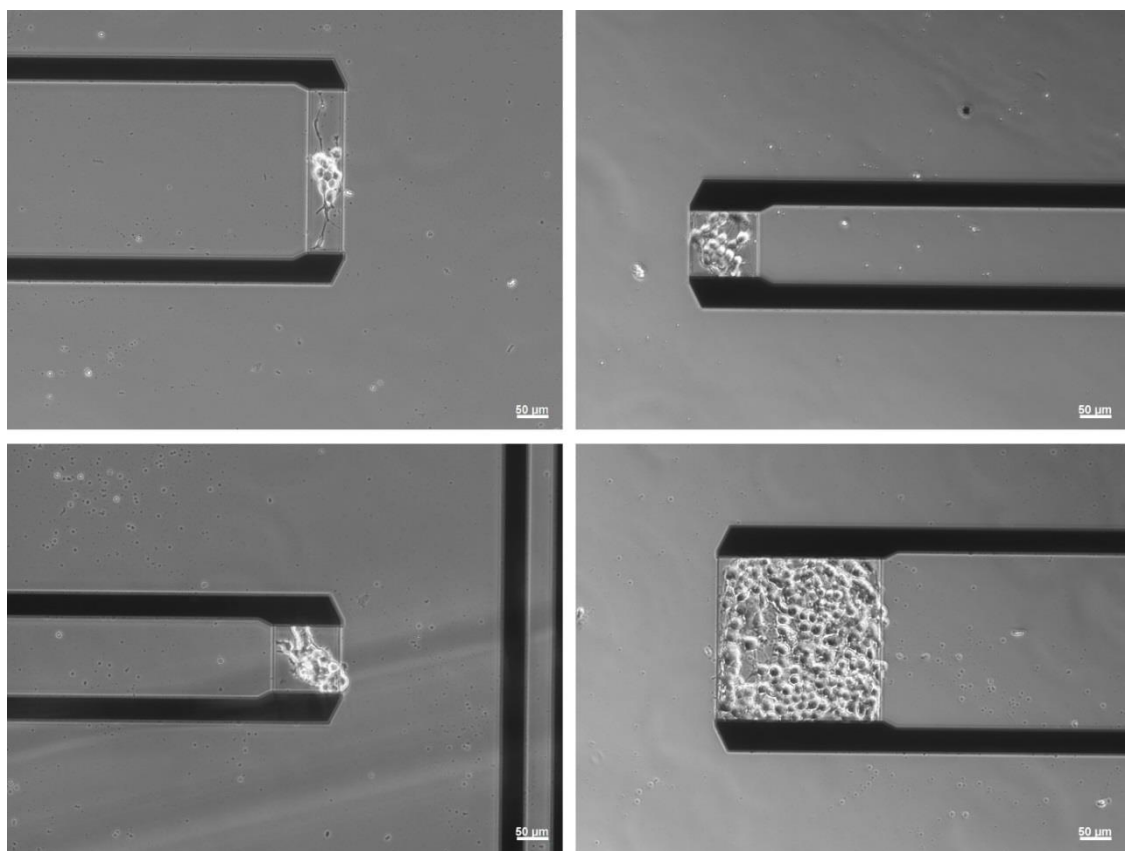


**Figure S3.1** Patterning of pc-12 cells on top of OECT channels with different geometries for further recordings. Scale bar 50  $\mu\text{m}$ .

### 3.6. References

1. Nakajima, N., and Ikada, Y. (1995) Mechanism of Amide Formation by Carbodiimide for Bioconjugation in Aqueous-Media, *Bioconjugate Chem* 6, 123-130.
2. Hermanson, G. (1996) *Bioconjugate techniques*, Academic Press, San Diego.
3. Berggren, M., and Richter-Dahlfors, A. (2007) Organic bioelectronics, *Adv. Mater.* 19, 3201-3213.
4. Owens, R. M., and Malliaras, G. G. (2010) Organic Electronics at the Interface with Biology, *Mrs Bull* 35, 449-456.
5. Jimison, L. H., Rivnay, J., and Owens, R. M. (2013) Conducting Polymers to Control and Monitor Cells, In *Organic Electronics*, pp 27-67, Wiley-VCH Verlag GmbH & Co. KGaA, Weinheim, Germany

6. Rivnay, J., Owens, R. M., and Malliaras, G. G. (2013) The Rise of Organic Bioelectronics, *Chem Mater*.
7. Shim, N. Y., Bernardis, D. A., Macaya, D. J., DeFranco, J. A., Nikolou, M., Owens, R. M., and Malliaras, G. G. (2009) All-Plastic Electrochemical Transistor for Glucose Sensing Using a Ferrocene Mediator, *Sensors-Basel* 9, 9896-9902.
8. Yan, F., Mok, S. M., Yu, J. J., Chan, H. L. W., and Yang, M. (2009) Label-free DNA sensor based on organic thin film transistors, *Biosens. Bioelectron.* 24, 1241-1245.
9. Abidian, M. R., Kim, D. H., and Martin, D. C. (2006) Conducting-polymer nanotubes for controlled drug release, *Adv. Mater.* 18, 405-+.
10. Simon, D. T., Kurup, S., Larsson, K. C., Hori, R., Tybrandt, K., Goiny, M., Jager, E. H., Berggren, M., Canlon, B., and Richter-Dahlfors, A. (2009) Organic electronics for precise delivery of neurotransmitters to modulate mammalian sensory function, *Nature Materials* 8, 742-746.
11. Jimison, L. H., Tria, S. A., Khodagholy, D., Gurfinkel, M., Lanzarini, E., Hama, A., Malliaras, G. G., and Owens, R. M. (2012) Measurement of Barrier Tissue Integrity with an Organic Electrochemical Transistor, *Adv. Mater.* 24, 5919-5923.
12. Khodagholy, D., Doublet, T., Quilichini, P., Gurfinkel, M., Leleux, P., Ghestem, A., Ismailova, E., Herve, T., Sanaur, S., Bernard, C., and Malliaras, G. G. (2013) In vivo recordings of brain activity using organic transistors, *Nature Communications* 4, 1575.
13. Kim, D. H., Wiler, J. A., Anderson, D. J., Kipke, D. R., and Martin, D. C. (2010) Conducting polymers on hydrogel-coated neural electrode provide sensitive neural recordings in auditory cortex, *Acta Biomaterialia* 6, 57-62.
14. Guimard, N. K., Gomez, N., and Schmidt, C. E. (2007) Conducting polymers in biomedical engineering, *Progress in Polymer Science* 32, 876-921.
15. Ismailova, E., Doublet, T., Khodagholy, D., Quilichini, P., Ghestem, A., Yang, S. Y., Bernard, C., and Malliaras, G. G. (2012) Plastic neuronal probes for implantation in cortical and subcortical areas of the rat brain, *Int J Nanotechnol* 9, 517-528.
16. Richardson-Burns, S. M., Hendricks, J. L., and Martin, D. C. (2007) Electrochemical polymerization of conducting polymers in living neural tissue, *Journal of Neural Engineering* 4, L6-L13.
17. Asplund, M. L. M., Thaning, E. M., Nyberg, T. A., Inganas, O. W., and von Hoist, H. (2010) Stability of Poly(3,4-ethylene dioxythiophene) Materials Intended for Implants, *Journal of Biomedical Materials Research Part B-Applied Biomaterials* 93B, 407-415.
18. Asplund, M., von Holst, H., and Inganas, O. (2008) Composite biomolecule/PEDOT materials for neural electrodes, *Biointerphases* 3, 83-93.
19. Collazos-Castro, J. E., Hernández-Labrado, G. R., Polo, J. L., and García-Rama, C. (2013) N-Cadherin- and L1-functionalised conducting polymers for synergistic stimulation and guidance of neural cell growth, *Biomaterials* 34, 3603-3617.

20. Nilsson, D., Kugler, T., Svensson, P. O., and Berggren, M. (2002) An all-organic sensor-transistor based on a novel electrochemical transducer concept printed electrochemical sensors on paper, *Sensors and Actuators B-Chemical* 86, 193-197.
21. Andersson, P., Nilsson, D., Svensson, P. O., Chen, M. X., Malmstrom, A., Remonen, T., Kugler, T., and Berggren, M. (2002) Active matrix displays based on all-organic electrochemical smart pixels printed on paper, *Adv. Mater.* 14, 1460-+.
22. Stavrinidou, E., Leleux, P., Rajaona, H., Fiocchi, M., Sanaur, S., and Malliaras, G. G. (2013) A simple model for ion injection and transport in conducting polymers, *J Appl Phys* 113.
23. Fabretto, M., Hall, C., Vaithianathan, T., Innis, P. C., Mazurkiewicz, J., Wallace, G. G., and Murphy, P. (2008) The mechanism of conductivity enhancement in poly(3,4-ethylenedioxythiophene)-poly(styrenesulfonic) acid using linear-diol additives: Its effect on electrochromic performance, *Thin Solid Films* 516, 7828-7835.
24. Xiong, S., Zhang, L., and Lu, X. (2013) Conductivities enhancement of poly(3,4-ethylenedioxythiophene)/poly(styrene sulfonate) transparent electrodes with diol additives, *Polymer Bulletin* 70, 237-247.
25. Ouyang, B. Y., Chi, C. W., Chen, F. C., Xi, Q. F., and Yang, Y. (2005) High-conductivity poly (3,4-ethylenedioxythiophene): poly(styrene sulfonate) film and its application in polymer optoelectronic devices, *Adv. Funct. Mater.* 15, 203-208.
26. Mengistie, D. A., Wang, P.-C., and Chu, C.-W. (2013) Effect of molecular weight of additives on the conductivity of PEDOT: PSS and efficiency for ITO-free organic solar cells, *Journal of Materials Chemistry A* 1, 9907-9915.
27. Nardes, A. M., Kemerink, M., de Kok, M. M., Vinken, E., Maturova, K., and Janssen, R. A. J. (2008) Conductivity, work function, and environmental stability of PEDOT : PSS thin films treated with sorbitol, *Org Electron* 9, 727-734.
28. Jimison, L. H., Hama, A., Strakosas, X., Armel, V., Khodagholy, D., Ismailova, E., Malliaras, G. G., Winther-Jensen, B., and Owens, R. M. (2012) PEDOT:TOS with PEG: a biofunctional surface with improved electronic characteristics, *Journal of Materials Chemistry* 22, 19498-19498.
29. Fabretto, M., Jariago-Moncunill, C., Autere, J.-P., Michelmore, A., Short, R. D., and Murphy, P. (2011) High conductivity PEDOT resulting from glycol/oxidant complex and glycol/polymer intercalation during vacuum vapour phase polymerisation, *Polymer* 52, 1725-1730.
30. Chen, C.-h., Torrents, A., Kulinsky, L., Nelson, R. D., Madou, M. J., Valdevit, L., and LaRue, J. C. (2011) Mechanical characterizations of cast Poly(3,4-ethylenedioxythiophene):Poly(styrenesulfonate)/Polyvinyl Alcohol thin films, *Synthetic Met* 161, 2259-2267.
31. Liu, N., Fang, G., Wan, J., Zhou, H., Long, H., and Zhao, X. (2011) Electrospun PEDOT:PSS-PVA nanofiber based ultrahigh-strain sensors with controllable electrical conductivity, *Journal of Materials Chemistry* 21, 18962-18966.

32. Cho, D., Hoepker, N., and Frey, M. W. (2012) Fabrication and characterization of conducting polyvinyl alcohol nanofibers, *Materials Letters* 68, 293-295.
33. Zuber, K., Fabretto, M., Hall, C., and Murphy, P. (2008) Improved PEDOT conductivity via suppression of crystallite formation in Fe(III) tosylate during vapor phase polymerization, *Macromol Rapid Comm* 29, 1503-1508.
34. Khodagholy, D., Rivnay, J., Sessolo, M., Gurfinkel, M., Leleux, P., Jimison, L. H., Stavriniidou, E., Herve, T., Sanaur, S., Owens, R. M., and Malliaras, G. G. (2013) High transconductance organic electrochemical transistors, *Nat Commun* 4, 2133.
35. Tang, H., Yan, F., Lin, P., Xu, J., and Chan, H. L. W. (2011) Highly Sensitive Glucose Biosensors Based on Organic Electrochemical Transistors Using Platinum Gate Electrodes Modified with Enzyme and Nanomaterials, *Advanced Functional Materials* 21, 2264-2272.
36. Tarabella, G., Santato, C., Yang, S. Y., Iannotta, S., Malliaras, G. G., and Cicoira, F. (2010) Effect of the gate electrode on the response of organic electrochemical transistors, *Appl Phys Lett* 97, 123304.
37. Cicoira, F., Sessolo, M., Yaghmazadeh, O., DeFranco, J. A., Yang, S. Y., and Malliaras, G. G. (2010) Influence of Device Geometry on Sensor Characteristics of Planar Organic Electrochemical Transistors, *Adv. Mater.* 22, 1012-+.
38. Yang, S. Y., DeFranco, J. A., Sylvester, Y. A., Gobert, T. J., Macaya, D. J., Owens, R. M., and Malliaras, G. G. (2009) Integration of a surface-directed microfluidic system with an organic electrochemical transistor array for multi-analyte biosensors, *Lab on a Chip* 9, 704-708.
39. Wan, A. M. D., Brooks, D. J., Gumus, A., Fischbach, C., and Malliaras, G. G. (2009) Electrical control of cell density gradients on a conducting polymer surface, *Chemical Communications*, 5278-5280.
40. Svennersten, K., Bolin, M. H., Jager, E. W., Berggren, M., and Richter-Dahlfors, A. (2009) Electrochemical modulation of epithelia formation using conducting polymers, *Biomaterials* 30, 6257-6264.
41. Svennersten, K., Berggren, M., Richter-Dahlfors, A., and Jager, E. W. H. (2011) Mechanical stimulation of epithelial cells using polypyrrole microactuators, *Lab on a Chip* 11, 3287-3293.
42. Lee, J. Y., Lee, J. W., and Schmidt, C. E. (2009) Neuroactive conducting scaffolds: nerve growth factor conjugation on active ester-functionalized polypyrrole, *Journal of the Royal Society Interface* 6, 801-810.
43. Lee, J. W., Serna, F., Nickels, J., and Schmidt, C. E. (2006) Carboxylic acid-functionalized conductive polypyrrole as a bioactive platform for cell adhesion, *Biomacromolecules* 7, 1692-1695.
44. Thompson, B. C., Richardson, R. T., Moulton, S. E., Evans, A. J., O'Leary, S., Clark, G. M., and Wallace, G. G. (2010) Conducting polymers, dual neurotrophins and pulsed electrical stimulation - Dramatic effects on neurite outgrowth, *J Control Release* 141, 161-167.
45. Gumus, A., Califano, J. P., Wan, A. M. D., Huynh, J., Reinhart-King, C. A., and Malliaras, G. G. (2010) Control of cell migration using a conducting polymer device, *Soft Matter* 6, 5138-5142.

46. Povlich, L. K., Cho, J. C., Leach, M. K., Corey, J. M., Kim, J., and Martin, D. C. (2013) Synthesis, copolymerization and peptide-modification of carboxylic acid-functionalized 3,4-ethylenedioxythiophene (EDOTacid) for neural electrode interfaces, *Biochimica et biophysica acta* 1830, 4288-4293.
47. Chikar, J. A., Hendricks, J. L., Richardson-Burns, S. M., Raphael, Y., Pflingst, B. E., and Martin, D. C. (2012) The use of a dual PEDOT and RGD-functionalized alginate hydrogel coating to provide sustained drug delivery and improved cochlear implant function, *Biomaterials* 33, 1982-1990.
48. Sessolo, M., Khodagholy, D., Rivnay, J., Maddalena, F., Gleyzes, M., Steidl, E., Buisson, B., and Malliaras, G. G. (2013) Easy-to-fabricate conducting polymer microelectrode arrays, *Adv Mater* 25, 2135-2139.
49. Yao, C., Xie, C., Lin, P., Yan, F., Huang, P., and Hsing, I. M. (2013) Organic Electrochemical Transistor Array for Recording Transepithelial Ion Transport of Human Airway Epithelial Cells, *Adv. Mater.*, n/a-n/a.
50. Stavrinidou, E., Leleux, P., Rajaona, H., Khodagholy, D., Rivnay, J., Lindau, M., Sanaur, S., and Malliaras, G. G. (2013) Direct Measurement of Ion Mobility in a Conducting Polymer, *Adv. Mater.* 25, 4488-4493.

## Chapter 4

---

### **4. Ionic liquid gels integrated with conformal electrodes for long-term cutaneous recordings and with organic electrochemical transistors for sensing applications.**

Cutaneous electrophysiological recordings are used in standard clinical tests to measure the integrity of an organ or a specific physiological function. For example, electroencephalography (EEG) is a diagnostic tool which typically uses metallic electrodes on the surface of the scalp to measure electrical activity in the brain<sup>1</sup>. When compared to other neurological diagnostic methods, EEG is less invasive and more cost-effective. For this reason, EEG continues to be the method of choice for clinicians when testing for neural pathologies<sup>2</sup>. It is often combined with other electrodes placed on the skin to simultaneously or independently measure cardiac activity (electrocardiography)<sup>3</sup> or muscular response (electromyography<sup>4</sup> – electrooculography<sup>5</sup>). Despite their widespread use in the majority of electrophysiological diagnostic procedures, currently used cutaneous electrodes have some shortcomings, especially in long-term measurements<sup>6</sup>: Temporal stability is an important characteristic for diagnostic tools, and in many cases, cutaneous recordings need to be performed over several days<sup>7</sup>. Ag/AgCl electrodes which are the current gold standard in cutaneous recordings require a liquid electrolyte to decrease the electrode/skin impedance. This is undesirable for several reasons: Firstly, the electrolyte often dries out over the course of only a few hours when exposed to open air<sup>8</sup>. As a result, the impedance of these electrodes usually increases and their ability to record meaningful signals is lost. Secondly, in cases where high density recordings are necessary, as in some EEG helmets, short circuits can occur if the liquid electrolyte leaks between two adjacent electrodes<sup>9</sup>. Thirdly, adding the electrolyte gel to each electrode is time-consuming and causes discomfort both to the patient and the caregiver. For these reasons, there is significant motivation to develop

alternative electrolytes for use in cutaneous measurements. Much effort has been put into improving dry electrodes which do not utilize a liquid electrolyte. One study reports the use of only a very small volume of gel which is released by pressure on the electrode, but this requires a system which is able to apply pressure to all the electrodes<sup>10</sup>. Several studies report the fabrication of micro-structures on the surface of the electrodes in order to increase the surface area and decrease the electrode impedance<sup>11-14</sup>. We recently reported the use of conducting polymers as dry electrodes with enhanced performance<sup>15</sup>. Another solution involves the use of spring-loaded contacts embedded in a flexible substrate<sup>8</sup>. Although these are promising ideas, the lack of an electrolyte means that movement artifacts are more likely to occur during recording.

Ionic liquids (ILs) are salts that are in a liquid state at room temperature<sup>16</sup>. They have recently inspired a great deal of research spanning a number of different fields due to their high chemical and thermal stability as well as their excellent ionic conductivity. ILs have been used in many biological applications, including as solvents that enhance the stability of proteins<sup>17</sup>. Although several IL families showing low cytotoxicity have been identified<sup>18-20</sup>, the establishment of general design rules for IL biocompatibility is the focus of ongoing work. ILs can be polymerized to yield gels which are especially appealing for use as a quasi-solid-state electrolytes<sup>21</sup>. Their lack of leakage makes them an ideal candidate for many electrochemical applications<sup>22</sup>, including bio-sensing electrodes<sup>23</sup> and transistors<sup>24</sup>. IL gels seem to be an appealing option for use with cutaneous electrodes because they do not leak or dry out and can be integrated with devices during fabrication, thereby addressing all short comings of electrodes currently used in electrophysiological recordings.

In this work we report the use of IL gel-assisted electrodes in long term cutaneous recordings. We incorporated the IL gel onto electrodes made of Au and of the conducting polymer poly(3,4-ethylenedioxythiophene) doped with poly(styrene sulfonate) (PEDOT:PSS). The latter was used as it was shown to yield high performance dry electrodes<sup>15</sup>. The electrodes were deposited on a thin film of parylene C to render them conformable to the skin. We show that the IL gel improves the performance of the electrodes and helps maintain a low impedance over longer periods of time than commercially available electrodes.

## 4.1. Fabrication and characterization of electrodes with ionic liquid gel

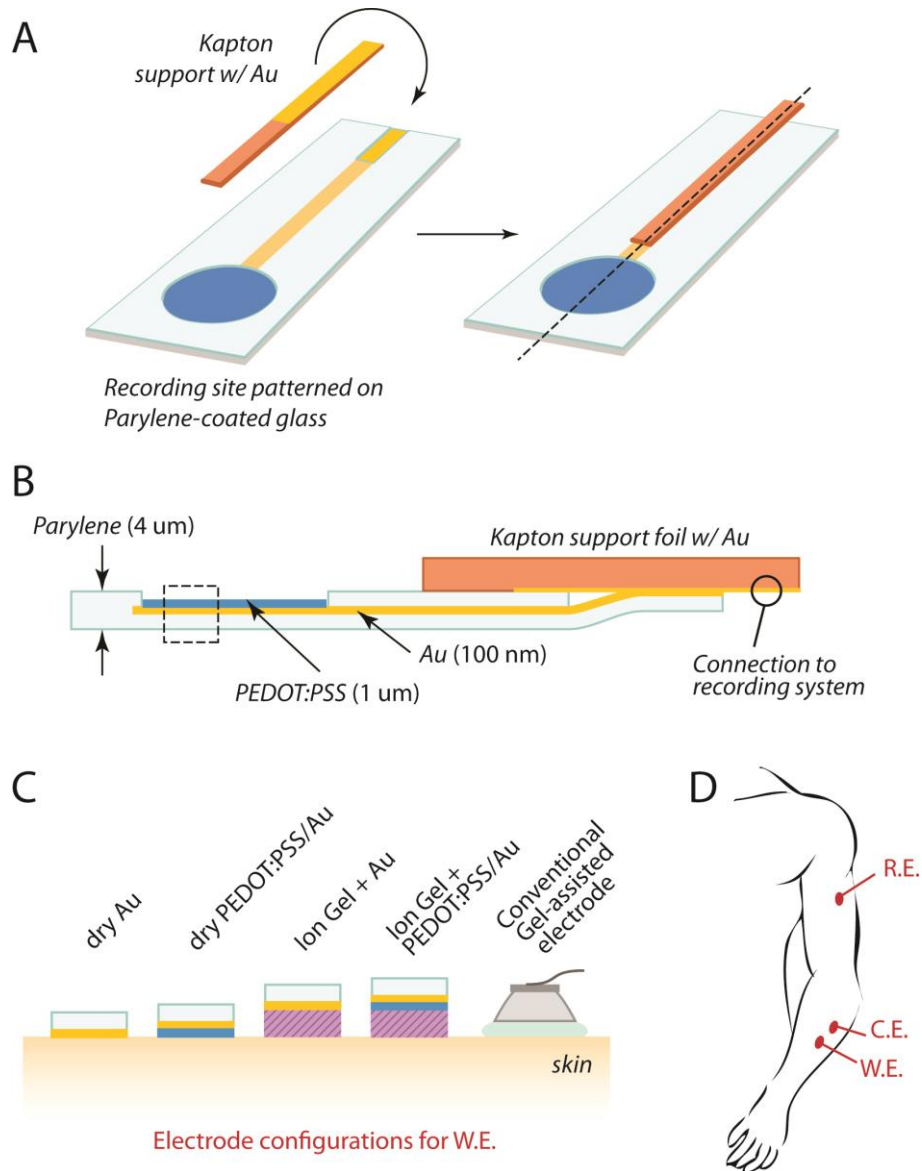


**Figure 4.1:** (A) Schematic of the electrode assembly, and (B) cross-section of an electrode. (C) The different electrode configurations tested. (D) Schematic of the electrode positions on a subject's arm. The working electrode (W.E.) and counter electrode (C.E.) were placed on the forearm, 5 cm away from each other. The reference electrode (R.E.) was placed on the arm, 30 cm away from the W.E.

Figure 4.1 illustrates the fabrication process for the devices. Gold electrodes were patterned using shadow mask evaporation onto a 2 micron thick layer of parylene

C. We then insulated the electrodes with two additional layers of parylene, with a thickness of 2 microns each. An anti-adhesive soap was included between these two layers, to allow the top layer to be peeled-off at a later stage. Subsequently, a standard photolithographic process was used to expose only the electrode sites to etching. Once the devices were etched down to the gold layer, the conducting polymer PEDOT:PSS was spun over the entire wafer. The top layer of parylene was peeled-off, patterning the PEDOT:PSS film over the electrode area and leaving the a parylene layer insulating only the interconnects (the details of this patterning technique were reported in <sup>25</sup>). This process yields electrodes with a total thickness of only  $\sim 4$  microns, a size which endows them with a high conformability. A support foil was laser-cut out of Kapton and gold was deposited on it. It was connected to the electrode using a small amount of adhesive placed on its periphery. Figure 4.1a shows how the electrode and support foil were attached to each other. Figure 4.1b shows how this fabrication process resulted in a conformal 4 micron thick electrode which was also strong enough to withstand connection. The gel was made using the IL (1-ethyl-3-methylimidazolium ethyl sulfate), the polymer poly(ethylene glycol)-diacrylate, and a photo initiator<sup>24</sup>. It was polymerized directly on the electrode during the fabrication process. A variety of electrodes were prepared using this general process (Figure 4.1c), including dry Au and PEDOT:PSS electrodes, Au and PEDOT:PSS electrodes with the IL gel, and a commercial Ag/AgCl electrode (which included an aqueous gel).

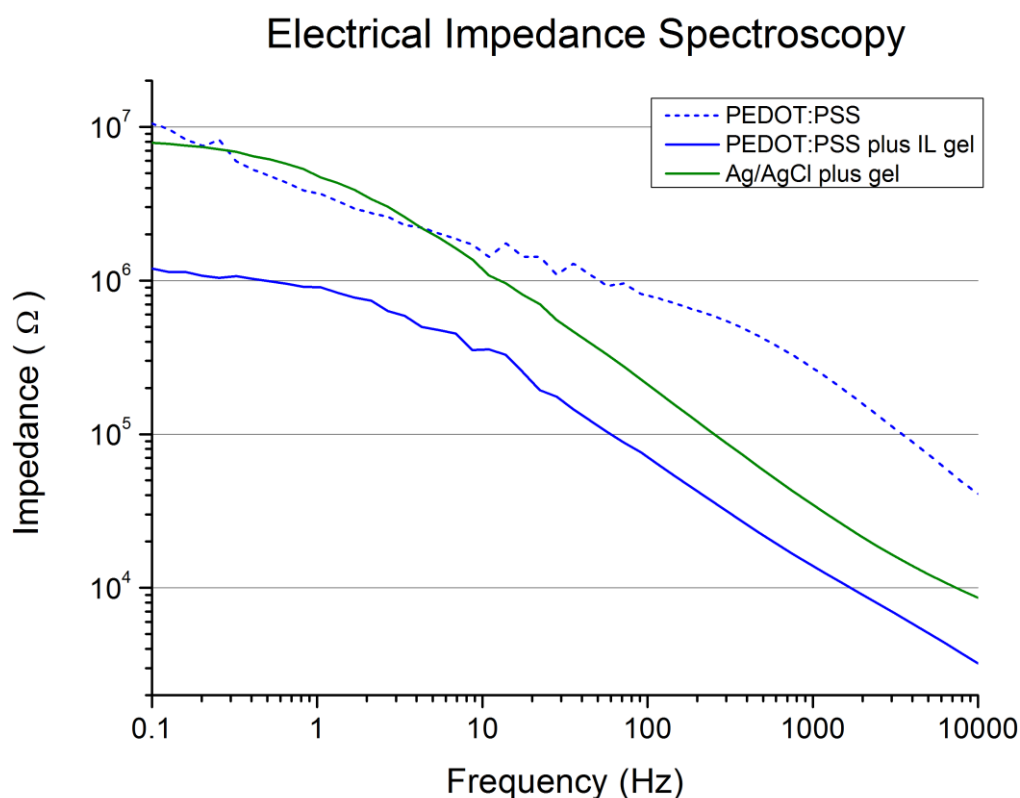


**Figure 4.2:** *Electrical impedance spectra corresponding to PEDOT:PSS electrodes, IL gel-assisted PEDOT:PSS electrodes, and a commercial Ag/AgCl electrode with an aqueous gel, all in contact with skin.*

In order to compare the performance of these electrodes in cutaneous recordings, we tested the electrode/skin impedance on a healthy volunteer. The electrodes were placed on the subject's arm as shown in Figure 4.1d using a 3-electrode configuration, where both counter and reference electrodes were commercial Ag/AgCl electrodes. Figure 4.2 shows typical electrical impedance spectra for all electrodes tested. In terms of dry electrodes, PEDOT:PSS demonstrated a lower impedance than Au, consistent with results obtained in microelectrode arrays *in vitro*<sup>25</sup>. Adding an IL gel decreases the impedance of both electrodes considerably: At 1 kHz, which is the frequency at which EEG electrodes are tested clinically, the impedance of the IL gel-assisted and aqueous gel-assisted electrodes is similar (see below for measurement error).

The temporal stability of the gel-assisted electrodes is shown in Figure 4.3. The same setup as for the previous measurement was used, and impedance was measured at 1 kHz on a healthy volunteer's arm over a period of 3 days. All three electrodes began in approximately the same range, but while the impedance of the commercial electrode steadily increased, the impedance of both IL gel-assisted electrodes remained relatively constant. Both IL gel-assisted electrodes were able to record with low impedance over 3 days, while the impedance of the commercial electrode increased dramatically after only 1 day. In fact, after 20 hours the Ag/AgCl electrode showed impedance that was too high for high quality cutaneous recordings and recordings from this electrode were stopped. Possible reason is the dehydration of the commercial gel, owing to its water based nature.

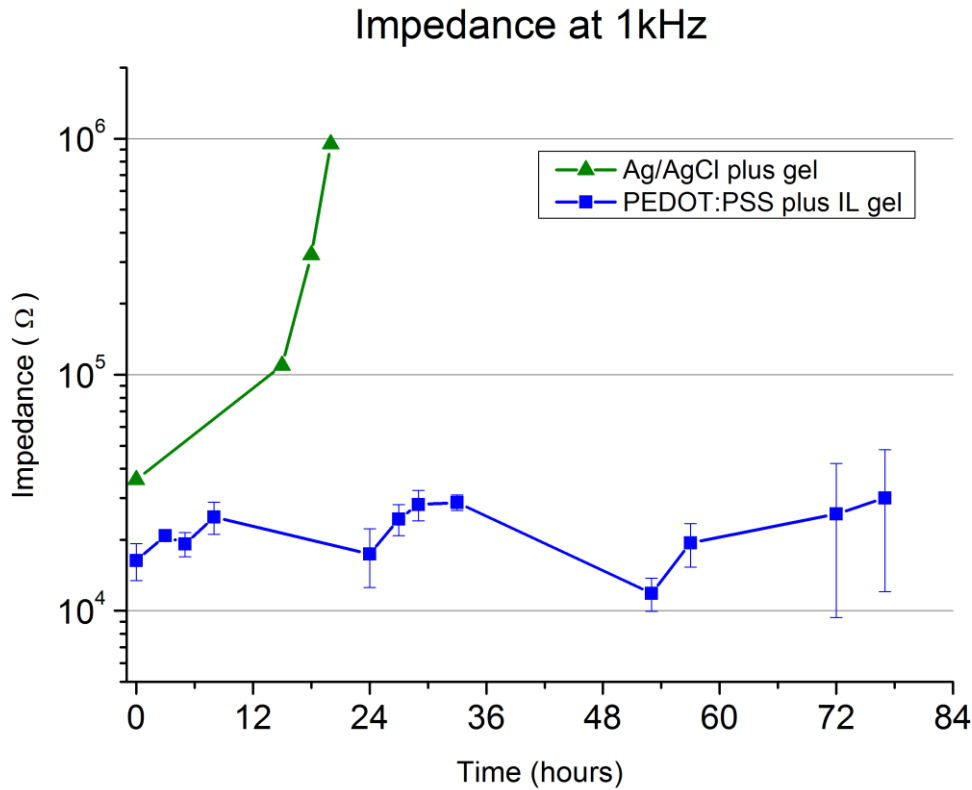


**Figure 4.3:** Electrode/skin impedance measured at 1 kHz for IL gel-assisted PEDOT:PSS electrodes and commercial Ag/AgCl electrode with an aqueous gel.

Although both IL gel-assisted electrodes showed similar values of impedance, the PEDOT:PSS electrodes performance exhibited less variation. The error bars in Figure 4.3 represent measurements recorded by 5 different devices for each type of IL gel-assisted electrode. The observed variations are due to a multitude of reasons, including device-to-device variations (fabrication, electrode work-function), and changes in the hydration of the skin. The conducting polymer-based electrode is shown to exhibit less variation than the Au-based one, owing to a more stable surface. This is consistent with work on implantable microelectrodes, which showed that conducting polymer electrodes offer lower drift *in vivo* than electrodes made from metals<sup>26, 27</sup>. As the measurements were carried out on a person's arm, many factors caused slight changes in the performance of the electrodes. After the subject showered, for example, the electrodes were partially rehydrated and the impedance decreased. As it can be seen in figure 4.3, both IL gel-assisted electrodes followed the same cycle: Lowering of impedance due to rehydration and subsequent increasing of impedance during the course of the day. This variation is due to a measurement protocol that represents an accurate model for cutaneous recordings under realistic conditions, as the latter are carried out on patients who inevitably sweat, particularly if bandages are used.

In this work we used a photo-crosslinkable IL gel to show that these materials help remedy the most important shortcoming of cutaneous electrodes, namely they can be used for long term measurements. Moreover, as IL gels do not flow, they can enable high density electrode arrays without causing short circuits. Finally, IL gels can be incorporated onto the electrodes during fabrication, yielding ready-to-use devices. The fabrication scheme outlined here is compatible with such an endeavor, and the IL gel can be patterned at the same time as the conducting polymer using the peel-off step. There exists a great variety in IL structures and in ways to render them in a gel form. Future research should focus on exploring the tradeoff between the conductivity and mechanical properties of these materials to deliver IL gel-assisted electrodes with even higher performance.

## **4.2. Ionic liquid gels integrated with OECTs for multianalyte sensors.**

The availability of sensitive, reliable and inexpensive biosensors is an important goal for the diagnostics industry. Many different technologies have been proposed for biosensing but, unfortunately, they often lack in terms of portability, cost, and sensitivity. The OECT has the potential to overcome these limitations owing to its amplification properties, ease of fabrication, and micrometer scale dimensions. OECTs have been used as glucose sensors by employing either aqueous electrolytes or liquid phase electrolytes<sup>27-31</sup>. Recently, OECTs using iongel as electrolyte have been used to detect lactate in the physiological range in the sweat<sup>31</sup>. Additionally, OECTs have been integrated with microfluidic for multianalyte purposes<sup>32</sup>.

We took advantage of the iongel's properties and used it to functionalize glucose oxidase (GOx), lactate oxidase (LOx), with ferrocene as a mediator in the electrolyte in order to fabricate an array of OECTs for multianalyte purposes. We further integrated the system with a PDMS microfluidic. In figure 4.4a we see the lay-out of the device. The sample, consisting of glucose and lactate, enters the inlet of the PDMS fluidic and by spontaneous flow on top of each device, where measurements take place. The spontaneous flow is realized because of a degassing step of the PDMS fluidic prior to the use of the device. During the thorough degassing step the air is removed from the structure of the PDMS. By subsequent exposure of the fluidic at atmospheric conditions, the fluidic sucks air to its structure resulting in a vacuum in the fluidic channel. This vacuum is pulling the droplet of the analyte, thus creating a flow without the help of

external pump. Figure 4.4b demonstrates multiple drops of analyte samples entering and flowing through the microfluidic.

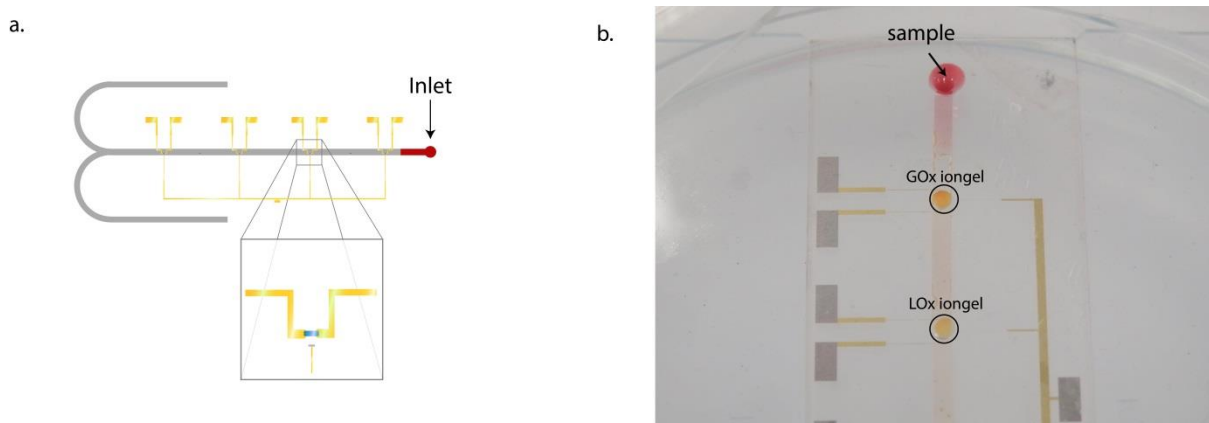


**Figure 4.4:** OECTs integrated with a PDMS pump-less microfluidic and an iongel electrolyte for continuous multianalyte measurements a. layout of the device b. figure showing flow of analyte without pump.

In order to test the device's sensing capabilities, we measured each device separately. For the enzymatic measurements a square pulse of 0.4 V for 180 sec was applied to the gate and therefore a current modulation was observed to the channel (figure 4.5). As expected, by addition of glucose to the system a modulation was observed, which was proportional to the glucose concentration. However, the modulation of the current was shifting to a direction which is opposite to the sensing mechanism. In more details, during the enzymatic redox reactions an electron is deposited at the gate of the OECT. This transfer of electrons causes a de-doping effect at the channel, thus decreasing the drain current. However, in figure 4.5 we observe a doping effect in the channel. This implies that upon multiple pulses, the ions existing in the iongel are stuffed into the channel and thus de-dope it. However, taking away the bias is not sufficient to bring the ions back to the electrolyte. Therefore, the channel remains de-doped. However, upon introducing an aqueous electrolyte such as PBS with small and highly mobile ions, its ions dominate the doping/de-doping process, thus a shift in the baseline is observed. An additional disadvantage of using an iongel of this type for enzymatic sensing is the low diffusion rates of the analytes to the gel. No further experiments were performed using the iongel, but an alternative approach using hydrogel as an electrolyte is under development.

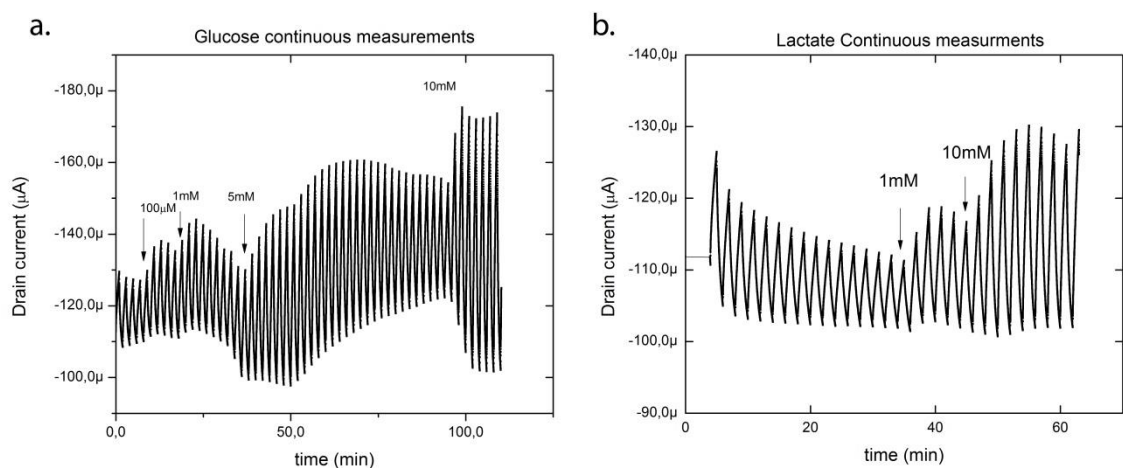


**Figure 4.5:** Drain current versus time upon application of gate voltage. *a.* addition of glucose with various concentrations *b.* addition of lactate with various concentrations.

### 4.3. Discussion

We demonstrate that ionic liquid gel-assisted electrodes can be used for long term cutaneous recordings. We fabricated conformal electrodes made of Au and PEDOT:PSS and compared their performance in a dry state as well as in conjunction with an IL gel. The IL gel decreases impedance at the interface with human skin to levels that are similar to those in commercial electrodes (at 1 kHz). The IL gel did not dry out and the electrodes continued to show a low impedance over the course of three days. The commercial electrode, on the other hand, gave up after only 20 hours. The IL gel-assisted electrodes provide a means of recording cutaneous electrophysiological data over extended periods of time, which is often necessary during diagnostic procedures. As such, they provide a path towards accurate and stable electrophysiological recordings, allowing clinicians to rely less heavily on more invasive diagnostic techniques.

We also used the iongel for sensing applications. However, the low diffusion rates of the analytes to the gel and the shift of the current baseline showed that the iongel is not the best solution for sensing applications.

## 4.4. Experimental section

*Fabrication of electrodes:* Parylene C was deposited on a silicon wafer in a SCS Labcoater 2 to a thickness of 2 microns (at which thickness parylene films are pinhole-free). Subsequently, 10 nm of chromium and 100 nm of gold were deposited using a metal evaporator. The metal was evaporated only onto the shape of the 8 mm diameter electrode using a shadow mask. This was followed by the deposition of an additional 2 micron thick layer of parylene, a non-adhesive layer, and a last 2 micron thick layer of parylene. AZ9260 photoresist was spun over the wafer and exposed to UV light using a SUSS MBJ4 contact aligner and a shadow mask. Following development of the photoresist using AZ developer, two layers of PEDOT:PSS were spun onto the wafer. The first layer was spun at 1500 rpm for 30 seconds; the second at 600 rpm for 30 seconds. The PEDOT:PSS was prepared by mixing 45 mL of aqueous dispersion (PH-1000 from H.C. Clark) with 5 mL of ethylene glycol, 6 drops of dodecyl benzene sulfonic acid (DBSA) and 0.5 mL of 3-glycidoxypropyltrimethoxysilane (GOPS, as a cross-linker). The PEDOT:PSS film on the wafer was baked at 140 C for 30 minutes and subsequently immersed in deionized water to remove any excess low-molecular weight compounds. The top layer of parylene was then removed, leaving behind the PEDOT:PSS only on the electrodes and contact pads. The remaining parylene C served to insulate the interconnects. A Au coated kapton support foil was glued to the device to give it some rigidity and enable an easy and stable connection to the recording system.

*IL Gel Preparation:* The IL gel was prepared by mixing the IL (1-ethyl-3-methylimidazolium ethyl sulfate) and the polymer poly(ethylene glycol) diacrylate (30% of the total weight solution). We then added 0.3% of the photo initiator 2-hydroxy-2-methylpropiophenone. We mixed until no phase separation was visible. Ten microliters of the solution were pipetted onto the electrode, and the gel was cross-linked using exposure to UV light for approximately one minute.

*Impedance Measurements:* Informed signed consent was obtained from the healthy volunteer on whom the impedance was measured. Impedance spectra were measured using an Autolab potentiostat equipped with a FRA module, with the electrodes placed on the subject's arm. The applied voltage was 0.01 V. Dry and IL gel-assisted electrodes were taped to the skin using surgical tape. Commercially available Ag/AgCl electrodes (Comepa Industries) for ECG were used (as received) as the aqueous gel-assisted working electrodes, and as the counter and reference electrodes for the impedance measurements. The latter were located 5 cm and 30 cm away from the working electrode, respectively. For the stability measurements shown in Fig. 4.3, fresh counter and reference

electrodes were used for each measurement. For all measurements and for all electrode types, we waited 10 min after the application of a fresh electrode before a measurement was taken.

*Electrochemical transistor fabrication and operation:* The fabrication process, similar to that reported previously included the deposition and patterning of gold, parylene, and PEDOT:PSS. Source/drain contacts were patterned by a lift-off process, using S1813 photoresist, exposed to UV light through a SUSS MJB4 contact aligner, and developed using MF-26 developer. 5 nm of chromium and 100 nm of gold were subsequently deposited using a metal evaporator, and metal lift-off was carried out in acetone. Metal interconnects and pads were insulated by depositing 2  $\mu\text{m}$  of parylene C using an SCS Labcoater 2, with a silane adhesion promoter. A dilute solution of industrial cleaner (Micro-90) was subsequently spin coated to act as an anti-adhesive for a second, sacrificial 2  $\mu\text{m}$  parylene C film. Samples were subsequently patterned with a 5  $\mu\text{m}$  thick layer of AZ9260 photoresist and AZ developer (AZ Electronic Materials). The patterned areas were opened by reactive ion etching with an oxygen plasma using an Oxford 80 Plasmalab plus. PEDOT:PSS + 1 wt% GOPS in solution, the usual formulation for *in vivo* applications, was spin coated at 3000 rpm, and baked for 90 sec in 100 °C. The second layer of parylene was peeled off with a subsequent rinsing in DI water and baking at 140 °C for 30 min.

*Fabrication of PDMS microfluidic:* uncured PDMS was poured on top of a silicon wafer. A 250  $\mu\text{m}$  thick PMMA was used as a mold and defined the fluidic channel size and geometry. A degassing step at 25 °C used to remove the bubbles and to create a smooth layer. After that, a curing step followed at 70 °C for 3 hours. Then the PDMS was peeled off from the pattern. An additional 1 mm layer for the bottom part of the fluidic was fabricated by using the same protocol.

*Iongel immobilization:* For the electrolyte the 1-ethyl-3-methylimidazolium ethyl sulfate was used as an ionic liquid, in combination with polyethylene glycol-diacrylate (PEG-DA) as a crosslinking polymer. All the chemicals were bought from Sigma-Aldrich. We used PEG-DA because of its property to self-polymerize under exposure of UV light. Another important property of the PEG-DA is the fast hydration, owing to its hydrophilicity. For the preparation of the Iongel, we mixed gently (30% optimized) of the enzyme in PBS and 70% of IL and we obtain a clear liquid. After that, PEG-DA 30% was added of the total solution. A small amount of 2  $\mu\text{l}$  was placed on top the devices. Post polymerization with an array of four UV-LEDs 365nm for 1 minute followed, and an Iongel with an immobilized enzyme acting as an electrolyte of our transistors was obtained.

## 4.5. References

1. Berger, H. (1929) Über das Elektrenkephalogramm des Menschen, *Archiv für Psychiatrie und Nervenkrankheiten* 87, 527-570.
2. Quinonez, D. (1998) Common applications of electrophysiology (EEG) in the past and today: the technologist's view., *Electroencephalogr. Clin. Neurophysiol.* 106, 108-112.
3. Gilchrist, J. M. (1985) Arrhythmogenic seizures: diagnosis by simultaneous EEG/ECG recording., *Neurology* 35, 1503-1506.
4. Achaibou, A., Pourtois, G., Schwartz, S., and Vuilleumier, P. (2008) Simultaneous recording of EEG and facial muscle reactions during spontaneous emotional mimicry, *Neuropsychologia* 46, 1104-1113.
5. Akerstedt, T., and Gillberg, M. (1990) Subjective and objective sleepiness in the active individual., *The International journal of neuroscience* 52, 29-37.
6. Green, R. M., Messick, W. J., Ricotta, J. J., Charlton, M. H., Satran, R., McBride, M. M., and Deweese, J. A. (1985) Benefits, shortcomings, and costs of EEG monitoring, *Annals of surgery* 201, 785-792.
7. Schad, A., Schindler, K., Schelter, B., Maiwald, T., Brandt, A., Timmer, J., and Schulze-Bonhage, A. (2008) Application of a multivariate seizure detection and prediction method to non-invasive and intracranial long-term EEG recordings, *CLINICAL NEUROPHYSIOLOGY* 119, 197-211.
8. Liao, L.-D., Wang, I.-J., Chen, S.-F., Chang, J.-Y., and Lin, C.-T. (2011) Design, fabrication and experimental validation of a novel dry-contact sensor for measuring electroencephalography signals without skin preparation., *Sensors (Basel, Switzerland)* 11, 5819-5834.
9. Tenke, C. E., and Kayser, J. (2001) A convenient method for detecting electrolyte bridges in multichannel electroencephalogram and event-related potential recordings, *CLINICAL NEUROPHYSIOLOGY* 112, 545-550.
10. Mota, A. R., Duarte, L., Rodrigues, D., Martins, a. C., Machado, a. V., Vaz, F., Fiedler, P., Haueisen, J., Nóbrega, J. M., and Fonseca, C. (2013) Development of a quasi-dry electrode for EEG recording, *Sensors and Actuators A: Physical* 199, 310-317.
11. Salvo, P., Raedt, R., Carrette, E., Schaubroeck, D., Vanfleteren, J., and Cardon, L. (2012) A 3D printed dry electrode for ECG/EEG recording, *Sensors and Actuators A: Physical* 174, 96-102.
12. Matteucci, M., Carabalona, R., Casella, M., Di Fabrizio, E., Gramatica, F., Di Rienzo, M., Snidero, E., Gavioli, L., and Sancrotti, M. (2007) Micropatterned dry electrodes for brain-computer interface, *Microelectronic Engineering* 84, 1737-1740.
13. O'Mahony, C., Pini, F., Blake, A., Webster, C., O'Brien, J., and McCarthy, K. G. (2012) Microneedle-based electrodes with integrated through-silicon via for biopotential recording, *Sensors and Actuators A: Physical* 186, 130-136.
14. Ng, W. C., Seet, H. L., Lee, K. S., Ning, N., Tai, W. X., Sutedja, M., Fuh, J. Y. H., and Li, X. P. (2009) Micro-spike EEG electrode and the vacuum-

- casting technology for mass production, *Journal of Materials Processing Technology* 209, 4434-4438.
15. Leleux, P., Badier, J.-M., Rivnay, J., Bénar, C., Hervé, T., Chauvel, P., and Malliaras, G. G. (2013) Conducting Polymer Electrodes for Electroencephalography, *Advanced healthcare materials*, 142-7.
  16. Armand, M., Endres, F., MacFarlane, D. R., Ohno, H., and Scrosati, B. (2009) Ionic-liquid materials for the electrochemical challenges of the future, *Nat. Mater.* 8, 621-629.
  17. Nakashima, K., Maruyama, T., Kamiya, N., and Goto, M. (2005) Comb-shaped poly(ethylene glycol)-modified subtilisin Carlsberg is soluble and highly active in ionic liquids., *Chemical communications (Cambridge, England)*, 4297-4299.
  18. Vrikkis, R. M., Fraser, K. J., Fujita, K., MacFarlane, D. R., and Elliott, G. D. (2009) Biocompatible Ionic Liquids: A New Approach for Stabilizing Proteins in Liquid Formulation, *Journal of Biomechanical Engineering* 131, 074514-074514.
  19. Weaver, K. D., Kim, H. J., Sun, J. Z., MacFarlane, D. R., and Elliott, G. D. (2010) Cyto-toxicity and biocompatibility of a family of choline phosphate ionic liquids designed for pharmaceutical applications, *Green Chem* 12, 507-513.
  20. Rebros, M., Gunaratne, H. Q. N., Ferguson, J., Seddon, K. R., and Stephens, G. (2009) A high throughput screen to test the biocompatibility of water-miscible ionic liquids, *Green Chem* 11, 402-408.
  21. Lu, J., Yan, F., and Texter, J. (2009) Advanced applications of ionic liquids in polymer science, *Prog Polym Sci* 34, 431-448.
  22. Buzzeo, M. C., Evans, R. G., and Compton, R. G. (2004) Non-haloaluminate room-temperature ionic liquids in electrochemistry - A review, *Chemphyschem* 5, 1106-1120.
  23. Safavi, A., Maleki, N., Moradlou, O., and Tajabadi, F. (2006) Simultaneous determination of dopamine, ascorbic acid, and uric acid using carbon ionic liquid electrode., *Analytical biochemistry* 359, 224-229.
  24. Khodagholy, D., Curto, V. F., Fraser, K. J., Gurfinkel, M., Byrne, R., Diamond, D., Malliaras, G. G., Benito-Lopez, F., and Owens, R. M. (2012) Organic electrochemical transistor incorporating an ionogel as a solid state electrolyte for lactate sensing, *J. Mater. Chem.* 22, 4440-4443.
  25. Sessolo, M., Khodagholy, D., Rivnay, J., Maddalena, F., Gleyzes, M., Steidl, E., Buisson, B., and Malliaras, G. G. (2013) Easy-to-Fabricate Conducting Polymer Microelectrode Arrays, *Adv. Mater.* 25, 2135-2139.
  26. Ludwig, K. A., Uram, J. D., Yang, J. Y., Martin, D. C., and Kipke, D. R. (2006) Chronic neural recordings using silicon microelectrode arrays electrochemically deposited with a poly(3,4-ethylenedioxythiophene) (PEDOT) film, *J. Neural Eng.* 3, 59-70.
  27. Kim, D.-H., Richardson-Burns, S., Povlich, L., Abidian, M. R., Spanninga, S., Hendricks, J., and Martin, D. C. (2008) Soft, Fuzzy, and Bioactive Conducting Polymers for Improving the Chronic Performance of Neural Prosthetic Devices, In *Indwelling Neural Implants: Strategies for Contending with the In-Vivo Environment* (Reichert, W. M., Ed.), pp 165-207, CRC Press, Taylor and Francis, Boca Raton, FL.

28. Bernardis, D. a., Macaya, D. J., Nikolou, M., DeFranco, J. a., Takamatsu, S., and Malliaras, G. G. (2008) Enzymatic sensing with organic electrochemical transistors, *Journal of Materials Chemistry* 18, 116-116.
29. Shim, N. Y., Bernardis, D. a., Macaya, D. J., DeFranco, J. a., Nikolou, M., Owens, R. M., and Malliaras, G. G. (2009) All-Plastic Electrochemical Transistor for Glucose Sensing Using a Ferrocene Mediator, *Sensors* 9, 9896-9902.
30. Yang, S. Y., Cicoira, F., Byrne, R., Benito-Lopez, F., Diamond, D., Owens, R. M., and Malliaras, G. G. (2010) Electrochemical transistors with ionic liquids for enzymatic sensing, *Chemical communications (Cambridge, England)* 46, 7972-7974.
31. Khodagholy, D., Curto, V. F., Fraser, K. J., Gurfinkel, M., Byrne, R., Diamond, D., Malliaras, G. G., Benito-Lopez, F., and Owens, R. M. (2012) Organic electrochemical transistor incorporating an ionogel as a solid state electrolyte for lactate sensing, *J. Mater. Chem.* 22, 4440-4443.
32. Yang, S. Y., DeFranco, J. a., Sylvester, Y. a., Gobert, T. J., Macaya, D. J., Owens, R. M., and Malliaras, G. G. (2009) Integration of a surface-directed microfluidic system with an organic electrochemical transistor array for multi-analyte biosensors, *Lab on a chip* 9, 704-708.

## Chapter 5

---

### 5. In vitro enzymatic sensing using biofunctionalized OECTs

Glucose is the main external source of energy for cells. The glucose uptake is a symporter mechanism that involves protein transporters, such as GLUT5, localized in the apical side of epithelial cells and Na<sup>+</sup> ions. Inside the cell, glucose can be degraded to produce energy or just transported to the basal side. The glucose exit is due to a uniporter mechanism termed GLUT2. The glucose effluxes can be taken up by other cells, such as endothelial cells. The cell degrades the glucose, in an oxygen-dependent manner, for generating ATP and other sub products that could be used for metabolic purposes. One of these products is lactate, which is mostly produced under anaerobic conditions and upon cell damage. The balance between glucose and lactate levels plays a key role in the cellular metabolism regulation. When this balance is upset diseases such as diabetes occur, in which a major diagnostic method is monitoring the glucose concentration in blood.<sup>1</sup> In tissue engineering, the quantification of these molecules is important to determine the metabolic activities of the cells in normal and under different stimuli, for instance the detection of lactate is considered an ideal non-invasive marker for evaluating cyclosporine and diclofenac toxicity in human proximal tubule cells.<sup>2, 3</sup>

Current methods for detecting glucose and lactate *in vitro* and *in vivo* are based on colorimetric reactions using tetrazolium salts<sup>4</sup>, glucose oxidase-based reactions, hydrogen peroxide detection, fluorescent-based sensors and nanomaterials as carbon nanotubes or graphene; however they cannot be use in long term detection and in some cases their cytotoxicity is still unclear.<sup>5</sup>

The OECT can potentially overcome such limitations. In the OECT the electrolyte is in direct contact with both the gate and the channel. This facilitates, first of all, better interface with the biological environment, and transduction of low magnitude ionic fluxes to high magnitude electronic currents.<sup>6</sup> In other words, it is a biological signal amplifier which operates in the closest proximity of the event of interest.<sup>7</sup> The OECT has been successfully used

in a variety of biological applications. These applications are ranging from the sensing of ions and metabolites such as glucose to the monitoring of cells viability and integrity.<sup>8-10</sup> Because of its high amplification properties, the use of robust materials, and the combination with metals that exhibit high catalytic activities, the OECT results in high sensitivity enzymatic sensors.<sup>11</sup> Moreover, for *in vitro* and *in vivo* applications stability is important. Biofunctionalization, which is the binding of biomolecules to the conducting polymer, can improve stability for a long period of time. Different types of biofunctionalization depending on the application and the nature of the bond have been used. For example, physical entrapment of enzymes with the use of membranes is a simple yet reliable functionalization method.<sup>12</sup> However, owing to the ionic interactions of the membranes with electrolytes, delamination of the enzyme can be observed. For increased stability over extensive periods of time the use of covalent bonding is preferred and can result in stable biosensors.<sup>13</sup>

Additionally, OECTs have been used in monitoring the integrity of epithelial and endothelial cells.<sup>9, 14</sup> In more details, the OECT has been shown that it can detect the integrity of a barrier tissue, and how the barrier is affected by pathogenic organisms in complex media.<sup>15</sup> However, a continuous detection of metabolic activities in cells and how these activities are affected by toxic compounds has not been performed, to the best of our knowledge.

In this section we demonstrate *in vitro* detection of metabolic activities from cells using OECTs. After the fabrication of the OECT, further functionalization steps are performed in order to fabricate sensitive, stable, and selective enzymatic sensors. Furthermore, optimization for integration with living cells has been performed.

## **5.1. Fabrication and functionalization process of the OECT**

It is mandatory for an enzymatic sensor to exhibit high sensitivity and stability for an extensive period of time in order to achieve *in vitro* continuous metabolite sensing from cells. Furthermore, an important property that has to be considered, when sensing occurs in complex media with acids creating interference, is the selectivity. Finally, the integration with live cells necessitates biocompatibility. The OECT due to its amplification properties and the use of biocompatible materials facilitates easy integration with cells.<sup>10, 14</sup> Furthermore, conducting polymers can be blended with non-conducting polymers and result biofunctionalized devices.

In this study, OECTs were fabricated using the double layer parylene C technique resulting micrometer scale transistors.<sup>16</sup> In order to maintain one step fabrication, the channel as well as the gate had a planar configuration, with the area of the gate ten times bigger than the area of the channel.

For the biofunctionalization of the device, PEDOT:PSS:PVA was used as the active material.<sup>13</sup> This formulation allows the deposition of a silane layer either by chemical vapor deposition or by aqueous deposition (figure 5.1a). Prior to the deposition of the silane, Pt-NPs were deposited by electrodeposition using a three electrode set up connected to a potentiostat. The gate of the OECT was used as a working electrode. A solution containing 5mM chloroplatinic acid ( $\text{H}_2\text{PtCl}_6$ ) and 100 mM sulfuric acid ( $\text{H}_2\text{SO}_4$ ) as a supporting electrolyte. Pt-NPs because of their high catalytic properties to the oxidation of hydrogen peroxide in combination with their high surface area can result highly sensitive enzymatic sensors.<sup>17</sup> The deposition of Pt-NPs was done by pulse voltammetry. During this process, Pt ions are reduced by a negative potential. The reduced ions precipitate and create small islands in the nanometer scale. In more details, by the application of a positive potential at  $V = 0.7 \text{ V vs Ag/AgCl}$  no reactions occurs at the gate-working electrode. The duration in this potential gives time to the Pt ions to diffuse in the bulk of PEDOT:PSS, in order to produce nanoparticles to the whole bulk of the electrode. As, the potential shifts to a negative value of  $V = -0.2 \text{ V vs Ag/AgCl}$ , the reduction of Pt ions occurs, resulting the creation of Pt-NPs. The Pt-NPs have sizes of 100 nm with high density into the PEDOT:PSS film (figure S5.1). The catalytic activity of the modified gate was tested by oxidation on  $\text{H}_2\text{O}_2$ . Upon application of a constant positive potential at the gate ( $V_g = 0.3 \text{ V}$ ), the  $\text{H}_2\text{O}_2$  is oxidized by the Pt-NPs, and a modulation of the drain current is observed.

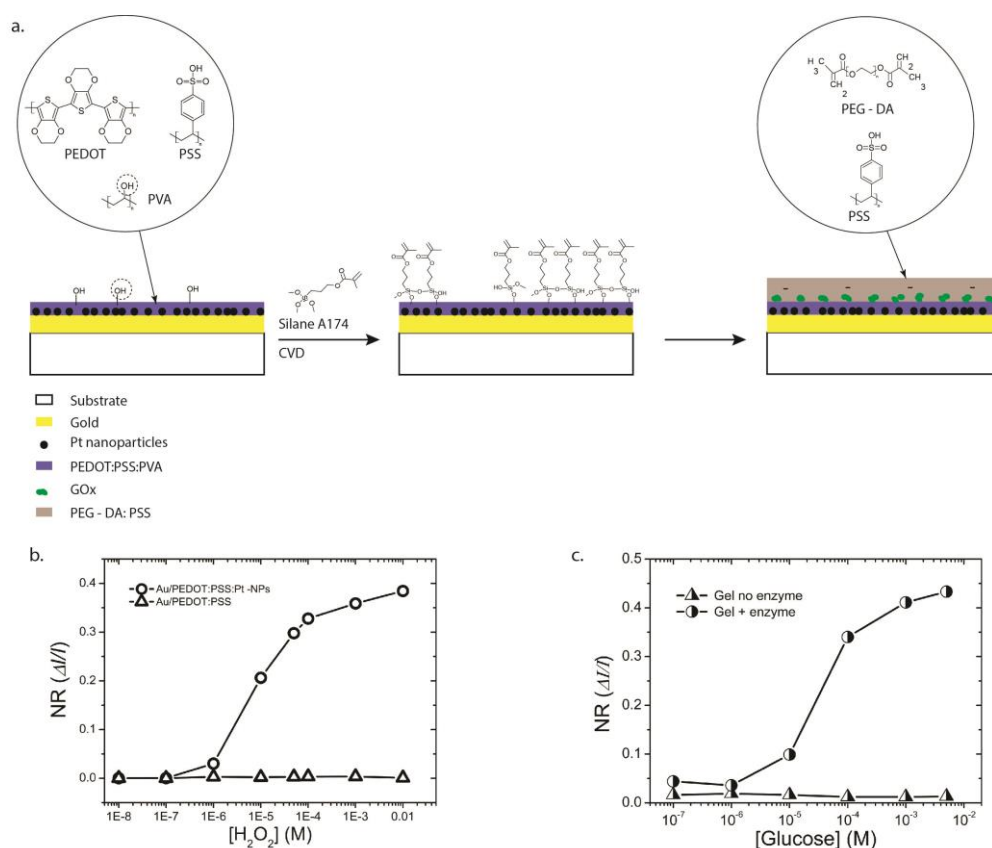


**Figure 5.1:** Biofunctionalization steps of the OEET. *a.* from left to right steps: deposition of Pt-NPs, chemical vapor deposition of silane A174 onto PEDOT:PSS:PVA and PEG-DA:PSS:GOx hydrogel deposition. *b.* Normalized current response  $NR(\Delta I/I)$  with concentration of  $H_2O_2$  for a control gate consisting of Au/PEDOT:PSS:PVA (triangles) and for the gate of interest Au/PEDOT:PSS:PVA:Pt-NPs (circles). *c.* Normalized current response  $NR(\Delta I/I)$  with a concentration of glucose for a functionalized gate with hydrogel with (circles) and without (triangles) GOx.

Figure 5.1b displays the normalized current response (NR) of an OEET with Pt-NP modified gate. The OEET exhibits an s-shape NR with  $H_2O_2$  concentration with a linear response in the micrometer range, and a limit of detection less than  $1\mu M$ . In the absence of Pt-NPs no oxidation of hydrogen peroxide is observed, validating the activity of the modified gate.

The enzyme was functionalized on top of the gate by entrapment on a photocrosslinkable hydrogel. The hydrogel consisted of polyethylene glycol diacrylate (PEG-DA) mixed with polystyrene sulfonate (PSS) and enzyme. Under UV light the PEG-DA is cross-linked. A small amount of photo-initiator (1 wt. % to PEG-DA) was added to start the polymerization. The hydrogel crosslinks, additionally, to the PEDOT:PSS:PVA, because of the deposition of a 3-(trimethoxysilyl)propyl methacrylate (A-174 silane). The covalent binding of the hydrogel to the PEDOT:PSS:PVA results in high stability of the sensor. Measurements carried

out after 20 days validate the stability of the enzyme for a long period of time (figure S5.2).

A NR versus glucose concentration in PBS is shown in figure 5.1c. The shape of the NR follows the same trend as the NR in figure 5.1b. In the case of hydrogel without enzyme no modulation is observed. The PSS in the hydrogel also acts as a negatively charged layer for the repulsion of acids (such as ascorbic acid, uric acid) that can interfere with the measurements.

The next step was to test the sensing of metabolites (glucose, lactate) in complex media. Devices functionalized with hydrogels consisting of glucose oxidase (GOx) lactate oxidase (LOx) and no enzyme as control were used for measurements of glucose and lactate in fresh media and in media that had been incubated with cells for 24 hours. The concentration of glucose in the fresh media was 5 mM. An initial PBS electrolyte with 45  $\mu$ L was used and 5  $\mu$ L of diluted media with different concentrations was added. In figure 5.2a we can see the NR response vs concentration of media for a device with and without GOx. The OECT with enzyme shows higher values of NR with a shift of the slope starting in lower values. For the control device we observe an interference background, which has, however, low changes compared to devices functionalized with GOx. The difference in the normalized response demonstrates that the device is capable of sensing glucose in a physiologically relevant background. Figure 5.2b, shows the NR versus the concentration of media incubated with cells for 24 hours. The concentration of glucose has decreased, with a substantial increase in the lactate concentration, while the interference of the background stays at the same level. This indicates that the glucose was converted to lactate by the cells.

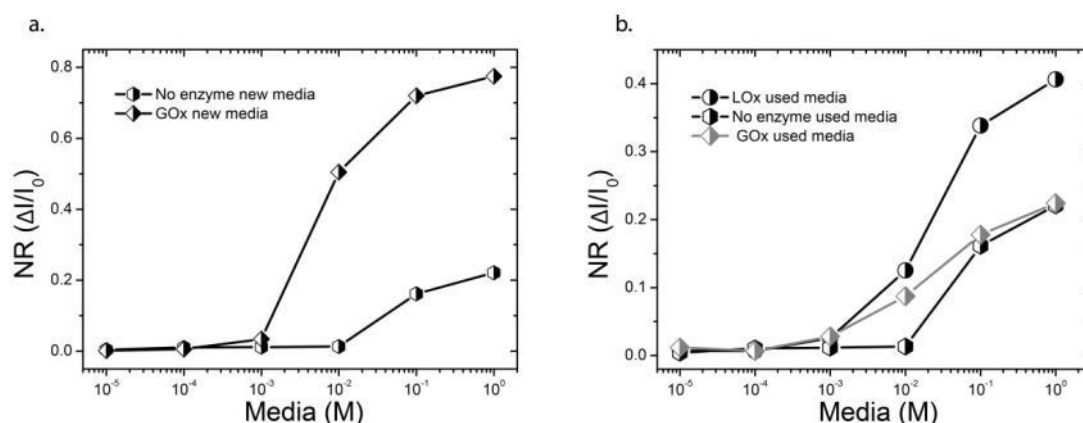


**Figure 5.2:** Measurements of glucose and lactate in complex media (DMEM). *a.* NR vs concentration of fresh media, which has initial glucose concentration of 5 mM. *b.* NR vs concentration of media incubated with cells for 24 hours.

Subsequently, an array of three devices: one with GOx functionalized gate, one with LOx functionalized gate, and one control device were incubated with MDCK cells for *in vitro* analyte measurements. A glass well was placed and glued on the substrate by using a thin layer of PDMS, in order to confine the electrolyte. Prior to the seeding of cells, collagen was added to improve their adhesion. In figure 5.3a we see the lay-out of the device with cells. After 48 hours the creation of a cell layer is observed for the control device and the device consisting of LOx. In the case of GOx the cells do not adhere to the substrate (figure S5.3). The reason is because the initial concentration of glucose in media is high, thus the immobilized enzyme converts the glucose to H<sub>2</sub>O<sub>2</sub>, which is toxic for the cells.<sup>9</sup> In the case of the control device and the device with LOx the cells created a healthy cell layer. This layer is extended in the whole area confined by the well, apart from the hydrogel (figure 5.3b), because of the bio-inert properties of PEG. An additional advantage of the gate not covered by cells is that the glucose and lactate can diffuse into the functionalized gate and redox reactions can take place figure 5.3a. *In vitro* measurements with cells were carried out inside an incubator and 37°C for two devices one with LOx and one control device. Fresh media was added to both devices prior to the measurements. Figure 5.3c shows the NR versus time for the two devices. As we can see from the plot the current in the control device stays at the same levels, whereas in the device functionalized with LOx, there is an increase in the NR. This validates the production of lactate from the cells. Further experiments are currently in progress for validating the metabolic activities and further studies of how toxic compounds affect these metabolic activities will potentially follow.

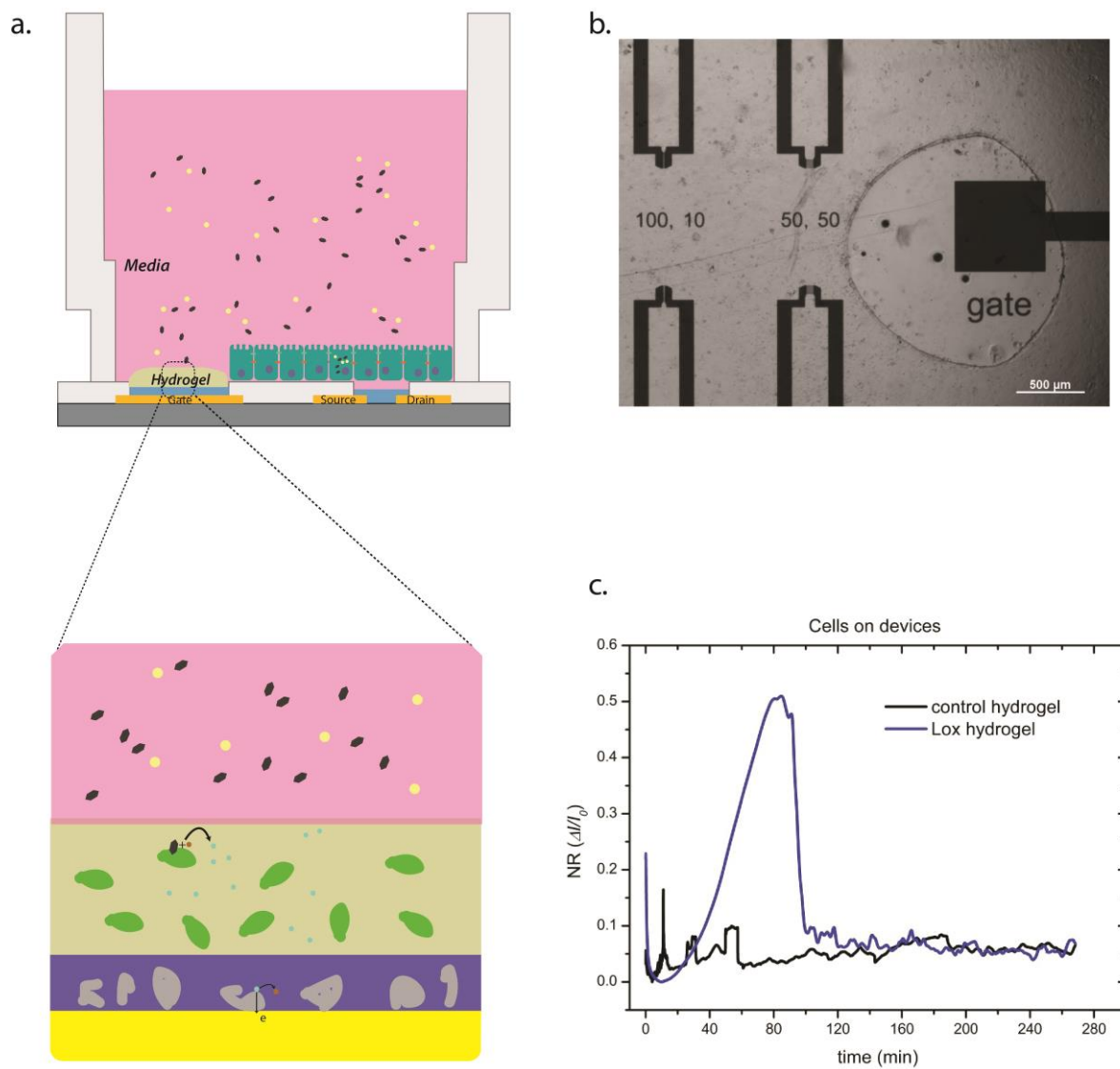


**Figure 5.3:** *In vitro* lactate sensing a. lay-out of the functionalized devices for *in vitro* measurements b. microscope image showing a cell layer covering the device except the gate. Scale bar 500 μm c. lay-out of the gate showing the diffusion of lactate its conversion to H<sub>2</sub>O<sub>2</sub> and the electron transfer to the gate. d. NR versus time for LOx and control device.

## 5.2. Discussion

To conclude, we demonstrate biofunctionalized OECTs that can be used for *in vitro* enzymatic measurements. The functionalization steps are: Pt-NP deposition to enhance sensitivity, modification of PEDOT:PSS with PVA for covalent binding with the silane and biomolecules. A further deposition of photo-cross linkable hydrogel overcomes multiple limitations: immobilization of enzymes for stability, deposition of a negatively charged membrane for selectivity. The OECTs exhibit high sensitivities for detection of the corresponding substrates over a background signal. It also shows stabilities over time. One limitation is that during the integration with cells, for *in vitro* measurements, the GOx functionalized device produces hydrogen peroxide from glucose which shows toxic effects to the cells (figure S5.3). For the devices with LOx we are able to measure the conversion of glucose to lactate *in vitro*. Further tests currently occur for the integration of cells to GOx functionalized devices by replacing a media containing glucose with a galactose one. In the presence of galactose the cells adhere to the devices and create layers. Finally, future work will study if and how the metabolic activities are being affected by toxic compounds.

## 5.3. Experimental section

*Electrochemical transistor fabrication and operation:* The process, similar to that reported previously<sup>13,16</sup> included the deposition and patterning of gold, parylene, and PEDOT:PSS:PVA. Source/drain contacts were patterned by a lift-off process, using S1813 photoresist, exposed to UV light through a SUSS MJB4 contact aligner, and developed using MF-26 developer. 5 nm of chromium and 100 nm of gold were subsequently deposited using a metal evaporator, and metal lift-off was carried out in acetone. Metal interconnects and pads were insulated by depositing 2  $\mu\text{m}$  of parylene C using an SCS Labcoater 2, using a silane adhesion promoter. A dilute solution of industrial cleaner (Micro-90) was subsequently spin coated to act as an anti-adhesive for a second, sacrificial 2  $\mu\text{m}$  parylene – C film. Samples were subsequently patterned with a 5  $\mu\text{m}$  thick layer of AZ9260 photoresist and AZ developer (AZ Electronic Materials). The patterned areas were opened by reactive ion etching with an oxygen plasma using an Oxford 80 Plasmalab plus. PEDOT:PSS:PVA in solution was spin coated at 3000 rpm, and baked for 90 sec in 100 °C. The second layer of parylene was peeled off with a subsequent rinsing in DI water and baking at 140 °C for 30 min. All characterization was done using a 100 mM NaCl solution in DI water as the electrolyte and a Ag/AgCl wire (Warner Instruments) as the gate electrode.

*Pt-NPs deposition:* The Pt-NPs were electrodeposited by reducing Pt ions. A Solution containing 5mM chloroplatinic acid ( $\text{H}_2\text{PtCl}_6$ ) and 50 mM sulfuric acid ( $\text{H}_2\text{SO}_4$ ) was used in a three electrodes set up connected to a Metrohm potentiostat. As reference electrode (RE) an Ag/AgCl was used, as Counter electrode a Pt layer, and as counter electrode (CE) the planar gate of the OECT. Pulse Voltametry was used with initial potential  $V_{\text{off}} = + 0.7$  vs Ag/AgCl – where no reduction occurs for 60 seconds and final potential  $V_{\text{on}} = - 0.2$  vs Ag/AgCl where deposition of Pt occurs was used for 3 sec. After that, the devices were soaked in DI water overnight for the removal of sulfuric acid, ethylene glycol, and DBSA. A cylindrical glass well with  $d = 8$  mm was used to confine the electrolyte.

*Hydrogel:* The hydrogel was consisted from polyethylene glycol-diacrylate 10 wt. % (MW ~ 6000), NaPSS 0.5wt.% (MW ~ 60000) and GOx 1 mg/ml in DI and 1wt.% of 2-Hydroxy-2-methylpropiophenone. The hydrogel was mixed thoroughly until a homogenous solution was obtained. A 2  $\mu\text{l}$  of the hydrogel was dropcasted / spincoated on top of the gate and photopolymerized with a UV led array for 3 min (in order to retain the structure and functionality of the enzyme). Prior to that, A 3-(trimethoxysilyl)propyl meth-acrylate (A-174 Silane) was deposited by chemical vapor deposition (CVD) under vacuum at 90 °C for 1 hour for tethering the PEDOT:PSS:PVA with the hydrogel. Finally, in the case of planar devices collagen was used as an adhesion promoter.

*Cell culture:* Epithelial MDCK II cells (Madin Darby kidney cells, kindly donated by Dr. Frédéric Luton, Institute of Cellular and Molecular Pharmacology, Valbonne, France) were routinely maintained at 37°C in a humidified atmosphere of 5%  $\text{CO}_2$  in complete DMEM (cDMEM) media (Dulbecco's Modified Eagle Medium, 10% fetal bovine serum, and Pen/Strep 5000 [U/mL] penicillin–5000 [ $\mu\text{g}/\text{mL}$ ] streptomycin). For all experiments, cells were plated at an initial density of  $6 \times 10^4$  cells/Transwell insert (0.4  $\mu\text{m}$  pore size, and area of 0.33  $\text{cm}^2$ ) and incubated until reach confluence. Before starting the experiments, the media was changed for fresh cDMEM. The inserts were placed into the device in the same conditions and glucose and/or lactate measurements were performed. All the experiments were done at 37°C and 5%  $\text{CO}_2$ .

*Device assembly and operation:* A 3d printed holder was designed using solidedge software, and printed by a Stratasys idea 3d printer. All the cells measurements were carried inside an incubator safe cell UV under 37 °C and 5%  $\text{CO}_2$ . The measurements were performed using a National Instruments PXIe-1062Q system. The channel of the OECT was biased using one channel of a source-measurement unit NI PXIe-4145. The gate voltage was applied using a NI PXI-6289 modular instrument. In the case of the IV-characteristics and transconductance characterization, the drain current was measured using the SMU channel used for the bias. Concerning the time response characterization of the OECT, one NI-PXI-4071 digital multimeter measured drain current, and a

channel of the NI PXI-6289 equipment measured gate voltage. All the measurements were triggered through the built-in PXI architecture.

## 5.4. Supplementary Information

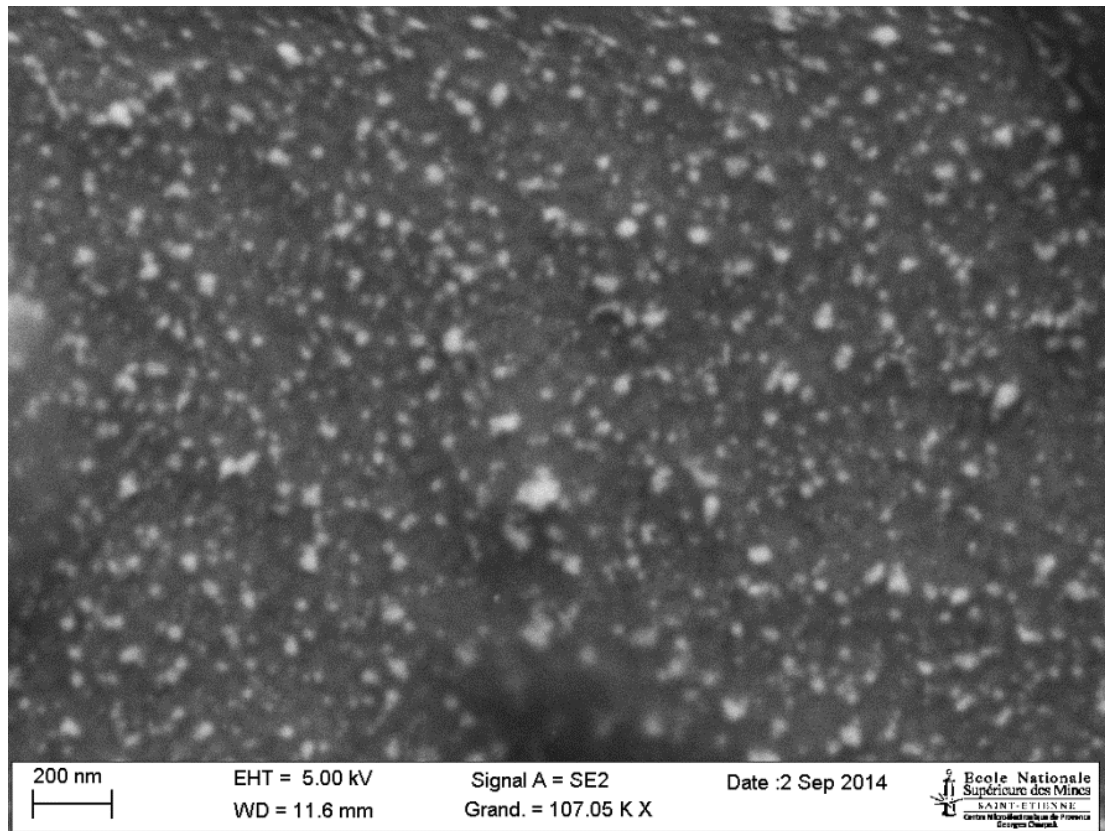


*Figure S5.1: SEM image of Pt-NPs into an Au/PEDOT:PSS:PVA gate.*

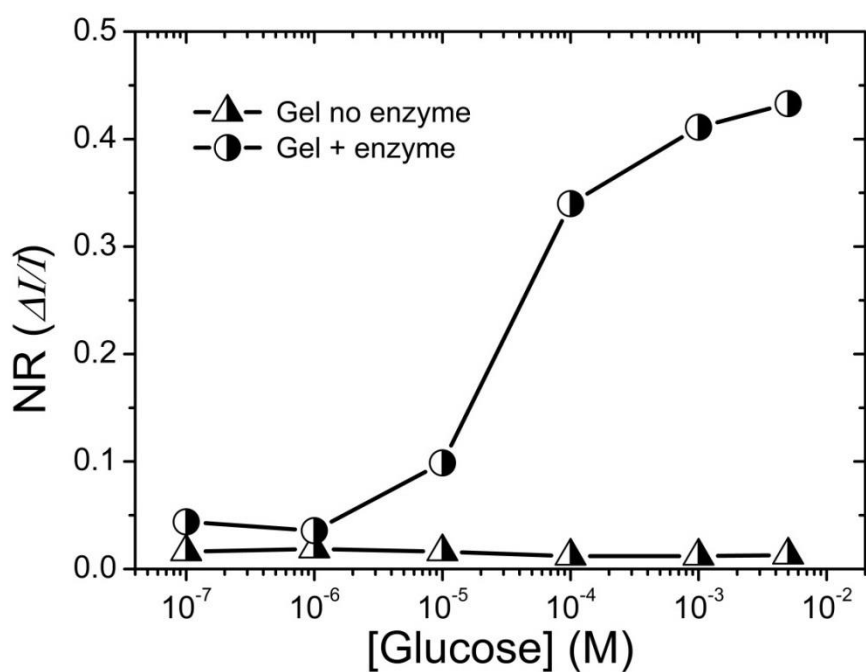


**Figure S5.2:** stability measurements of a device after 20 days. The electrolyte is media with and without glucose.



**Figure S5.3:** Barrier tissue layer of MDCK II cells 24 hours after seeding. a. for a functionalized device without enzyme into the hydrogel. b. for a device with LOx hydrogel. c. for a device with GOx hydrogel. Numbers indicate channel width and length in microns.

## 5.5. References

1. Yoo, E. H., and Lee, S. Y. (2010) Glucose biosensors: an overview of use in clinical practice, *Sensors (Basel)* 10, 4558-4576.
2. Limonciel, A., Aschauer, L., Wilmes, A., Prajczek, S., Leonard, M. O., Pfaller, W., and Jennings, P. (2011) Lactate is an ideal non-invasive marker for evaluating temporal alterations in cell stress and toxicity in repeat dose testing regimes, *Toxicol In Vitro* 25, 1855-1862.
3. Hasan, A., Nurunnabi, M., Morshed, M., Paul, A., Polini, A., Kuila, T., Al Hariri, M., Lee, Y. K., and Jaffa, A. A. (2014) Recent advances in application of biosensors in tissue engineering, *Biomed Res Int* 2014, 307519.
4. Babson, A. L., and Phillips, G. E. (1965) A rapid colorimetric assay for serum lactic dehydrogenase, *Clin Chim Acta* 12, 210-215.
5. Taguchi, M., Ptitsyn, A., McLamore, E. S., and Claussen, J. C. (2014) Nanomaterial-mediated Biosensors for Monitoring Glucose, *J Diabetes Sci Technol* 8, 403-411.
6. Rivnay, J., and Malliaras, G. G. (2013) The Rise of Organic Bioelectronics.
7. Khodagholy, D., Doublet, T., Quilichini, P., Gurfinkel, M., Leleux, P., Ghestem, A., Ismailova, E., Hervé, T., Sanaur, S., Bernard, C., and Malliaras, G. G. (2013) In vivo recordings of brain activity using organic transistors, *Nature communications* 4, 1575-1575.
8. Sessolo, M., Rivnay, J., Bandiello, E., Malliaras, G. G., and Bolink, H. J. (2014) Ion-Selective Organic Electrochemical Transistors, *Adv. Mater.* 26, 4803-4807.
9. Jimison, L. H., Tria, S. A., Khodagholy, D., Gurfinkel, M., Lanzarini, E., Hama, A., Malliaras, G. G., and Owens, R. M. (2012) Measurement of barrier tissue integrity with an organic electrochemical transistor, *Adv Mater* 24, 5919-5923.
10. Lin, P., Yan, F., Yu, J., Chan, H. L., and Yang, M. (2010) The application of organic electrochemical transistors in cell-based biosensors, *Adv Mater* 22, 3655-3660.
11. Tang, H., Yan, F., Lin, P., Xu, J., and Chan, H. L. W. (2011) Highly Sensitive Glucose Biosensors Based on Organic Electrochemical Transistors Using Platinum Gate Electrodes Modified with Enzyme and Nanomaterials, *Advanced Functional Materials* 21, 2264-2272.
12. Liao, C., Zhang, M., Niu, L., Zheng, Z., and Yan, F. (2013) Highly selective and sensitive glucose sensors based on organic electrochemical transistors

- with graphene-modified gate electrodes, *Journal of Materials Chemistry B* 1, 3820-3820.
13. Strakosas, X., Sessolo, M., Hama, A., Rivnay, J., Stavrinidou, E., Malliaras, G. G., and Owens, R. M. (2014) A facile biofunctionalisation route for solution processable conducting polymer devices, *Journal of Materials Chemistry B* 2, 2537-2537.
  14. Ramuz, M., Hama, A., Huerta, M., Rivnay, J., Leleux, P., and Owens, R. M. (2014) Combined optical and electronic sensing of epithelial cells using planar organic transistors, *Adv Mater* 26, 7083-7090.
  15. Tria, S. A., Ramuz, M., Huerta, M., Leleux, P., Rivnay, J., Jimison, L. H., Hama, A., Malliaras, G. G., and Owens, R. M. (2014) Dynamic monitoring of *Salmonella typhimurium* infection of polarized epithelia using organic transistors, *Advanced healthcare materials* 3, 1053-1060.
  16. Khodagholy, D., Rivnay, J., Sessolo, M., Gurfinkel, M., Leleux, P., Jimison, L. H., Stavrinidou, E., Herve, T., Sanaur, S., Owens, R. M., and Malliaras, G. G. (2013) High transconductance organic electrochemical transistors, *Nature communications* 4, 2133-2133.

# Chapter 6

---

## 6. Conclusion

The major work of this thesis is the development of functionalization methods compatible with OECTs. The overall goal is to produce devices that will be more stable, sensitive, biocompatible, and cheap. For example, for *in vitro* measurements of neurons it is important to pattern the neurons as close as possible to the channel of the OECT for better recordings and by functionalizing only the conducting channel it can be achieved. Furthermore, in the case of biosensors, stability as well as sensitivity is important, and by functionalizing the enzymes on the device, stable and reproducible biosensors can be produced for continuous measurements.

In more detail, in chapter 2 we explored two different functionalization methods for PEDOT:TOS, a CP which is obtained by vapor phase polymerization. The first biofunctionalization method was using surface chemistry to functionalize biomolecules to the conducting polymer. In order to create functional groups on the surface of PEDOT:TOS polymers which contains such groups were introduced prior to the polymerization process. Interestingly PEG, which was used for its alcohol groups increased the conductivity of PEDOT:TOS and additionally, its functional groups were available to chemically bind biomolecules. An alternative approach, is also to directly incorporate biomolecules into PEDOT:TOS. This approach facilitates polymerization and functionalization in the same step. By integration of gelatin with PEDOT:TOS the adhesion of BBB bovine cells was increased compared to the pristine polymer. For more fragile biomolecules such as enzymes, the incorporation occurs by stuffing the enzyme after the polymerization step avoiding its degradation in high temperatures. This method, results direct wiring of the enzyme to the polymer, however, the enzyme activity is affected.

In chapter 3 we use a functionalization method with PEDOT:PSS that can be used for multiple applications. This functionalization method employs the use of silanes for binding the biomolecules. Silanes have one part called silanol that crosslinks to alcohol groups and one side group that can be altered and tuned according to the chemical site of interest for binding. In order to induce alcohol groups into the PEDOT:PSS, PVA was blended, creating the composite

PEDOT:PSS:PVA. This functionalization method has been successfully used for two different applications: neuron-like cell patterning, and glucose sensing.

In chapter 4 we explore the use of ionic liquid in combination with crosslinkable polymers as alternative to liquid electrolytes. Ionic liquids exhibit many properties such as large electrochemical window of operation, non-flammability, low evaporation rates. When mixing with crosslinkable polymers they can result solid state electrolytes. The use of these solid state electrolytes can increase the stability of recordings in electrodes that are in contact with the skin, because they don't dry. Moreover, enzymes and can be entrapped inside the iongel resulting stable enzymatic sensors. However, slow diffusion of the analyte inside the iongel makes the sensors impractical.

In chapter 5 we record *in vitro* metabolic activities of cells, namely the conversion of glucose to lactate. The employment of crosslinkable hydrogel is used for the functionalization of the enzyme. The hydrogel approach serves multiple purposes. First of all, the amount of enzyme can be tuned, and the functionality is tuned and maintained. It also allows the use of a negative membrane for increasing the selectivity. Finally, it crosslinks with the conducting polymers, and thus it increases the stability. The use of Pt nanoparticles is used in order to make the planar gate functional to the catalysis of hydrogen peroxide. These OECTs are capable of recording *in vitro* the production of lactate and potentially the consumption of glucose.

## 6.1. Outlook

The need for novel biomedical tools that will address and overcome problems is mandatory. The development of multifunctional devices that will combine sensing, and recording capabilities as well as treatment capabilities will lead to new therapeutic methods. Take for example the case of epilepsy; in order to fire, neurons need energy, and the main energy source is glucose. So, if a device can record *in vivo* the levels of glucose and at the same time record electrical activities, it will be capable of recognizing when an epileptic crisis will occur. At the same time, the device should be capable of delivering drugs before the crisis occurs. Organic bioelectronics has made a tremendous progress towards the development of these devices.

# 7. Publications

## Chapter 1

**X. Strakosas**, M. Bongo, R. M. Owens “*The organic electrochemical transistor for biological applications.*” *Journal of Applied Polymers Science* 15, (2015).

## Chapter 2

Jimison, L. H., Hama, A., **Strakosas, X.**, Armel, V., Khodagholy, D., Ismailova, E., Malliaras, G. G., Winther-Jensen, B., and Owens, R. M. “*PEDOT:TOS with PEG: a biofunctional surface with improved electronic characteristics*”, *Journal of Materials Chemistry* 22, (2012) 19498-19498.

M. Bongo, O. Winther-Jensen, S. Himmelberger, **X. Strakosas**, M. Ramuz, A. Hama, E. Stavrinidou, G. G. Malliaras, A. Salleo, B. Winther-Jensen and R. M. Owens, “*PEDOT:Gelatin composites mediate brain endothelial cell adhesion*” *Journal of Materials Chemistry B*, 1, (2013) 3860-3860.

## Chapter 3

**Strakosas, X.**, Sessolo, M., Hama, A., Rivnay, J., Stavrinidou, E., Malliaras, G. G., and Owens, R. M. “*A facile biofunctionalisation route for solution processable conducting polymer devices*”, *Journal of Materials Chemistry B* 2, (2014) 2537-2537.

## Chapter 4

Leleux, Pierre. Johnson, Camryn. **Strakosas, Xenofon.** Rivnay, Jonathan. Hervé, Thierry Owens, Róisín M. Malliaras, George G. “*Ionic Liquid Gel-Assisted*

*Electrodes for Long-Term Cutaneous Recordings” Advanced Healthcare Materials*  
(2014) 1377-1380.

## **Chapter 5**

*In-vitro metabolite sensing using organic electrochemical transistors: work in progress.*

## 8. Glossary

Ag/AgCl: silver/silver chloride

BBB: blood brain barrier

BBEC: bovine brain endothelial cells

BSA: bovine serum albumin

CHIT: chitosan

Chox: cholesterol oxidase

CPs: conducting polymers

CV: cyclic voltammetry

DBSA: dodecyl benzene sulfonic acid

DC: direct current

DI: di-ionized water

DMEM: dulbecco's modified eagle medium

ECM: extra cellular matrix

ECoG: electrocorticography

EDC: 1-Ethyl-3-(3-dimethylaminopropyl)carbodiimide

EDL: electrical double layer

EDOT: 3,4-Ethylenedioxythiophene

EDTA: ethylenediaminetetraacetic acid

EEG: electroencephalography

EG: ethylene glycol

EGT: electrolyte gated transistor

EGTA: ethylene Glycol Tetraacetic Acid

EGOFET: electrolyte Gated Organic Field Effect Transistor

FAD: flavin adenine dinucleotide

FBS: fetal bovine serum

GOPS: 3-glycidoxypropyltrimethoxysilane

GOx: glucose oxidase

$I_d$ : drain current

$I_g$ : gate current

IgG: immunoglobulin G

LOx: lactate oxidase

MDCK: madin darby canine kidney

MW: molecular weight

MWCNT: multiwall carbon nanotubes

NHS: N-hydroxysuccinimide

NR: normalized response

OECT: organic electrochemical transistor

PAL: phosphatase alkaline

PBMEC: porcine brain microvessel endothelial cell

PBS: phosphate buffered Saline

PDMS: polydimethylsiloxane

PEDOT: poly(3-4 ethylene)dioxythiophene

PEG: poly(ethyleneglycol)

PEG-DA: poly(ethyleneglycol)-diacrylate

PLL: poly-L-lysine

Pt: platinum

Pt – NPs: platinum nanoparticles

PSS: polystyrene sulfonate

PVA: polyvinyl alcohol

QCM: quartz crystal microbalance

RTIL: room temperature ionic liquid

SEEG: stereoelectroencephalography

SEM: scanning electron microscopy

SNR: signal-to-noise ratio

TER or TEER: trans electrical endothelial resistance

TJ: tight junctions

TOS: tosylate

$V_d$ : drain voltage

$V_g$ : gate voltage

$V_{g,eff}$ : effective gate voltage

VPP: vapor Phase Polymerization

XPS: x-ray Photoelectron Spectroscopy